This is to certify that the

dissertation entitled

Kinetics and Mechanism of the Reaction Between
Ozone and Chlorinated Alkenes in the Aqueous Phase

presented by

Clayton Edward McCormack

has been accepted towards fulfillment
of the requirements for

_____MS_____ degree in Environmental Engineering

Susan J. Masten
Major professor

Date 20 September 1995

O-12771

```
+---------------------------+
|        LIBRARY            |
|   Michigan State          |
|    University             |
+---------------------------+
```

PLACE IN RETURN BOX to remove this checkout from your record.
TO AVOID FINES return on or before date due.

DATE DUE	DATE DUE	DATE DUE
————————	————————	————————
————————	————————	————————
————————	————————	————————
————————	————————	————————
————————	————————	————————
————————	————————	————————
————————	————————	————————

MSU Is An Affirmative Action/Equal Opportunity Institution

c:\circ\datedue.pm3-p.1

KINETICS AND MECHANISM OF THE REACTION BETWEEN OZONE AND CHLORINATED ALKENES IN THE AQUEOUS PHASE

By

Clayton Edward McCormack

A THESIS

Submitted to
Michigan State University
in partial fulfillment of the requirements
for the degree of

MASTER OF SCIENCE

Department of Civil and Environmental Engineering

1995

ABSTRACT

KINETICS AND MECHANISM OF THE REACTION BETWEEN OZONE AND CHLORINATED ALKENES IN THE AQUEOUS PHASE

By

Clayton Edward McCormack

The purpose of this work was to investigate the kinetics and mechanism of the reaction between ozone and low molecular weight chlorinated alkenes in the aqueous phase using second order reaction conditions. An airtight, glass syringe was used as the reaction vessel to minimize the loss of reactants and to permit modeling the kinetics of the system as a completely mixed, batch process. An aliquot from the syringe was withdrawn at regular time intervals to monitor the concentration of both reactants during the reaction. The stoichiometry of the reaction with several chlorinated alkenes was found to be greater than the 1:1 (VOC:ozone) stoichiometry predicted by the Criegee mechanism. The reaction rate coefficient was determined by fitting the concentration data of one or both reactants to kinetic modeling expressions. The stoichiometric ratio was observed to affect the fit of the experimental data to the modeling expression and the precision of the calculated reaction rate coefficients from the models. The observed stoichiometry and modeling problems were explained by the formation of an epoxide species as a result of an indirect reaction between a reaction intermediate and the unreacted chlorinated alkene.

ACKNOWLEDGMENTS

Well, this monstrosity has finally been completed and I can hardly believe it. This thing (thesis) represents the culmination of over a year of hard work with many a light nights (or early mornings), but more importantly the completion of this thesis represents the conclusion of over 20 years of education to prepared for a career in the cut-throat "real world". Along the way, I have learned a great deal about science, but I have also learned alot about myself at the same time. No one is going to be able to hold your hand in the "real world" and, in the end, its going to take your own personal skills, education, and self-dedication to a project to see it from conception to completion. Along the way there have been many people who have help me towards achieving the goal of getting a Masters degree and I am very great to their assistance.

Although it might be very strange, I need to acknowledge the work of people like Rudoff Criegee, Philip S. Bailey, and Jürg Hoigné for dedicating a lifetime of work attempting to develop an understanding of ozone chemistry and reactions. Without an understanding of the fundamentals of the chemistry of ozone, engineers would not be able to use their science to develop engineered applications to solve environmental problems.

I need to thank the other graduate students who have done research in the Chemical Oxidation group with Susan and Simon. Thanks in particularly to J.J. and Michael Hsu for being so helpful in accommodating my needs to use the ozone equipment and being patient with my messy laboratory habits. I wish the both of you much success in the future with completing your degrees.

me that inorder to achieve in science, I need at least a Masters degree. Mom and Dad, all I wanted is for you to be proud of me and my accomplishments. I am grateful for your strength and encouragement. I hope that I have always lived up to all your expectations. This Masters degree will be able to open many doors along my pathway that otherwise would be closed tight. My family has always provided the foundation by which my pathway has been built. With the doors open, its now up to me to take the first steps out of the familiar and secure side of the door in academia and out into the rough "real world". I am both excited and at the same time nervous about what the future holds, but with the continued strength of my family to help even out the bumps, all I can do is to try to do my best to continue to excel in my future endeavors.

"The man who works for something greater than himself
will ultimately benefit himself the most"

Clay

August, 1995

TABLE OF CONTENTS

LIST OF TABLES

LIST OF FIGURES

LIST OF SYMBOLS, ABBREVIATIONS, NOMENCLATURE, AND UNITS

SYMBOLS

ν_{O3} Stoichiometry Coefficient for Ozone

ν_M Stoichiometry Coefficient for any organic molecule

k Second Order Reaction Rate Coefficient (M^{-1} s^{-1})

k_{O3} Second Order Reaction Rate Coefficient Determined using Ozone Concentration Data (M^{-1} s^{-1})

k_m Second Order Reaction Rate Coefficient Determined using any Organic Molecule Concentration Data (M^{-1} s^{-1})

k' Pseudo-first Order Reaction Rate Coefficient (M^{-1})

$[M]_o$ Initial Molar Concentration of any Organic Molecule

pK_a Acid Dissociation Constant (M^{-1})

K Equilibrium Constant (M^{-1})

ABBREVIATIONS

trans-DCE   *trans*-dichloroethylene

cis-DCE   *cis*-dichloroethylene

1,1-DCE   1,1-dichloroethylene

TCE   trichloroethylene

PCE   tetrachloroethylene

1,1-DCP   1,1-dichloropropene

1,1,3-TCP   1,1,3-trichloropropene

M	Any Organic Molecule
NMR	Nuclear Magnetic Resonance
VOC	Volatile Organic Compound. Generic term organic compound used in this study.
CD	Coefficient of Determination
r^2	Correlation Coefficient

NOMENCLATURE

Ea	Activation Energy
E°	Standard Reduction Potential (volts)
$\Delta G°$	Standard Gibbs Free Energy (J or cal / mole)
$\Delta H°$	Standard Enthalpy
$\Delta S°$	Standard Entropy

UNITS

V	volts
Å	angstrom (1Å = 0.1 nm)
m	meter
M or [X]	concentration. (moles / L)
L	liter
J	joule
cal	calorie
s	second
min	minute
g	gram
ppm	parts per million (mg/L for aqueous solutions)

CHAPTER 1

INTRODUCTION

The presence of synthetic organic compounds (VOCs) in groundwater aquifers has been of great concern since they were first detected in groundwater-supplied drinking water about 20 years ago. Contaminated groundwater poses a great threat to the general population because 80% of all public water supply systems in the US. rely on groundwater resources for portable water (Handbook of Public Water Systems, 1986). The magnitude of groundwater contamination became apparent as a result of the 1980-81 Groundwater Supply Survey (GWSS) which showed that of 500 random samples, approximately 20% showed the presence of at least one VOC at detectable levels and about 5% had three of more VOCs present (The Conservation Foundation, 1987). The five compounds that occurred most frequently included: 1,1-dichloroethane (DCA), *cis/trans* 1,2-dichloroethylene (*cis/trans* DCE), trichloroethane (TCA), trichloroethylene (TCE), and 1,1,1-, tetrachloroethylene (PCE). These and many other volatile organic compounds have been used widely in many types of industrial, commercial, agriculture, and household applications. Table 1 shows the US demand for these compounds, their principle industrial uses, and their chemical hazards.

Table 1. Demand, Industrial Uses, and Hazards of the Five Most Common VOCs Found in Groundwater

Compound	1989 US Demand[1] 10^3 metric tons	Principle Industrial Uses	Hazards
DCA	7146	Manufacture of Polymers[2]	C, F
DCE		Extraction Solvent for Organics[3]	F, I
TCA	338	Industrial Solvent[2]	C, I, T
TCE	108	Vapor Degreasing Metal Parts[4]	C, M, I
PCE	218	Dry Cleaning Solvent[5]	C, I, M

Hazards Codes: C-Cancer Suspect Agent, F-Flammable, I-Irritant, M-Mutagen, T-Toxic.

(1) Reed, D., 1993. (2) The Conservation Foundation, 1987. (3) Mertens, J., 1993. (4) Mertens, J., 1993. (5) Reich, D. and Cormany, C., 1982.

Most contamination has occurred from the improper surface or underground disposal of hazardous wastes from industrial activities, although some groundwater contamination has also resulted from non-waste disposal activities such as accidental spills or leaking storage tanks.

Because of wide spread contamination of groundwater by VOCs and the hazardous properties of those contaminants, the USEPA has developed maximum contaminant level regulations for the presence of VOCs in drinking water under the Safe Drinking Water Act. Those regulations have forced environmental engineers to develop treatment strategies to remove regulated contaminants from drinking water. Although, treatment technologies such as air stripping and carbon adsorption have been used successfully to remove many VOCs from drinking water, these processes simple transfer the contaminants from one phase to another. For example, air stripping transfers the contaminants from the water to the air while carbon adsorption transfers the contaminants from the water to the carbon particles which then require regeneration or disposal. For these reasons, treatment technologies that degrade or destroy the organic contaminants are being increasingly considered. Such a treatment technology is chemical oxidation using ozone.

Ozone has been used for the treatment of drinking water for approximately 100 years. The ability of ozone to disinfect polluted surface waters resulted in the first full scale application of the technology for the treatment of drinking water in 1893 at Oudshoorn in the Netherlands (Brink, Langlais, and Reckhow, 1991). Since that time, ozonation has become the predominant treatment technology for the disinfection of drinking water throughout Europe. In the United States, chlorination is the principal technology for disinfection of drinking water because residual chlorine protects the distribution system from contamination. Concern relating to the formation of trihalomethanes (THMs) and disinfection by-products upon chlorination has generated increased interest for using ozone as a primary disinfectant. In 1990, some 40 drinking

water plants in the US were using ozone for primary disinfection and chlorine addition to provide protection in the distribution system (Brink, Langlais, and Reckhow, 1991).

In addition to disinfection, ozone has been used as an oxidizing agent for the treatment of water containing a wide variety of other contaminants. These uses of ozone other than for disinfection in water treatment are listed in Table 2.

Table 2. Uses of Ozone in Water Treatment

Algae Removal	Oxidation of Organics (Detergents, Pesticides, Phenol)
Color Removal	
Taste and Odor Removal	Oxidation of Inorganics (Cyanide, Nitrite, Sulfide)

(from Weber and Posselt, 1972)

Ozone is one of the most powerful commercially available oxidants and is capable of oxidizing almost all reduced inorganic and most organic compounds that may be present in polluted waters. Ozonation has been used favorably when compared to chlorination for the oxidation of contaminants because it can be produced relatively easily from oxygen or air using electrical energy. Ozone does not impart taste or odor to the water as does chlorination. The major disadvantage seen with using the ozonation technology for oxidation or disinfection is the very high capital and/or operating costs. For example, Montgomery (1985) estimated the costs for ozonation to be 4.6 times greater than chlorination in terms of dollars per pound equivalent weight. However, ozonation has been successfully applied to treat specific contamination problems in a cost effective manner using well engineered treatment systems.

In order to design a well-engineered ozone treatment system, it is imperative that the kinetics and mechanisms of the reactions of concern be well understood. In this study, I have focused on investigating the reaction of ozone with low molecular weight chlorinated alkenes in water that have been identified as contaminants in groundwater aquifers and other water sources. There were four principle objectives of this study.

(1) The first objective was to develop an experimental apparatus and/or experimental procedures to obtain kinetic data for the reaction between two volatile reactants. Bandemehr (1992) investigated the reaction of ozone with chlorinated ethylenes using a 22 mL GC headspace vial as the reaction vessel. Partitioning of the reactants from the aqueous phase to the gas headspace was believed to have affected the reaction rate coefficients calculated in the study.

(2) The second objective was to measure the order of the reaction with respect to each reactant. It was important to verify that the correct form of the reaction rate law expression was used in the derivation of the kinetic modeling expressions. Order can also be used to reject a proposed mechanism if the experimentally determined order does not agree with the order predicted by the proposed mechanism.

(3) The third objective was to measure the reaction stoichiometric coefficient with respect to each reactant. Measuring the stoichiometry of the reaction was important for an understanding of the overall reaction mechanism and the fitting of the concentration data to the kinetic modeling expressions.

(4) The final objective of this study was to calculate the reaction rate coefficient (k) for the reaction between ozone and low molecular weight chlorinated alkenes. Previous researchers have studied the reaction of ozone with chlorinated ethylenes using pseudo-first order reaction conditions, but a ten fold excess of ozone relative to the target compound is not feasible for an engineered treatment system. When using second order reaction conditions, the reaction rate coefficient was calculated using three methods and the values obtained for all methods were expected to agree. If it is found through this study that the values from the three methods do compare favorable, than the conclusion can be made that the reaction rate coefficient can be calculated using concentration data from only one reactant when using second order reaction conditions. The calculated reaction rate coefficients for a series of compounds will produce an insight into the chemical properties and electronic configuration of the target compounds which dictates

its reactivity towards ozone. The trends and observations previously observed for the chlorinated ethylenes can be expanded to include chlorinated propenes. Chlorinated propenes have not been commonly observed as a groundwater contaminant, these compounds have been used in a commercial formulation called "D-D Mixture" as a control of nematodes and other soil organisms (Hadler, 1982). Chlorinated propenes are also regulated as a priority pollutant in the 1977 Clean Water Act (Davis and Cornwell, 1991). The chemical properties of the chlorinated propenes (see Appendix A) made working with these compounds in the laboratory much easier than the chlorinated ethylenes because of the higher solubility limits and lower Henry's Law constants of the chlorinated propenes as contrasted with the chlorinated ethylenes. The location of the chlorine atoms on the carbon chain and their relationship to the carbon-carbon double bond are structural properties of the compounds which govern the reactivity of chlorinated alkenes towards ozone.

CHAPTER 2

THEORY

OZONE CHEMISTRY

Ozone (O_3) exists at normal temperature and pressure as an unstable gas having a strong, pungent odor. The gas occurs predominantly on Earth in the upper layers of the stratosphere where it adsorbs harmful UV radiation emited by the sun. In the lower atmosphere, ozone is the principle photochemical oxidant produced as a consequence of the natural atmospheric reactions associated with the nitrogen oxide photolytic cycle (Davis and Cornwell, 1991). The gas can be produced for commercial applications by passing an oxygen containing gas (usually either purified air or pure oxygen) through an electrified corona discharge cell. A very high potential, on the order of 8,000 to 30,000 volts, is applied across two electrodes in the cell causing free electrons to interact with the oxygen molecules in the gas and ultimately resulting in the formation of ozone (Carling and Clark, 1982). As such, ozone is produced by the following reactions that occur in the electrified corona discharge cell.

$$O_2(g) + e^- \dashrightarrow 2O(g) + e^- \tag{1}$$
$$O(g) + O_2(g) + M(g) \dashrightarrow O_3(g) + M(g) \tag{2}$$
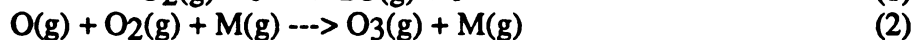
where M = any other gas phase molecule (siphons off excess energy)
e- = electron

At the same time, ozone can be consumed by two competing reactions.

$$O(g) + O_3(g) \dashrightarrow 2O_2(g) \tag{3}$$
$$O_3(g) + e^- + M(g) \dashrightarrow O_2(g) + O(g) + M(g) \tag{4}$$

6
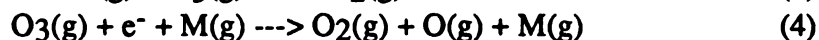
The summation of the four reaction results in the net production of an ozone enriched gas having an ozone concentration of about 5% (by volume) if oxygen is used and about 2% if air is used as the feed gas. The quality of the feed gas can greatly effect the net yield of ozone produced by the corona discharge cell. The gas must be extremely dry, free of particles, and have no hydrocarbon contamination for the maximum possible yield to be achieved. Cooling of the corona cell assembly is extremely important for optimal ozone production because 95% of the electrical energy supplied to the cell is dissipated as heat. Optimal operating conditions must be used for the treatment technology to be economical.

A good engineering design is also an important consideration for economic operation and performance of the system because of the low yields of ozone production and the low solubility of the gas in aqueous solution. Roth and Sullivan (1981) observed that the saturation concentration of ozone in water is dependent upon pH, temperature, and the percent ozone in the feed gas. In general, ozone is between five and ten times more soluble than oxygen in water. The Henry's Law constant for ozone is an order of magnitude less than that for oxygen. A large Henry's Law constant is an indication that at equilibrium, more of the compound will partition into the gas phase than in the liquid phase. For an engineer to design an ozone treatment system to achieve a desired ozone dose in the water capable of achieving a specific treatment objective (e. g., a three log reduction in pathogens or a percentage decrease in apparent color), the ozone generation capacity needs to be large enough to overcome the problems of low yield and low solubility. The economics of the treatment system may become prohibitive if the capital costs associated with providing enough ozone generation capacity become excessive.

Despite the large capital costs associated with using the ozone treatment technology, ozone continues to be used in water and wastewater treatment generally because it is one of the most powerful oxidants available. The strength of an oxidant is generally measured by its standard reduction potential ($E°$). The strongest oxidant has

the largest $E°$ value. Table 3 lists the $E°$ values of the common oxidants used in water and wastewater treatment.

Table 3. Standard Reduction Potential of Oxidants in Water Treatment

Oxidant	Reduction Reaction	$E°(V)$
Hydroxyl Radical	$\cdot OH + e^- <---> OH^-$	3.06
Ozone	$O_3 + 2H^+ + 2e^- <---> O_2 + H_2O$	2.08
Chlorine (pH<7.5)	$HClO + H^+ + 2e^- <---> Cl^- + H_2O$	1.48
Chlorine Dioxide	$ClO_2 + e^- <---> ClO_2^-$	0.95
Chlorine (pH>7.5)	$ClO^- + H_2O + e^- <---> Cl^- + 2OH^-$	0.81

(from CRC Handbook, 1990)

Ozone is sufficiently strong as an oxidant to be capable of oxidizing almost all reduced inorganic compounds and some simple organic compounds via an oxidation/reduction type reaction. Ozone has also been observed to react with many organic molecules by reactions other than the oxidation/reduction type (for examples see Bailey, 1972; Hoigné, 1982). The following list of functional groups have been observed to react with ozone via a non-redox type reaction: carbon-carbon double and triple bonds; aromatic, carbocyclic, and heterocyclic molecules; carbon-nitrogen and similar unsaturated molecules; nucleophilic molecules such as amines, sulfides, sulfoxides, phosphines, etc.; carbon-hydrogen bonds in alcohols, ethers, aldehydes, amines, and hydrocarbons. The reactivity of ozone towards organic molecules can be partially explained by an understanding of the electronic configuration of the ozone molecule.

ELECTRONIC STRUCTURE OF THE OZONE MOLECULE

During the early 1950s, the identification of the electronic structure of the ozone molecule helped to explain the observed reactivity of the molecule towards organic molecules. The microwave spectrum of the ozone molecule in its ground state revealed that the molecule has an obtuse angle of $116°45"\pm 35"$ and an oxygen-oxygen bond

length of 1.278±0.003 Å (Hughes, 1956; Trambarolo *et al.*, 1953). On this basis, the molecule can be described by a resonance hybrid structure.
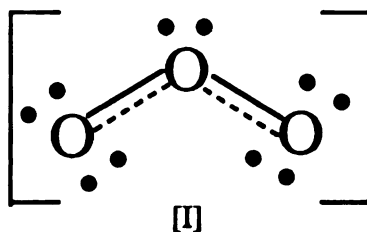
Figure 1. Resonance Hybrid Structure of the Ozone Molecule

In Figure 1, the two dashed lines represents a pair of bonding electrons. The resonance hybrid structure can be thought of as a combination of the four contributing resonance forms shown below in Figure 2.
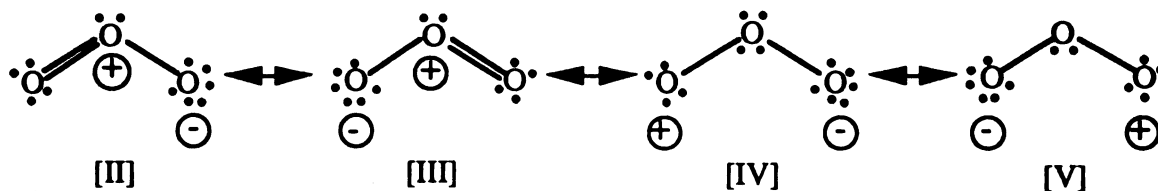
Figure 2. Resonance Forms Contributing to Resonance Hybrid Structure

Trambarolo *et al.* (1953) explained that the experimental evidence suggested that the actual observed bond length was intermediate between the double bond length in O_2, 1.21 Å, and the single bond length in hydrogen peroxide, 1.47 Å. The oxygen-oxygen bond in the ozone molecule can be thought of as an averaging of a single and a double bond. This explains the existence for structures [II] and [III]. Structures [IV] and [V] are included because the observed obtuse bond angle is just slightly less that 120° as would be expected for an sp^2 hybridization of the oxygen atoms. The opposite charges on the

terminal atoms in the molecule would tend to decrease the observed bond angle in the molecule.

The four resonance forms reveal the reason why the ozone molecule can react with organic compounds via non-oxidation/reduction type reaction pathways. The ozone molecule can act as either an electrophile, a nucleophile, or a 1,3-dipole in reactions with organic molecules (Bailey, 1978). Structures [IV] and [V] shows that a terminal oxygen atom can be positively charged so as to act an electrophile to attack a nucleophilic site of an organic molecule. Aromatic compounds with electron donating substitutent groups (such as OH, NH_2, alkyl groups) cause the carbon atom with the substitution to have a strong electron density thus acting as a nucleophile site, available to attack by the ozone molecule which acts as an electrophile. All four structures have a negatively charged terminal oxygen atom causing ozone to act as a nucleophile to attack an electrophilic site on an organic molecule. Ozone, acting as a nucleophile, can attack electron deficient sites on aliphatic compounds, or more frequently, electron deficient carbon atoms in aromatic compounds which are substituted with functional groups such as NO_2, NR_3, and carboxyl containing groups. Structures [IV] and [V] show that ozone can act as 1,3-dipoles and undergo 1,3-dipole cycloaddition with unsaturated bonds to result in the formation of a primary ozonide. This reaction is the classical Criegee Mechanism which will be discussed in greater detail later in this chapter.

The electronic configuration of the ozone molecule can also be described by invoking the molecular orbital theory. Each oxygen atom in the ozone molecule is said to have sp^2 hybridization. An sp^2 hybrid molecular orbital is constructed by a linear combination of the 2s, $2p_x$, and $2p_y$ valence atomic orbitals. The hybrid orbital has three s-type orbital lobes at 120° to each other in a single plane in addition to the pure p-type orbital normal to the plane of the other lobes. Two of the three sp^2 orbitals in the plane of the apex atom form a localized sigma molecular bond by overlapping with the lobe of the sp^2 orbital on each of the terminal atom. The remaining nonbonding lobe of the sp^2

orbital(s) in the plane contains a nonbonding electron pair. This configuration is illustrated in Figure 3.
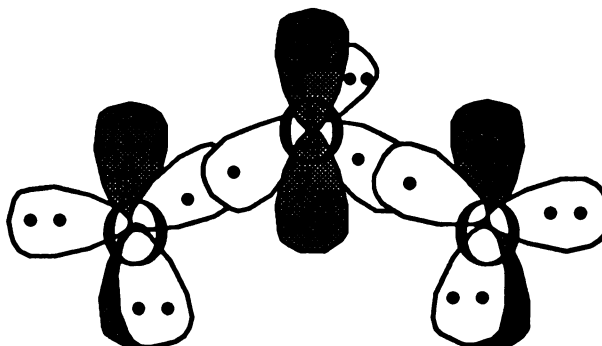
Figure 3. Molecular Orbital Configuration of the Ozone Molecule

There are four electrons in the ozone molecule which are delocalized over the pi orbital system, creating a so-called pi-electron cloud. The electron density of the pi-orbitals can shift from one atom of the molecule to another in response to the presence of a charged or an induced charged region on an adjacent molecule. The ability of the electron density of the pi-electrons to delocalize on the molecule dictates the reactivity of the molecule with respect to the 1,3-dipole cycloaddition reaction.

CRIEGEE MECHANISM

During the period 1949-1957, Rudolf Criegee at the University of Karlsruhe (Germany) developed a mechanism to explain the active oxygen-containing products observed after the ozonation of a wide variety of unsaturated compounds in different types of solvents (for a review, see Bailey, 1958, 1978). The ability to postulate a reaction mechanism was only possible after the electronic configuration of the ozone molecule was determined. The complete mechanism can be seen in Figure 4. Ozone, acting as a 1,3-dipole, attacks the carbon-carbon double bond through a 1,3-dipole cycloaddition reaction to give a 1,2,3-trioxolane species [VIII], which is sometimes called a "primary ozonide". Various papers in the literature have called the initial adduct
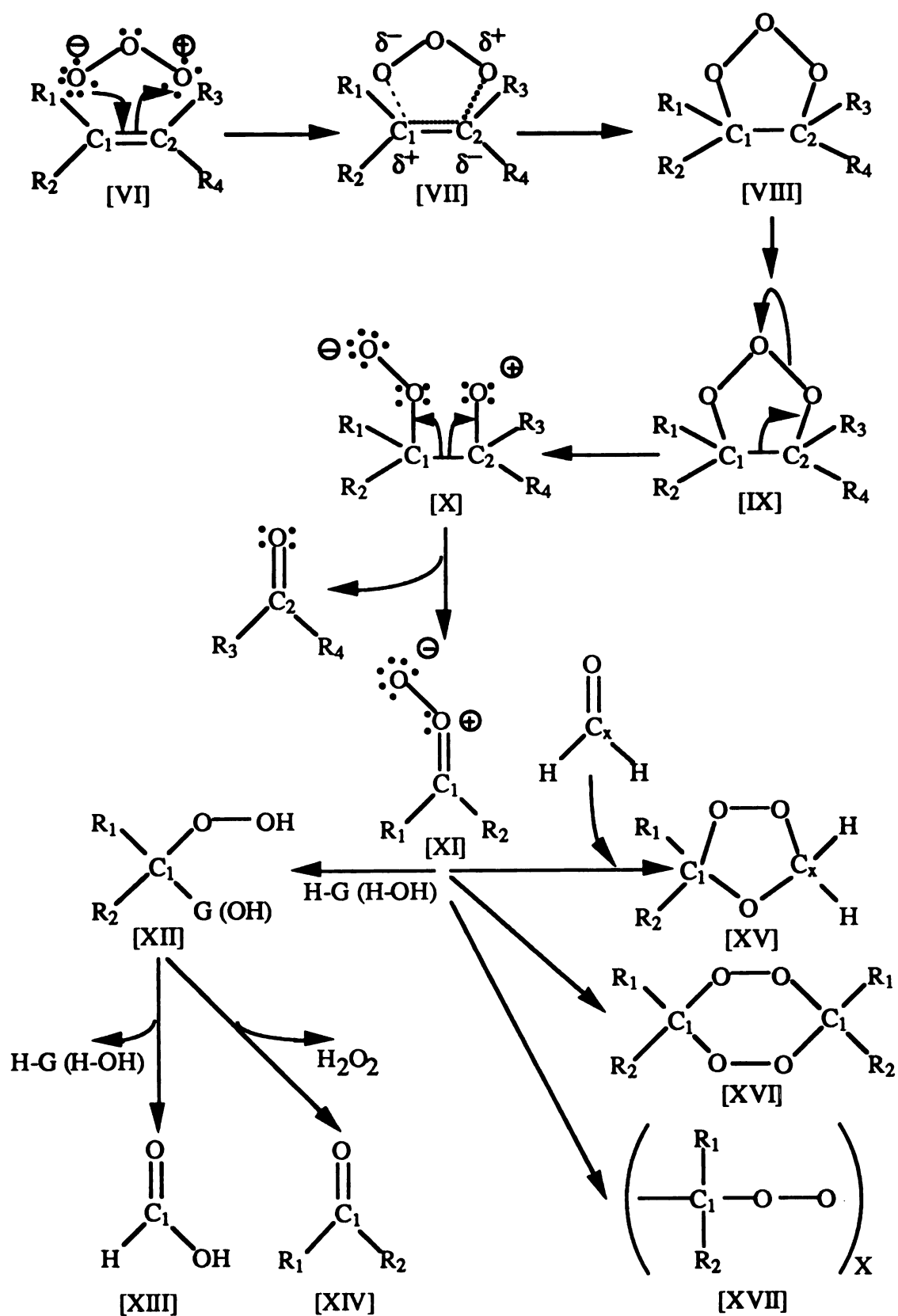
Figure 4. Overall Criegee Mechanism (After Bailey, 1978)

species simply an "ozonide" or a "molozonide", however these terms are more appropriately used to describe the initial adduct species of other proposed mechanisms for this reaction that have since been disproved (Bailey, 1978).

The five member cyclic structure of the primary ozonide is very unstable and cleaves to produce the key intermediate of the mechanism, a carboxyl oxide zwitterion [XI], while releasing an aldehyde or a ketone. This highly energetic zwitterion species must be stabilized further by reacting through one of the following pathways: (1) reaction with a protic, participating solvent to give a hydroxy hydroperoxide species [XII]; (2) reaction with an aldehyde to give a stable, five member cyclic ozonide containing an ether and a peroxide linkage [XV]; (3) dimerization to give a stable, six member cyclic ozonide containing two peroxide linkages [XVI]; or (4) polymerization [XVII]. The fate of the zwitterion [XI] depends on its structure, but more importantly on its environment.

Water is an example of a protic solvent, so that in an aqueous environment, the zwitterion can be expected to stabilize itself predominately through the reaction with the participating solvent (water). The product of the reaction between the carboxyl oxide zwitterion [XI] with the protic solvent is a hydroxy hydroperoxide species [XII] that easily decomposes by releasing either a water molecule or hydrogen peroxide to create as a final product of the reaction either an a carboxylic acid [XIII], an aldehyde [XIV], or a ketone [XIV]. Simple carboxyl containing compounds, particularly when chlorinated, as is the case upon the ozonation of chlorinated ethylenes, are not stable in water and would be expected to hydrolyze to produce Cl^-, H_2O, and CO_2 (Masten, 1986).

$$\underset{\substack{\text{phosgene}\\ \text{(chloroformaldehyde)}}}{\underset{Cl}{\overset{O}{\underset{\|}{C}}}Cl\,(H)} \xrightarrow{H_2O} \underset{Cl}{\overset{O}{\underset{\|}{C}}}OH \;+\; Cl^-\,(H^+)$$

(5)

$$\underset{Cl}{\overset{O}{\underset{\diagup C \diagdown}{\parallel}}} \underset{OH}{} \xrightarrow{\ H_2O\ } \quad CO_2(g) \ + \ HCl \tag{6}$$
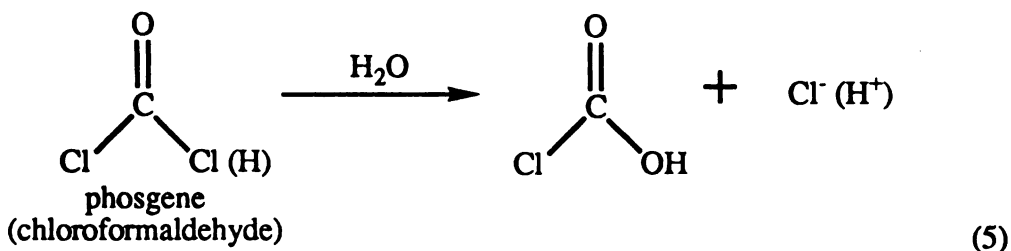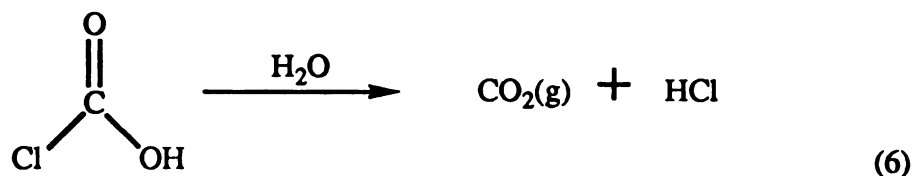
When the solvent is aprotic, the carboxyl oxide zwitterion [XI] must be stabilized by reacting via one of the other pathways. When an aldehyde is released upon the formation of the carboxyl oxide zwitterion from the primary ozonide, the released aldehyde is expected to react with [XI] to form a five membed cyclic ozonide [XV]. If a ketone is released, it will not react with the carboxyl oxide zwitterion because it is generally less susceptible to nucleophilic attack than are aldehydes. The carboxyl oxide zwitterion can also be stabilized by dimerizing to form a six member cyclic structure [XVI] or by polymerizing to form [XVII].

The 1,3-cyclic addition reaction is an example of a unique class of reaction mechanisms called a pericyclic mechanism (McMurry, 1988). This type of reaction occurs through a concerted process where all bond changes occur at the same time, in a single step. Cycloaddition reactions are a particular group of pericyclic mechansims where a cyclic product is formed from two unsaturated molecules through the formation of two new s-type bonds from the pi-orbital electrons from each molecule. The reaction between ozone and ethylenes is similar to the classical Diels-Alder cycloaddition reaction between a diene and a dienophlie (McMurry, 1988). Both the diene and the ozone molecules have 4 pi-electrons while the ethylene and the dienophile molecules have only two pi-electrons. Thus, these reactions are termed [π4s + π2s] cycloaddition reactions. Figure 5 shows the overlap of the π HOMO (highest occupied molecular orbital) of the ethylene molecule and the π* LUMO (lowest unoccupied molecular orbital) of the ozone molecule. The symmetry of these frontier orbitals on the two molecules are such that the lobes are on the same face of each molecule. This geometric arrangement of the

overlaping frontier orbitals is termed suprafacial cycloaddition and it permits the reaction between these molecules to occur under very mild reaction conditions.
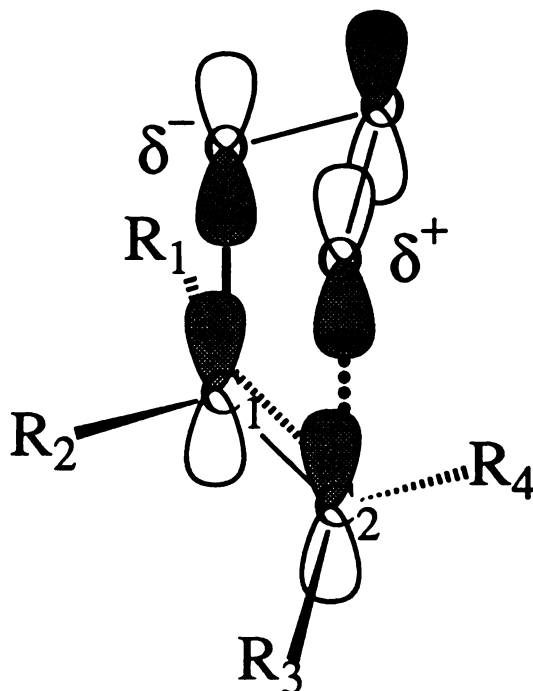
Figure 5. Overlap of Molecule Orbitals for the 1,3 Cycloaddition Reaction

In general, not only must the kinetic pathway of the reaction be favorable, but the thermodynamics of the reaction must also be favorable for the reaction to proceed. A reaction is considered thermodynamically favorable if the ΔG° (standard Gibbs Free Energy) of the reaction is negative. The equation for the standard Gibbs free energy ($\Delta G^{\circ} = \Delta H^{\circ} - T\Delta S^{\circ}$) is the combination of the standard reaction enthalpy (ΔH°; the amount of heat released or consumed by the reaction) and the standard reaction entropy (ΔS°; the amount of disorder of the system). In particular for the reaction between ozone and ethylenes, the entropy term makes a significant contribution to the ΔG° value. Figure 5 shows that the reactants must be precisely aligned with respect to each other for the reaction to occur. Huisgen (1963) said when speaking of the orientation of the molecules required for the reaction, "... the lock will be closed with a low expenditure of energy

only when the key is fitted into properly. The interplay of entropy and enthalpy controls the rate-determining activation process." The high degree of order required for the 1,3-cycloaddition reaction causes the entropy of activation for a series of electron-deficient alkenes to be calculated as -31 ± 2.5 cal/mole degree (Pryor *et al.*, 1983). The observed value is within the typical range of -29 to -40 cal/mole degree predicted by Huisgen (1963).

The enthalpy of the reaction has been difficult to quantify because is has been impossible to measure the enthalpy of formation (ΔH°_f) of the intermediate of the reaction. However, several authors have made use of *ab initio* theoretical calculations using different basis sets and procedures to attempt to model the reaction and calculate the ΔH°_f of the intermediates of the reaction (Wadt and Goddard, 1975; Harding and Goddard, 1978; Cremer, 1981a, 1981b; Dewar *et al.*, 1991). Figure 6 shows the ΔH°_f profile of the reaction between gas phase ethylene and ozone using the data presented by Dewar *et al.* (1991). Overall, the reaction is exothermic giving off about 60 kcal/mole upon the formation of the carboxyl oxide zwitterion. The reaction has a very small activation energy estimated to be 11 kcal/mole, which compares favorable with the data presented by Pryor *et al.* (1983) for the ozonation of various chlorinated ethylenes in CCl_4 at 25°C (see Table 4 for data) (Pryor *et al.*, 1983). A very small value for the activation energy is consistent with the 1,3-cycloaddition mechanism proposed by Criegee.

For the Criegee mechanism to be accepted by the scientific community after it was proposed in the 1950s, it was necessary to obtain experimental evidence to support the existence of the two key intermediates of the proposed reaction mechanism. In the 1960s, the initial focus of the attempts to verify the mechanism involved identifying the structure of the primary ozonide molecule. This was first attempted by making a derivative of the primary ozonide molecule. The primary ozonide species was postulated to be highly unstable requiring very low temperatures to be used to trap the species and to
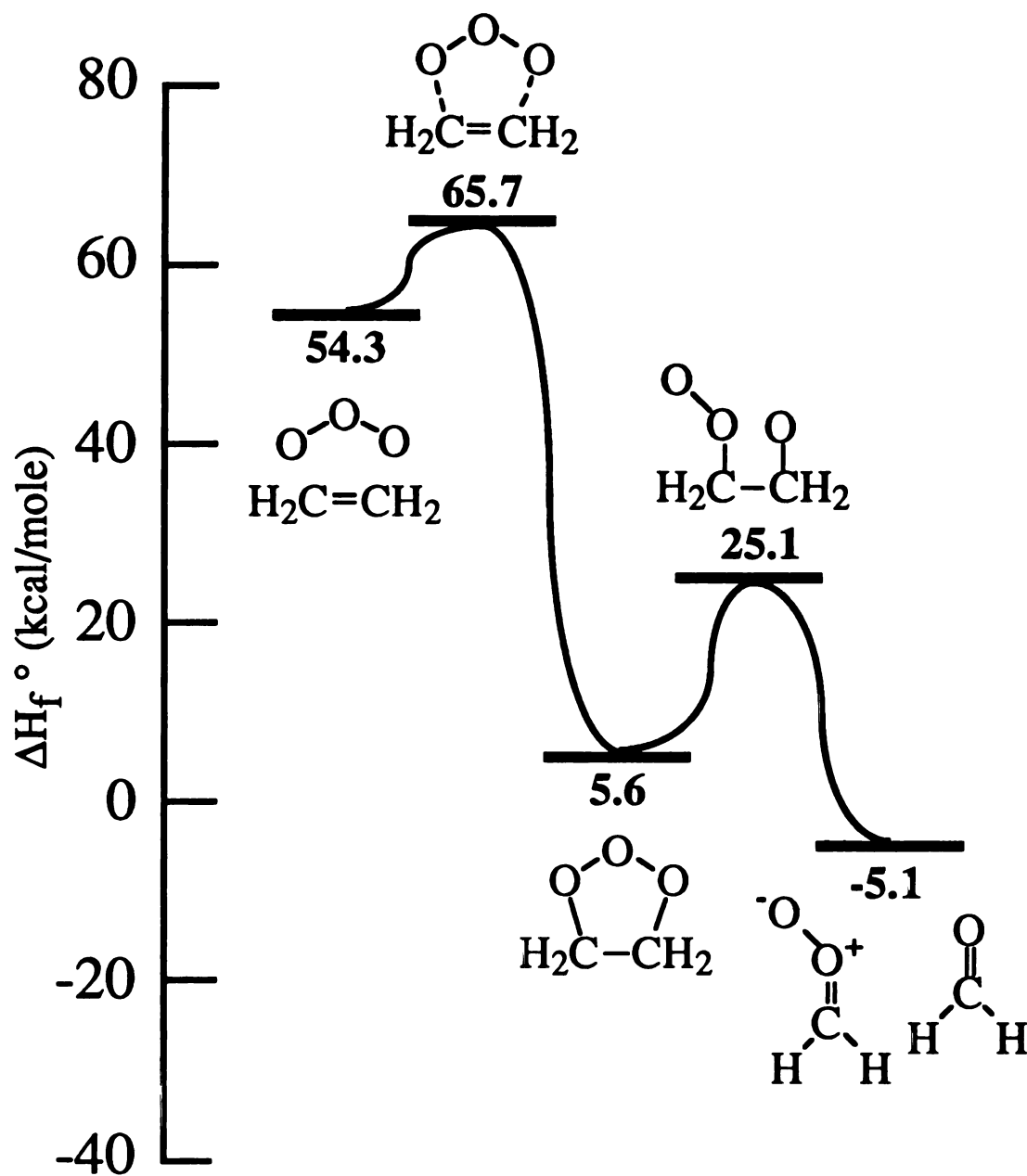
Figure 6. Estimated Enthalpy of the Ozonation of Ethylene in the Gas Phase
(Data taken from Dewar *et al.* 1991)

conduct the derivative experiment. A white crystalline precipitate believed to be the primary ozonide was produced upon the ozonation of 3-octene at -95°C using pentane as the solvent. However, the crystals violently decomposed upon warming the reaction mixture to -65°C (Greenwood and Cohen, 1963). In a second experiment, the ozonated reaction mixture, produced at -95°C, was treated with an isopropyl Grignard reagent and the product of that reaction tested positive for a 1,2-diol with periodic acid (HIO_4). The 1,2-diol was cleaved by oxidation to yield two carbonyl compounds through a cyclic intermediate. This reaction scheme is presented below in Figure 7.
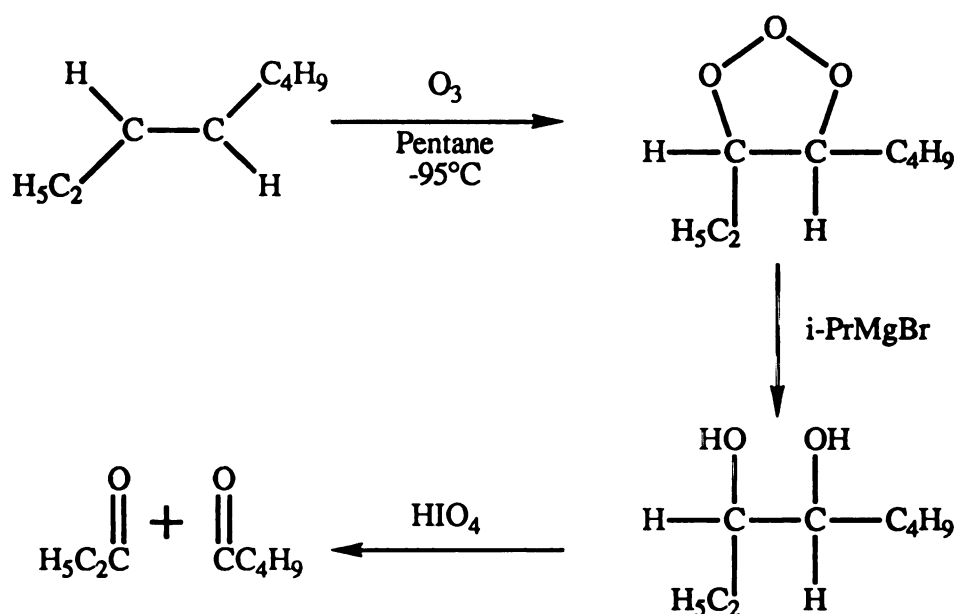
Figure 7. Derivatization Reactions Used to Identify the Primary Ozonide

Using a similar reaction scheme, Greenwood established the existence of the primary ozonide for a variety of simple alkenes: trans-3-hexene, trans-2-pentene, 1-pentene, trans-2-butene, 1-butene (Greenwood, 1964, 1965). The derivative experiments established the existence of the primary ozonide, but the exact shape and size of the molecule was not established for several few more years.

Criegee did not postulate a structure for the ozone-alkene adduct (primary ozonide) when the mechanism was proposed, several structures were later proposed for the primary ozonide (Bailey, 1978). Structure [XIX] is a modernization of structure [XVIII].
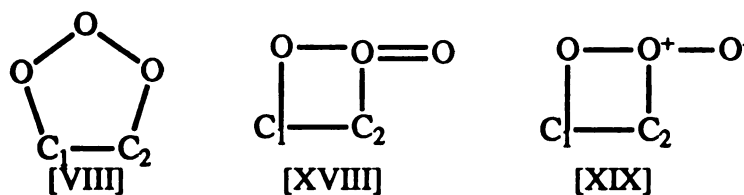
Figure 8. Proposed Structures for the Primary Ozonide

The question regarding the structure of the primary ozonide was answered in 1966 through low temperature NMR by Bailey, Thompson, and Shoulder (1966) who obtained the NMR spectrum of the initial ozonide of *trans*-1,2-di-t-butylethylene at -110°C in Freon 11 and observed a spectrum containing only two singlet peaks. The location of these peaks were consistent with t-butyl and methine protons in the expected ratio of 9:1. The NMR spectrum indicated that the primary ozonide was a symmetrical molecule thus discrediting the proposed four member cyclic primary ozonide [XIX] because this non-symmetrical molecule would have caused a more complex NMR spectrum. Following along on the work done by Bailey, the 1,2,3-trioxolane structure of the primary ozonide for both *cis* and *trans* alkenes was further identified by low temperature NMR spectroscopy (Durham and Greenwood 1968a, 1968b). However, it was observed that the primary ozonide from the *cis*-alkene was considerably less stable than the *trans*-alkene. The NMR spectrum of the solution was monitored for a period of time and as the temperature was increased. The methine peak on the spectrum for the primary ozonide from the *cis*-alkene disappeared within two hours at -130°C. The similar peak for the primary ozonide for the *trans*-alkene was stable at -130°C. and only disappeared upon warming the reaction solution to -100°C. From these early experiments, the existence

and structure of the five member, 1,2,3-trioxolane primary ozonide was experimentally determined and this added credability to the original mechanism proposed by Criegee.

Additional evidence in support of the Criegee mechanism was obtained when it was observed that a foreign aldehyde reacted with the carbonyl oxide zwitterion to form the five member cyclic ozonide. This work help to discredit other proposed mechanisms. A ^{18}O labeled aldehyde was shown to react with the zwitterion to form the cyclic ozonide with the ^{18}O atom located in the ether oxygen linkage position in the molecule (Fliszár, Carles, and Renard, 1968; Fliszár and Carles, 1969a, 1969b).

where $O^* = {}^{18}O$

(7)
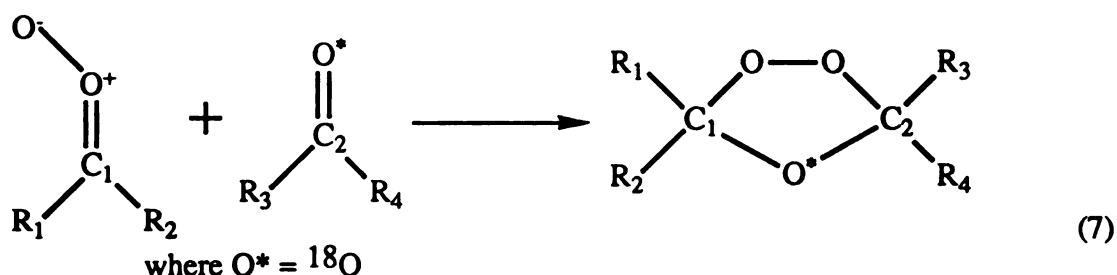
The ^{18}O was found in the ether oxygen linkage upon the ozonation of *cis* and *trans* stillbene in the presence of benzaldehyde-^{18}O at -78°C in pentane. The location of the ^{18}O was identified by the fragment pattern of the mass spectrum of the isolated reaction products. This work helped to disprove other proposed mechanisms because the labeled oxygen atom was incorporated at the ether linkage position rather that at the peroxide linkage as predicted by other proposed mechanisms. As experimental evidence was obtained, other proposed mechanisms were disproved thus leaving the original Criegee mechanism as the only mechanism that was supported by the experimental data.

DERIVATION OF THE REACTION RATE LAW EXPRESSION

The development and validation of the Criegee mechanism to describe the pathway by which ozone reacts with carbon-carbon double bonds serves as a theoretical

foundation for the development of the reaction rate law expression. The reaction rate law mathematically describes the rate of change of the reactants during the course of the reaction. The overall reaction can be written in simplest terms as shown below in equation (8).

$$\upsilon_{O_3}\, O_3 + \upsilon_M\, M \longrightarrow Z + H_2O \longrightarrow \text{Acids, Aldehydes, and Ketones} \tag{8}$$

$$\begin{aligned}
\text{where } M &= \text{any alkene molecule}\\
O_3 &= \text{ozone}\\
Z &= \text{zwitterion}\\
\upsilon &= \text{stoichiometric coefficient}
\end{aligned}$$
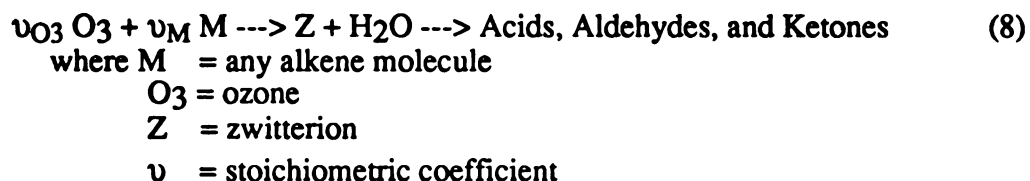
The rate determining step, or the slowest step, of the overall reaction mechanism is the initial 1,3-cycloaddition of the ozone at the carbon-carbon double bond resulting in the formation of the primary ozonide species. This step is believed to be the rate determining step of the overall mechanism because it requires a high degree of order to form the primary ozonide and because the theoretical *ab inito* calculations indicated the formation of a transition state with an activation energy of about 11 kcal/mole prior to the formation of the primary ozonide. Because the rate determining step of the overall mechanism is an elementary reaction (meaning that the reaction cannot be further simplified using a more basic reaction mechanism), the reaction rate law expression can be written as a second order overall reaction.

$$\frac{1}{\upsilon_{O_3}}\frac{[O_3]}{dt} = \frac{1}{\upsilon_M}\frac{d[M]}{dt} = -k[O_3]^1[M]^1 \tag{9}$$

$$\begin{aligned}
\text{where } [M] &= \text{any alkene molecule}\\
[O_3] &= \text{ozone}\\
k &= \text{second order reaction rate coefficient } (M^{-1}\,s^{-1})
\end{aligned}$$

The rate law for this bimolecular reaction can be interpreted as meaning that the rate of the reaction is dependent on the rate at which the reactants collide in solution, which

inturn is proportional to the solution concentration of the reactants. In addition, the expected reaction stoichiometry, based on the Criegee mechanism, would be one ozone molecule to one alkene molecule.

PREVIOUS RESEARCH REGARDING THE KINETICS OF THE REACTION BETWEEN CHLORINATED ETHYLENES AND OZONE

The reaction of the chlorinated ethylenes with ozone in the condensed phase has been studied by several researchers (for example, see Hoigné and Bader, 1983; Pryor *et al.*, 1983; Williamson and Cvetanovic, 1968). The complex nature of the reaction system required simplifying reaction conditions to be used. For example, carbon tetrachloride (CCl_4) was used as a solvent by Pryor *et al.* (1983) and Williamson & Cvetanovic (1968) as it is not a participating solvent and it does not react with the zwitterion. The solvent was pretreated with ozone to reduce the rate of ozone self-decomposition in the solvent from 30% hr^{-1} to 2-3% hr^{-1}(Williamson and Cvetanovic, 1968). A pH 2 phosphate buffer solution was used as the aqueous solvent by Hoigné and Bader (1983) to minimize ozone self-decomposition.[1] A closed, airtight stop flow apparatus was used by all researchers to prevent volatilization of the reactants during the reaction. The rate of the reaction was determined by monitoring the decrease in ozone concentration using a spectrophotometer. Again, all researchers used pseudo-first order reaction conditions so that the reaction rate coefficient (k) could be calculated using the concentration data from one reactant. The initial molar concentration of the reactants was chosen so that the chlorinated ethylene was in excess relative to ozone by 10-100 times. By using these reaction conditions, the change in the concentration of the chlorinated ethylene is small

---

[1] The self-decomposition of aqueous ozone has been observed to be pH dependent with hydroxide ion (OH^-) initiating the chain reaction mechanism that consumes ozone (Staehelin and Hoigné, 1982, 1985; Grasso and Weber, 1989; Sehested *et al.*, 1991). Hydrogen phosphate ion (HPO_4^{2-}) and dihydrogen phosphate ion ($H_2PO_4^-$) also acts to scavenge hydroxyl radicals ($OH\cdot$) produced as a result of the chain reaction mechanism causing ozone self-decomposition. Hydroxyl radicals are powerful, nonspecific oxidants capable of oxidizing organic compounds via a so-called non-direct pathway (Hoigné and Bader, 1976; Masten and Hoigné, 1992).

relative to the change in the ozone concentration. The second order reaction rate

expression can be simplified by using pseudo-first order reaction conditions.

$$\frac{1}{vO_3}\frac{[O_3]}{dt} = -k[O_3]^1[M]^1 \qquad \text{Second Order Kinetics} \qquad (10)$$

$$\frac{1}{vO_3}\frac{[O_3]}{dt} = -k'[O_3]^1 \qquad \text{Pseudo-First Order Kinetics} \qquad (11)$$

where $k' = k[M]$ = reaction rate coefficient (s^{-1})

The second order reaction rate coefficients calculated from the experimentally determined

pseudo-first order reaction rate coefficients for a series of chlorinated ethylenes can be

found in Table 4.

Table 4. Reported Reaction Rate Coefficients and Other Kinetic Information for the
Reaction of Chlorinated Ethylenes with Ozone in the Liquid Phase

Compound	Water [1,3]	k (M^{-1} s^{-1}) CCl4 [2,4]	CCl4 [2,5]	Ea [4] (kcal/mole)	Stoichiometry [5] VOC/O3
trans - DCE	5700±100	590	591	5.0	
cis - DCE	<800	21.3	35.7	7.0	0.98
1,1 - DCE	110±20	25.4	22.1	6.2	1.05
TCE	17±4	2.06	3.6	8.1	
PCE	<0.1	0.007	1.0	11	

(1) at 20°C. (2) at 25°C. (3) Hoigné and Bader, 1983. (4) Pryor *et al.*, 1983.
(5) Williamson and Cvetanovic, 1968.

The data shown in Table 4 illustrates two trends relevant to an understanding of

the reactivity of chlorinated ethylenes with ozone. In general, the rate of the reaction

decreases as the alkene backbone becomes more substituted with chlorine, an electron-

withdrawing substituent group. The observed reaction behavior is consistent with

chlorine exerting an inductive electron-withdrawing effect at the double bond thereby

reducing the electron density at that site. There is some evidence that ozone has an

electrophilic (electron-demanding) reaction character when behaving as a 1,3-dipole

(Carles and Fliszár, 1972; Williamson and Cvetanovic, 1968; Nakagawa, Andrews, and

Keefer, 1960). A reaction site with less electron density would cause the rate of the ozone attack at that site to be slower.

The other trend shown in Table 4 is that the *cis*-substituted alkene reacts slower than the *trans*-substituted alkene. This trend is generally observed for all 1,3-cycloaddition reactions because as the central carbon atoms go from sp^2 to sp^3 hybridization, the bond angle compresses from 120° to 109° (Pryor *et al.*, 1983; Huisgen, 1963). Compression of the van der Waals radius occurs causing an increased repulsion between *cis*-substituent groups and hence a high activation energy. Increased repulsion does not occur with *trans*-substituted alkenes. The consequence of the slightly higher activation energy for the *cis*-substituted alkenes is a slightly slower rate of reaction relative to the *trans*-substituted compounds.

DERIVATION OF SECOND ORDER REACTION RATE MODELS

Using reaction conditions where pseudo-first order kinetics cannot be assumed, the reaction rate coefficient can be experimentally determined using either of two models. Model I was originally developed by Bandemehr (1992) and later corrected in this study. When using this model, the concentration data for only one reactant is required to calculate the reaction rate coefficient. The assumptions used to derive the model are that: (1) ozone self-decomposition is slow relative to the rate of the reaction; (2) the reaction of the alkene with hydroxyl radicals is not important because the concentration of OH• is negligible; (3) the reaction of the alkene with ozone is first order with respect to ozone and first order with respect to alkene, or second order overall. The model is derived here using ozone concentration data, but an analogous derivation can be performed using alkene concentration data.

Model I is based upon the reaction rate law expression being given as equation (9).

$$\frac{1}{vO_3}\frac{[O_3]}{dt} = -k_{O3}[O_3]^1[M]^1 \tag{9}$$

where k_{O3} is the reaction rate coefficient calculated using ozone concentration data.

Equation (9) contains two interdependent variables making the integration quite difficult. A simpler expression with only one variable can be derived using the following substitution.

$$[M]_t = \left\{ [M]_0 - v_M([O_3]_0 - [O_3]_t) \right\} \tag{12}$$

where $[M]_0$ and $[O_3]_0$ are the initial concentration and v_M is a constant throught the course of the reaction.

This equation equates the extent of reaction of the alkene in terms of the amount of ozone that has reacted. Equation (12) can be substituted into equation (9), resulting in the following differential equation.

$$\frac{1}{vO_3}\frac{[O_3]}{dt} = -k_{O3}[O_3]^1\left\{ [M]_0 - v_M([O_3]_0 - [O_3]_t) \right\} \tag{13}$$

The details of the integration of equation (13) can be found in Appendix I-1 in Bandemehr (1992). Integration of equation (13) results in the following equation.

$$[O_3]_t = e^{-(kO3/vO3)t([M]_0 - vM[O3]_0)}\left[\frac{[M]_0}{[O3]_0([M]_0 - vM[O3])} \right] - \frac{vM}{([M]_0 - vM[O3]_0)} \tag{14}$$

The reaction rate coefficient, k_{O3}, calculated using the ozone concentration data can be determined using a nonlinear modeling program written by Bandemehr (1992) using Pro-Matlab© (The Mathworks, Inc. version 3.5). The independent variable is t, the dependent

variable is [O3], and the modeling parameter is k_{O3}. The modeling algorithm determines the best fit of the experimental data to equation (14) by finding the k_{O3}, which produces the greatest coefficient of determination. The 95% confidence interval for the calculated reaction rate coefficient is found using the likelihood ratio method (Ratkowsky, 1983).

The reaction rate coefficient can also be calculated using the concentration data from both reactants. Model II is based on the reaction rate law expression being given as equation (9).

$$\frac{1}{\nu O_3} \frac{[O_3]}{dt} = \frac{1}{\nu M} \frac{d[M]}{dt} = -k[O_3]^1[M]^1 \tag{9}$$

A progress variable, χ, which measures the progress of the reaction is defined as follows.

$$\chi = ([O_3]_o - [O_3]_t) = ([M]_o - [M]_t) \tag{15}$$

The rate law expression given in equation (9) can be rewritten in term of the new variable χ.

$$\frac{d\chi}{dt} = k([O_3] - \chi)([M] - \chi) \tag{16}$$

Integration of equation (16) yields:

$$\int_{\chi(0)}^{\chi(t)} \frac{d\chi}{([O_3] - \chi)([M] - \chi)} = k \int_0^t dt \tag{17}$$

To solve equation (17), the variables are separated and the method of partial fractions is used, yielding as the solution, the following equation (Hill, 1977; Steinfeld *et al.*, 1989; Bandemehr, 1992).

$$\ln\left[\frac{[M]}{[O_3]}\right] = -\ln\left[\frac{[O_3]_o}{[M]_o}\right] + (v_M[O_3]_o - v_{O3}[M]_o)kt \qquad (18)$$

The reaction rate coefficient (k) can be found by plotting t versus $\ln\left[\frac{[M]}{[O_3]}\right]$. The slope of the resulting linear relationship can be used to calculate the reaction rate coefficient.

$$k = \frac{\text{slope}}{(v_M[O_3]_o - v_{O3}[M]_o)} \qquad (19)$$

The computer algorithms coded in Pro-Matlab® that were used to determine the reaction rate coefficient were verified by Bandemehr (1992) to prevent coding or mathmatical errors. A data set was generated using a second order irreversible reaction model (obtained for the MINSQ® chemical kinetic library). The two models accurately predicted the second order reaction rate coefficient produced by MINSQ® to three significant figures. In theory, the reaction rate coefficients obtained using the two kinetic models to analyze experimental data would also be expected to produce the same value.

CHAPTER 3

MATERIALS AND METHODS

REAGENT PREPARATION

All solutions were prepared in house R. O. water purified by a Technic Series 300 model reverse osmosis unit followed in series by a Zyza Tech Activated Carbon cartridge filter and a Zyza Tech Nuclear Grade Deionization Resin cartridge filter. The water had a resistivity of 18 Mohm or greater and had a total organic carbon (TOC) content of less than 100 ppb. This water will be, herein, referred to as R.O.-Filtered water. All chemicals used were reagent grade (>95% purity) and were obtained from Aldrich Chemical Co., Milwaukee, WI, unless otherwise specified.

Buffer Stock Solution. The 0.05 M phosphate buffer solution was prepared using 85% phosphoric acid (Malinckrodt, Paris, KY). The pH was adjusted to 2.0 using a 3 M solution of sodium hydroxide (Columbus Chemical Industries Inc., Columbus, WI) The buffer solution was prepared daily.

Indigo Stock Solution. The indigo stock solution was prepared by dissolving a known mass of 5,5',7-indigo trisulfonic acid potassium salt (Sigma Chemical Co., St. Louis, MO, 75% purity) in phosphate buffer solution at a pH of 2.0. The bottle containing the indigo solution was wrapped in aluminum foil to prevent photo-decomposition. The solution was prepared fresh daily.

VOC Aqueous Stock and Calibration Stock Standard Solutions. The aqueous VOC stock solution was prepared gravimetrically using a known mass of chilled phosphate buffer solution (4°C) in a 60 mL serum bottle. Headspace in the serum bottle was minimized by the addition of 5 mm diameter clean glass beads. The bottle was sealed with a Mininert® valve and wrapped in aluminum foil to prevent photo-decomposition. A known mass of VOC was added to the bottle using a 50 µL syringe. The bottle was placed on a wrist-action shaker (Model 75, Burrell, Pittsburgh, PA)

overnight and then stored at 4°C until use. New solutions were prepared for every experiment. The concentration of the VOC stock solution was prepared to ensure that the aqueous solubility limits of the compound were not exceeded. The VOC calibration stock standards and the fluorobenzene (FB) internal standard stock solutions were prepared in a similar manner, except that methanol was used as the solvent. The stock standard solutions were stored at 4°C and held for no longer that 14 days.

Aqueous Ozone Solution. Gaseous ozone was produced by passing dried oxygen (AGA Gas Co., Columbus, OH, high purity) through a corona discharge, water-cooled ozone generator (Polymetrics, Inc., San Jose, CA, Model T-408, rated at 0.33 lb O3/day). After passage through the ozone generator, the oxygen gas contained about 2% ozone (by wt.). The ozone enriched oxygen gas was bubbled into a covered 1 L contact vessel containing fresh phosphate buffer solution at a pH of 2.0 and at room temperature. The voltage setting on the ozone generator and the oxygen pressure was adjusted to obtain the desired aqueous ozone concentration in solution. The aqueous ozone concentration was determined spectrophotometrically using a Diode Array UV-VIS Spectrophotometer (Hewlett-Packard, Palo Alto, CA, Model 8452A). The absorbance of the solution was measured in a 1.0 cm quartz UV cell. An extinction coefficient of 3200 $M^{-1} cm^{-1}$ was used to convert absorbance units to the units of concentration (Hoigné, 1995).

PREPARATION OF OZONE DEMAND-FREE GLASSWARE

All ozone demand-free glassware was prepared by soaking the glassware for 30 minutes in a 2% SP Brand MICRO All-Purpose Liquid Cleaning solution (Baxter Diagnostics, Deerfield, IL) prepared in R.O.-Filtered water. The glassware was rinsed three times in tap water followed by rinsing three times in R.O.-Filtered water. A 2.0 mg/L aqueous ozone solution was prepared and the glassware was allowed to soak in that

solution for 30 minutes. The glassware was removed from the ozonated solution and placed in a 105°C drying oven for 4 hours.

EXPERIMENTAL PROCEDURES

Ozone Losses using Different Mixing Scheme Determination. All mass transfer experiments were conducted at room temperature (22±2 °C). The aqueous ozone solution was pumped from the contact vessel at a flow rate of 5.0 ± 0.05 mL min^{-1} (Fluid Metering Inc., Oyster Bay, NY, Labpump Model QC150). The flow rate was checked during the experiment after every ten samples. The initial concentration of the solution was determined by pumping the solution through a 1.0 cm quartz UV flow-through cell placed in a diode array UV-VIS spectrophotometer (Hewlett-Packard, Palo Alto, CA, Model 8452A). An extinction coefficient of 3200 M^{-1} cm^{-1} was used to determine the aqueous ozone concentration (Hoigné, 1995). Before any experiments were conducted, the aqueous ozone concentration was allowed to reach a constant concentration which indicated that the contact reactor had reach steady state conditions. Phosphate buffer solution was pumped into the contact vessel to maintain a constant volume in the reactor.

For each sample, a known volume of solution was pumped into a clean 20 mL headspace vial (Sun Brokers, Inc., Wilmington, NC) containing a 1.27 cm long by 0.32 cm diameter octagonal micro-stirbar (FischerBrand, Fischer Scientific, Pittsburgh, PA). The loss of ozone was minimized by holding the end of the Teflon® tubing through which the ozone was flowing under the surface of the rising solution. The top of the vial was capped with a Teflon® coated rubber stopper (Sun Brokers, Inc., Wilmington, NC). The solution in the vial was mixed using the appropriate method for a specific length of time before the rubber stopper was partially removed to permit the addition of 1.0 mL of the indigo stock solution with a syringe to quench the remaining ozone in the solution. The vial was stored in the dark and analyzed for ozone concentration within 6 hours.

Reaction Order and Rate Constant Determination. All reaction order and rate

coefficient determination experiments were conducted at room temperature (22±2 °C).

The aqueous, calibration standard, and internal standard stock VOC solutions were kept

in an ice-water bath (4°C) to minimize volatilization. For the aqueous ozone

concentration determination, 10 mL of indigo stock solution was transfered by pipette to

a 12.5 cm high by 1.5 cm diameter, 16 mL clean disposable culture tube (FischerBrand,

Fischer Scientific, Pittsburgh, PA) of known mass. The volume of the indigo stock

solution added to the culture tube was determined from the difference in the mass of the

culture tube before and after addition of the indigo stock solution. For the aqueous VOC

determination, 10 mL of the indigo stock solution was transfered by pipette to clean 20

mL headspace vial (Sun Brokers, Inc., Wilmington, NC). The mass of the vial headspace

containing the indigo stock solution and topped by a aluminum crimp top/Teflon coated

rubber stopper was measured. The vial was placed in a ice-water bath (4°C) for at least

30 minutes prior to the experiment.

A 50 mL glass, airtight syringe (Hamilton Co., Reno, NV, Model 1050)

containing a 1.27 cm long by 0.32 cm diameter octagonal micro stirbar (FischerBrand,

Fischer Scientific, Pittsburgh, PA) was rinsed three times with ozonated buffer solution

from the contact reactor and completely drained after each rinse. The 50 mL glass

syringe was refilled with ozonated phosphate buffer solution (pH of 2.0) to obtain a

known ozone concentration. Pumping was accomplished at a rate slow enough so as to

prevent cavitation or degassing of the solution. Any headspace and/or gas bubbles were

removed from the syringe prior to conducting the experiment. The syringe was placed on

a mini-stirrer (VWR Scientific, Plainfield, NJ, Model 200) and the speed (or rpms) of the

stirrer was adjusted to result in the complete dispersion of a slug of dye within 2 seconds.

A glass micro-syringe was used to add a known volume of chilled aqueous VOC stock

solution to the syringe containing the ozonated phosphate buffer solution. After a

specific length of time, an aliquot of approximately 2 mL of the reaction solution was

delivered from the glass syringe to the culture tube or headspace vial containing the indigo dye stock solution. The time interval between the removal of aliquot from the syringe was selected to provide for the collection of at least 5 data points while ensuring that at least a 70% decrease in the concentration of the VOC was observed. A 15 cm long by 0.3 cm diameter Teflon® tube (total volume 0.75 mL) was used to deliver the aliquot from the glass syringe to the culture tube or headspace vial. The solution in the tube was drained prior to the aliquot being delivered to the tube or vial. The end of the tubing was placed below the liquid surface to minimize losses due to volatilization. While the headspace vial was in a ice-water bath (4°C) after the addition of the aliquot, the rubber stopper from the headspace vial was partially removed for the addition of the internal standard stock solution. The vial was allowed to return to room temperature before the final mass of the vial was measured and the sample analyzed for VOC concentration. Samples were stored in the dark prior to being analyzed for final aqueous ozone concentration within 12 hours.

For each kinetic experiment, a control run was performed for each reactant to ensure that any decrease in concentration with time was the result of the desired reaction and not an artifact of other losses. A VOC control run was performed by filling the 50 mL glass syringe with non-ozonated phosphate buffer solution and adding a known volume of chilled aqueous VOC stock solution. Aliquots were withdrawn at regular intervals for analysis. An ozone control run was performed by filling the syringe with ozonated phosphate buffer solution but without the addition of the aqueous VOC stock solution. Again, aliquots were withdrawn at regular intervals for analysis.

Determination of the Rate of Ozone Auto-Decomposition. A 50 mL glass, airtight syringe (Hamilton Co., Reno, NV, Model 1050) was rinsed and completely drained twice with ozonated phosphate buffer solution from the ozone contact reactor. The syringe was refilled with ozonated phosphate buffer solution at a rate slow enough so as to prevent cavitation or degassing of the solution. A 1.0 cm quartz UV-Vis

spectrophotometric cell was rinsed twice with ozonated phosphate buffer solution from the syringe. For the analysis, the cell was refilled with ozonated phosphate buffer solution from the 50 mL glass syringe ensuring that the end of the tube was kept below the rising liquid surface level in the cell to prevent ozone loss. The cell was completely filled and capped with a Teflon® coated cap. The absorbance of the solution at 258 nm was measured using a diode array UV-VIS spectrophotometer (Hewlett-Packard, Palo Alto, CA, Model 8452A) equipped with a colored glass filter (Oriel Corp., Stratford, CT, Filter # 51650). The filter was used prevent high energy light above 240nm from reaching the solution as the high energy light would initiate the auto-decomposition of ozone. An extinction coefficient of 3200 M^{-1} cm^{-1} (Hoigné, 1995) was used to calculate ozone concentration from the measured absorbance. A first order kinetic model was used to calculate an observed first order auto-decomposition rate for the ozone in the phosphate buffer solution. This experiment was repeated three times at the conclusion of the order or kinetic experiments.

ANALYSIS OF SAMPLES

VOC Concentration Determination. Analysis of the aqueous samples for VOC concentration was performed using gas chromatography with flame ionization detection (See Appendix B for GC analysis specifications). The Perkin Elmer Corporation AutoSystem Gas Chromatograph (Norwalk, CT) was equipped with a DG 624 fused silica glass capillary column (J & W Scientific catalog no. 125-1334). The headspace vials were sampled using a headspace sampler (Perkin Elmer Corporation, Norwalk, CT., Model HS40). Peak integration and data reduction were performed using an on-line software package (PE Nelson, Cupertino, CA, PE Nelson Turbochrom 3.0).

The gas chromatograph was calibrated on a mass basis using the internal standard method of calibration. One blank and eight standards, with a concentration range that bracketed that of the samples, were prepared and analyzed daily. The mass of the internal

standard added to each standards and sample was kept constant. A calibration curve was prepared daily from the results of the analysis of the standards by plotting the ratio of the observed peak areas of the compounds versus the mass ratio of the VOC to the internal standard versus The concentration of the VOC in the aqueous samples from the order and reaction experiment was calculated using the mass of the VOC in the aliquot as determined from the calibration curve divided by the volume of the aliquot delivered to the headspace vial (as measured by the mass of the aliquot). A high and low check standard along with a matrix and reagent blank were prepared and analyzed every 15 reaction samples. All samples and standards were analyzed on the gas chromatograph within 12 hours of being prepared or collected. A typical calibration curve is illustrated in Figure 9.
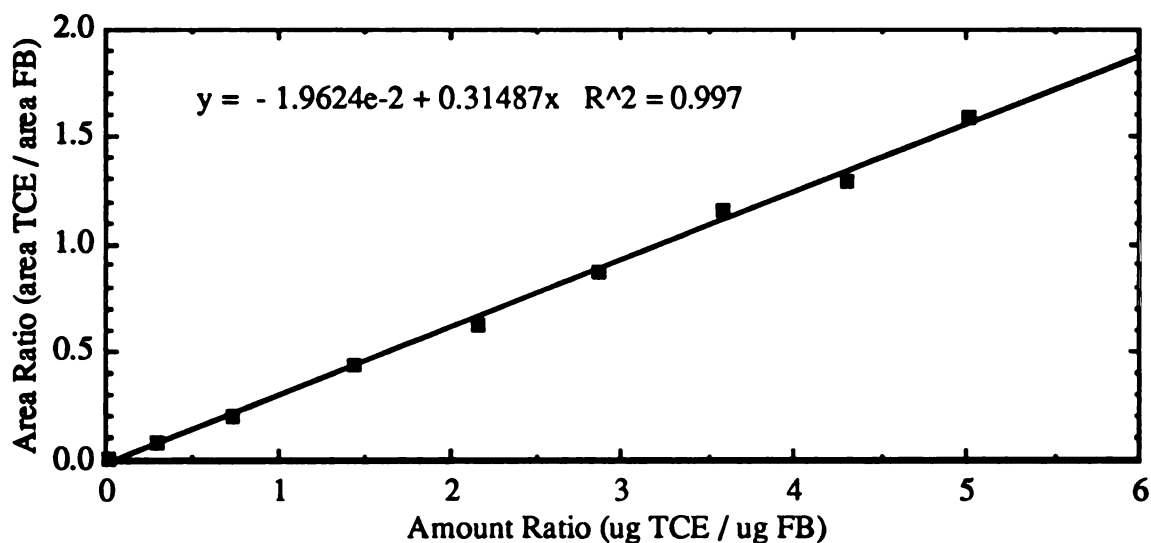
Figure 9. TCE Internal Standard Calibration Curve for 11/15/94
7.0 μg Fluorobenzene Used as Internal Standard.

The calibration samples were prepared by filling a 20 mL headspace vial with 10 mL of the indigo stock concentration and 2 mL of non-ozonated phosphate buffer solution at a pH of 2.0. After the vials were cooled in a ice-water bath (4°C), a known mass of VOC from the VOC calibration stock solution was added to the headspace vial.

A known mass of fluorobenzene (FB) was added to each headspace vial as an internal standard. The exact mass of internal standard was selected so that the peak area of the internal standard was about equal to the peak area of the middle calibration standard.

Aqueous Ozone Concentration Determination. Analysis of the aqueous samples for ozone concentration was performed using a modified procedure developed after Bader and Hoigné (1981, 1982). The aqueous ozone concentration was determined from the difference in the absorbance at 600 nm of an indigo dye solution before and after the addition of an aqueous sample containing ozone to the indigo dye solution. Ozone reacts with indigo dye in an acidic solution with a 1:1 reaction stoichiometry. The product of the indigo-ozone reaction does not absorb at 600 nm. The ozone concentration of the solution added to the indigo dye can be determined from the observed decrease in the absorbance of the solution.

The initial absorbance of the indigo dye solution was calculated based on an indigo dye standard curve. The standard curve was necessary because the it was impossible to ensure that the volume of the aliquot added to the culture tube containing the indigo stock solution was constant for each sample. The initial absorbance of the indigo stock solution varied because of dilution according to the volume of the aliquot added to the indigo stock solution.

Indigo dye standards, which consisted of at least one blank and eight standards with an indigo concentration which spanned the range expected of the samples, were prepared and analyzed daily. The indigo standards were prepared by adding 10 mL of the indigo dye stock solution with a pipette into a 12.5 cm high by 1.5 cm diameter, 16 mL clean disposable culture tube (FischerBrand, Fischer Scientific, Pittsburgh, PA) of known mass. The mass of the indigo stock solution added to the culture tube was determined. Another clean pipette was used to deliver a volume of non-ozonated phosphate buffer solution (pH of 2.0) to the culture tube. The mass of the buffer solution added to the culture tube already containing the indigo dye stock solution was determined. After

being prepared, the culture tubes were stored in the dark and analyzed within 12 hours.
The indigo standard curve was prepared by plotting the indigo concentration after
dilution with phosphate buffer solution versus the measured absorbance of the solution at
600 nm. Three check standards were prepared in a similar manner and analyzed for every
15 reaction samples.

Ozone standards consisting of one blank and at least six standards with an ozone
concentration that spanned the range expected of the samples was prepared and analyzed
daily. The ozone standards were prepared in a manner similar to that of the indigo dye
standards except that the phosphate buffer solution contained aqueous ozone. The
ozonated phosphate buffer solution was withdrawn from the ozone contact reactor using a
50 mL glass syringe at a rate slow enough as to prevent cavitation or degassing of the
solution. The ozone concentration of the phosphate buffer solution was determined after
rinsing the 1.0 cm quartz UV-VIS cell three times with ozonated phosphate buffer
solution and discarding the rinse solution. After refilling the cell and placing it in a diode
array UV-VIS spectrophotometer (Hewlett-Packard, Palo Alto, CA, Model 8452A), the
absorbance of the solution at 258 nm was measured. The ozone concentration was
calculated using Beer's law and an extinction coefficient of 3200 M^{-1} cm^{-1} (Hoigné,
1995). The direct absorbance method was considered to result in a primary standard
solution. The ozonated buffer solution of known concentration was added to the indigo
stock solution in the culture tube by placing the end of the Teflon© tube from the 50 mL
glass syringe below the liquid surface in the tube to minimize any losses of ozone. After
being prepared, the culture tubes were stored in the dark and analyzed within 12 hours.
The ozone standard curve was prepared plotting the ozone concentration of the solution,
considering dilution, in the indigo stock solution versus the change in absorbance of the
indigo dye solution, considering dilution, before and after the addition of the ozone-
containing sample. A typical ozone calibration curve is illustrated in Figure 10. A high
and low check standard were prepared and analyzed for every 15 reaction samples.

All samples for ozone determination (indigo dye standards, ozone standards, or order/rate samples) were analyzed sequentially after the completion of the reaction rate experiment. The solution in the culture tube was mixed using a vortex Touch-Mixer (FischerBrand, Fischer Scientific, Pittsburgh, PA; Model 231) for 15 seconds. A 1.0 cm quartz UV-Vis spectrophometic cell was rinsed twice with solution from the culture tube and discarded. After being refilled, the cell was placed in a diode array UV-VIS spectrophotometer (Hewlett-Packard, Palo Alto, CA, Model 8452A). The absorbance of the solution at 600nm was measured.
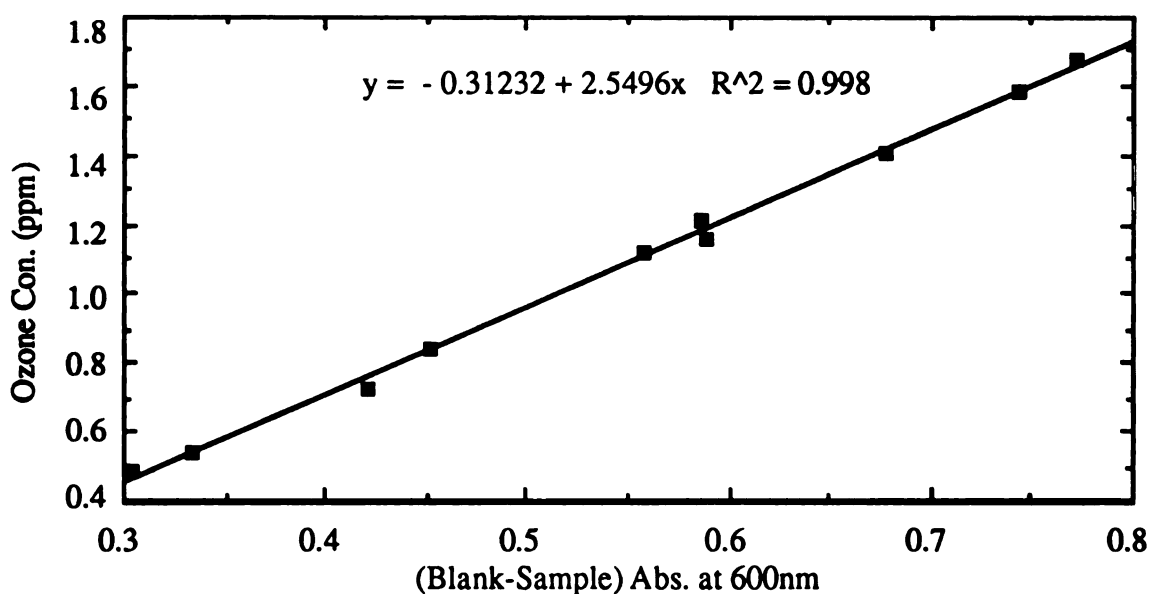
Figure 10. Ozone Calibration Curve using the Indigo Method for 11/15/94

DATA ANALYSIS PROCEDURES

Order Determination. The Van't Hoff Plot analysis method was used to calculate the reaction order with respect to each reactant (Steinfeld, Francisco, and Hase, 1989). Concentration data for one reactant was obtained at specific time intervals using pseudo-first order reaction conditions. A plot of time versus concentration was prepared for each trial and a quadratic least-squares regression analysis was used to obtain the parameters of the quadratic equation which best fit the data. The initial rate of the

reaction (the rate of the reaction at zero time) was determined by taking the derivative of the quadratic equation at zero time. The Van't Hoff plot was constructed by plotting the logarithm of the initial concentration versus the logarithm of the initial rate of the reaction for a series of experimental trials where the initial concentration of the reactant not present in excess was varied. A linear relationship was observed on the Van't Hoff plot and a linear least-squares regression analysis was performed. The calculated slope of the line obtained using the linear least-squares regression was taken as the order of the reaction with respect to the reactant not present in excess. The 95% confidence interval of the calculated order was determined using the student t-test (Anderson, 1987) by calculating the 95% confidence interval for the slope of the line.

Stoichiometry Determination. The ratio of the stoichiometry coefficients (υ_M/υ_{O3}) was determined by plotting the change in the measured VOC concentration during the a time interval as the ordinate versus the change in the measured aqueous ozone concentration over the same time interval as the abscissa. A linear relationship was observed and a least-squares regression analysis was performed to determine the slope and intercept of the line which best fit the data. The calculated slope of the line was taken as the observed ratio of the reactant stoichiometric coefficients. The 95% confidence interval of the calculated order was determined using the student t-test (Anderson, 1987) by calculating the 95% confidence interval for the slope of the line.

Reaction Rate Coefficient Determination. The reaction rate coefficient (k) was determined using two kinetic models (see Chapter 2 for derivation). For each experimental run, the reaction rate coefficient was determined in triplicate; twice using model I and once using model II. In theory, the values from the three reaction rate coefficient determination would be expected to agree to within experimental error.

Model I was a non-linear kinetic model which used concentration data from only one reactant to determine the reaction rate coefficient. A modeling algorithm to determine the best fit of the data to the modeling equation was written by Bandemehr

(1992) using Pro-Matlab© (The Mathworks, Inc., version 3.5) operating on a SPARC IPX (Sun, San Diego, CA) workstation located at the Case Center at Michigan State University. The best fit of the data to the modeling equation was determined by finding the maximum of the coefficient of determination. The 95% confidence interval for the calculated reaction rate coefficient was found using the likelihood ratio method (Ratkowsky, 1983).

Model II was a linear kinetic model which used concentration data from both reactants to determine the reaction rate coefficient. A plot of time versus $\ln\left[\dfrac{[M]}{[O_3]}\right]$ was prepared and a linear relationship was observed. A least-squares linear regression was performed to obtained the slope and intercept of the equation which best fits the data. The value of the slope calculated using the linear least-squares regression was used as a term in Equation 19 to calculate the reaction rate coefficient. The 95% confidence interval for the reaction rate coefficient was calculated based on the 95% confidence interval of the slope of the line using the student t-test (Anderson, 1987) and the propagated experimental error for the initial concentration of each reactant.

CHAPTER 4

RESULTS AND DISCUSSION

This chapter is divided into five sections: in the first four sections I will discuss the data and results associated with each of the objectives of this research. These four sections are: (1) Development of the experimental apparatus; (2) Determination of reaction order; (3) Determination of reaction stoichiometry; and (4) Calculation of the reaction rate coefficient. In the final section, I will discuss a possible cause of the experimental observations. Further details of each experiment, including raw data, can be found in Appendix C.

DEVELOPMENT OF EXPERIMENTAL APPARATUS

In a previous study, Bandemehr (1992) used a 22 mL GC headspace vial as the reaction vessel to investigate the rate of the reaction between ozone and chlorinated ethylenes in the aqueous phase. The reaction rate coefficients calculated in the study were found to be significantly greater than the reaction rate coefficients reported in the literature. Bandemehr suggested that partitioning of the reactants from the aqueous phase to the gas headspace in the closed vial was the major cause for the deviation from literature values. In that study, mixing was provided only at the start of the reaction by "shaking the vial for several seconds". The reactants would have partitioned into the gas headspace during the period of mixing and caused the rate of the reaction to appear to be greater than that observed in a system where partitioning was not occurring. It was concluded that the experimental method used by Bandemehr (1992) did not permit the accurate determination of the reaction rate coefficient for the reaction between two volatile reactants because the method of mixing facilitated the partitioning of the reactants from the aqueous phase to the gas headspace.

40

22 mL Headspace Vial. One of the original objectives of this study was to develop an experimental apparatus to obtain accurate kinetic data for the reaction between two volatile reactants. Selection of the method of mixing was the most important factor when considering an experimental apparatus because a constant mixing intensity was required to permit the modeling of the system as a completely mixed, batch process while at the same time minimizing the partitioning of the reactants. Three mixing schemes (with constant mixing intensity and using the 22 mL GC headspace vial as the reaction vessel) were tested to determine the significance of partitioning with each scheme. In these experiments, the concentration of an aqueous ozone solution was monitored with time using the three mixing schemes. Any decrease in the aqueous ozone concentration by another mechanism other than self-decomposition must have been attributed to partitioning of ozone from the aqueous phase into the gas headspace.

The selection of the reactant to be monitored in the experiments was based on the calculations which demonstrated which compound would be transported across the interface at the fastest rate. Schwarzenbach, Gschwend, and Imboden (1993) derived the following equation from first principles using the stagnant two-film model:

$$F = \left(\frac{1}{\left({}^{z_w}\!/_{D_w} \right) + \left({}^{z_a}\!/_{D_a K_H} \right)} \right) \left(C_w - \frac{C_a}{K_H} \right) \qquad (20)$$

or

$$F = v_{tot} \left(C_w - \frac{C_a}{K_H} \right) \qquad (21)$$

where F = Flux of Molecule Across Interface (mol cm^{-2} s^{-1})
  z_w = Thickness of Stagnant Water Layer (cm)
  z_a = Thickness of Stagnant Air Layer (cm)
  D_w = Molecular Diffusion Coefficient in Water (cm^2 s^{-1})
  D_a = Molecular Diffusion Coefficient in Air (cm^2 s^{-1})
  C_w = Bulk Water Concentration (mol/L)
  C_a = Bulk Air Concentration (mol/L)
  K_H = Henry's Law Constant (C_a/C_w)
  v_{tot} = Total Mass Transfer Velocity (cm s^{-1})

The total mass transfer velocity (v_{tot}) reflects the speed at which a compound can partition across the interface. The molecular diffusion coefficient in water and air along with the Henry's law constant are the physical properties of a compound which controls the rate of partitioning across an air-water interface. Assuming two compounds are present in solution in equal molar concentrations, then the compound with the greater total mass transfer velocity will have the greater mass flux across the interface. The total mass transfer velocity for ozone was calculated to be 0.017 cm s^{-1} compared to 0.007 cm s^{-1} for TCE. Under equal driving forces, ozone will have a greater mass flux across the interface than TCE. Based on these calculations, ozone was selected as the reactant to be monitored during the partitioning experiments. (See Appendix E for further details of the calculations).

Figure 11 shows how the normalized aqueous ozone concentration varied with time when three different schemes were used to provide mixing of the aqueous ozone solution in 22 mL GC headspace vials. The data has been corrected for ozone self-decomposition. The aqueous ozone concentration was observed to decrease with time for each mixing scheme. The greatest rate of ozone loss (as visually determined by the slope of the line in Figure 11) occurred when the shaker plate was used to provide mixing. The shaker plate caused the solution to be violently mixed resulting in the increased turbulence near the gas-liquid interface. The thickness of the stagnant layer was reduced and the result was a greater rate of mass transfer across the interface because the total mass transfer velocity (defined in equation 20 and 21) was increased. The slowest rate of mass transfer was observed when a micro-stirrbar was used to provide mixing because turbulence near the interface did not increase. For the two mixing schemes using a micro-stirrbar, the rate of mass transfer was observed to decrease as the volume of the headspace decreased from 12 mL to 2 mL. Decreasing the headspace volume did not effect the mass transfer coefficient, but rather affected the magnitude of the driving force $\left(C_w - \dfrac{C_a}{K_H} \right)$ for mass transfer. A smaller headspace volume would cause the gas phase

reactant concentration to increase. The concentration difference or driving force of mass transfer was reduced for the mixing scheme with the smaller gas headspace volume. The overall rate of mass transfer was reduced when the gas headspace volume was the minimized.

Mixing Schemes Tested

Symbol	Volume Liquid	Headspace	Mixing	Date
■	10 mL	12 mL	Shaker Plate	07/06/94
●	10 mL	12 mL	Micro-Stirrbar	07/10/94
▲	20 mL	2 mL	Micro-Stirrbar	07/14/94
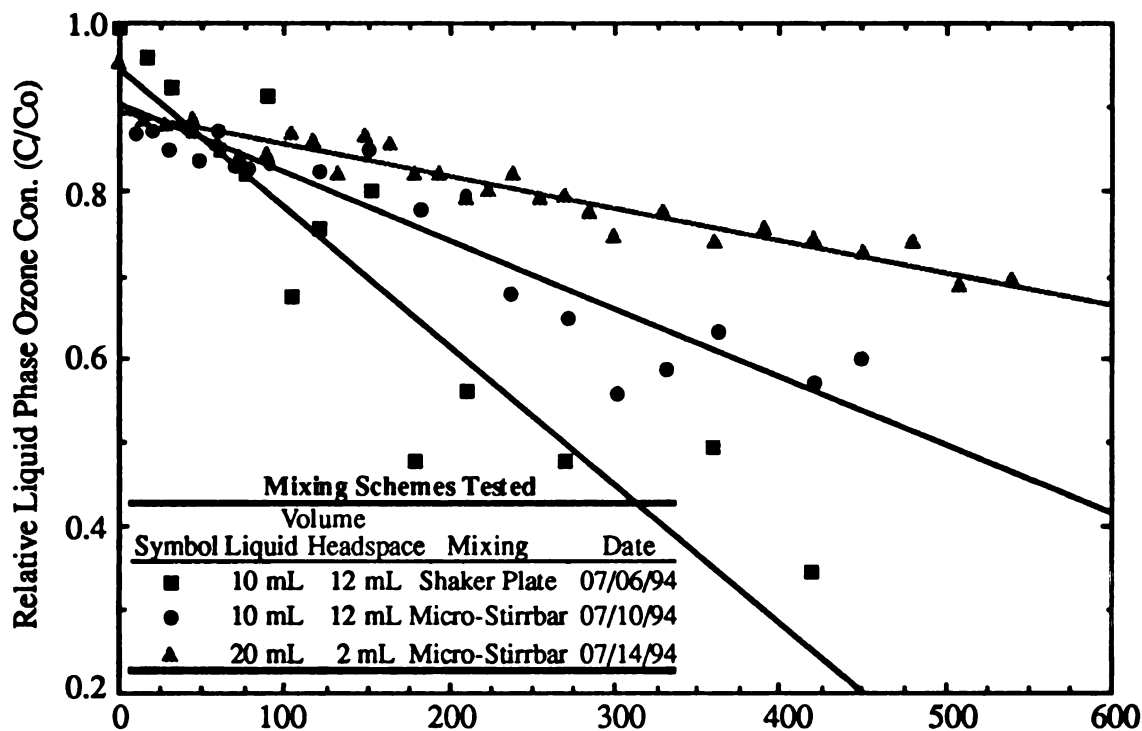
Figure 11. Normalized Liquid Phase Ozone Concentration
using Different Mixing Schemes

Partitioning was observed to be significant with all three mixing schemes because a gas headspace was present in all cases. The determination of the reaction rate coefficient would be greatly complicated if a reaction vessel was used where partitioning was known to be an important process. Under such conditions, the rate of mass transfer for both reactants, in addition to the rate of the reaction between the reactants in the gas phase, would be required to derive the expression to model the changes in the VOC and ozone concentration in the reaction vessel. The 22 mL GC headspace vial was rejected as

being too complex of a system to accurately model the kinetics of the aqueous phase reaction.

50 mL Glass Syringe. A 50 mL airtight, glass syringe was suggested as a possible reaction vessel to overcome the problems of partitioning.[2] All gas headspace in the syringe could be removed by squeezing on the plunger of the syringe. Aliquots of the reaction solution could be removed from the syringe at regular time intervals for analysis. A micro-stirrbar could be added to the syringe to provide sufficient mixing during the reaction to ensure completely mixed reaction conditions and to allow for the system to be modeled as completely mixed, batch process.

Again, an experiment was performed to assess losses of the reactants when using the 50 mL glass syringe as the reaction vessel. It was identified that the new potential causes for losses when using the 50 mL glass syringe included: (1) adsorption of the VOCs on the Teflon® coated plunger; (2) degassing of the ozonated buffer solution after long reaction times; (3) volatilization losses during the transfer of the aliquot to the collection vessel; and (4) increased ozone self-decomposition due to reactions of the ozone with the glass surface. The results of separate experiments where ozone and TCE solutions were mixed with a micro-stirbar using a 50 mL glass syringe as the reaction vessel are shown in Figure 12. The concentration of both reactants, when tested independently, remained constant during a 10 minute testing interval. Some variability due to the sample collection and analysis procedures was observed during the experiment, particularly with the TCE concentration data. Variability decreased in later experiments (see Figures 16 and 17 for control runs) when an analytical balance was used to gravimetrically measure the effluent aliquot samples.
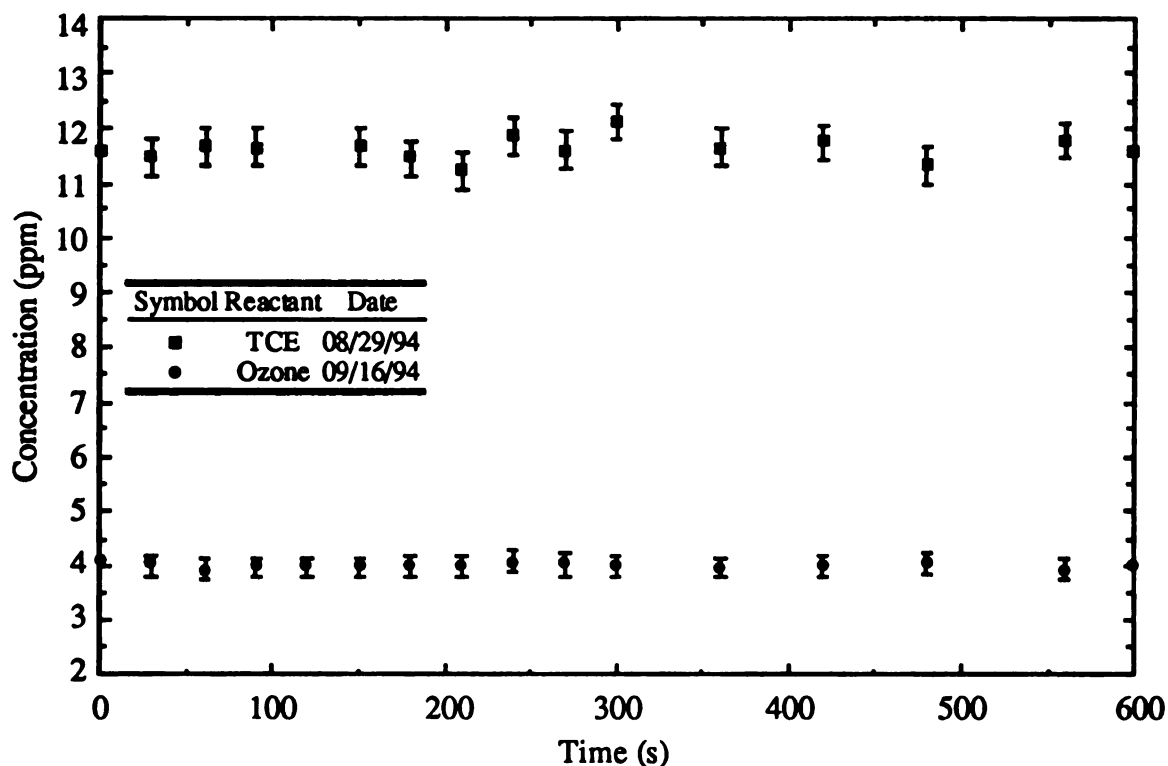
Figure 12. Results of Recovery Experiment using 50 mL Glass Syringe
with Micro-Stirrbar as the Reaction Vessel
(Error Bars Show 95% Confidence Interval of the Data)

DETERMINATION OF REACTION ORDER

An objective of this study was to calculate the order of the reaction with respect to each reactant. Determining the order of the reaction was important to be able to verify that the correct form of the reaction rate law expression was being used as the basis to derive the kinetic modeling expressions. Determining order was also important to be able to disprove a proposed reaction mechanism. A proposed mechanism may be rejected only if the experimentally determined order disagrees with the order of the proposed mechanism. The reaction between ozone and alkenes was expected to be second order overall, or first order with respect to each reactant. The Criegee mechanism served as the theoretical basis for being able to predict the order of the mechanism.

A Van't Hoff plot was used to calculate the observed order of the reaction with respect to each reactant. Each reactant was tested separately by using initial conditions

where the concentration of one reactant was present in 10-fold excess relative to the concentration of the other reactant. For each trial, a series of three or four runs were performed by varying the initial molar ratio of the reactant being tested. A linear relationship was obtained, for each trial, when the logarithm of the initial rate of the reaction at zero time was plotted versus the logarithm of the initial concentration of the reactant being tested . Figure 13 shows a typical Van't Hoff plot for the determination of the order of the reaction with respect to TCE. The line shown on the figure represents the line calculated by the least-squares linear regression of the data and the error bars represents the 95% confidence interval in the slope of the line. A corresponding series of experiments was conducted to determine the order of the reaction with respect to ozone.
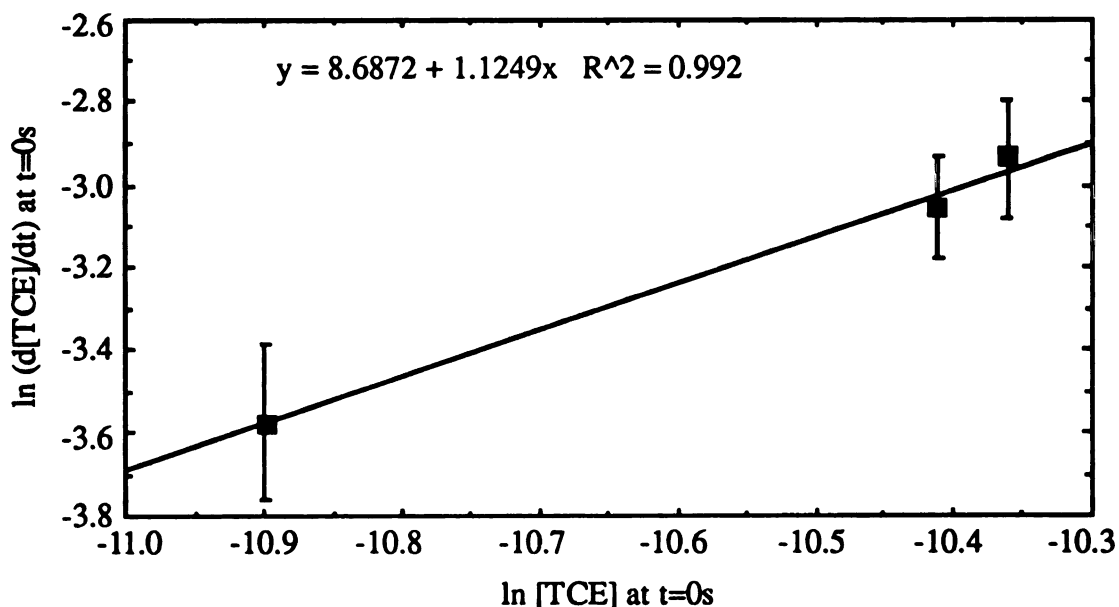
Figure 13. Typical Van't Hoff Plot. TCE Order Determination. 10/21/94
(Error Bars Show 95% Confidence Interval of the Line)

A summary of the calculated order with respect to each reactant can be found in Figure 14. The observed order with respect to each reactant was slightly greater (0.05 to 0.32) greater than one. The order of a non-radical mechanism, such as the Criegee mechanism, would be expected to be either an integer or half-integer (Atkines, 1990).

There has never been experimental evidence suggesting that the reaction between ozone
and simple alkenes in the aqueous phase occurs through a radical mechanism (Bailey,
1972, 1978). As a result, it was believed that the deviation of the calculated values from
integer values was a consequence of using only three or four data points in the linear
regression. The 95% confidence interval was unusually large relative to the observed
variation between trials. This observation was also caused by having only three or four
data points comprise the linear regression. The inclusion of additional data points would
have reduced the range of the 95% confidence interval and caused the calculated orders to
be closer to integer values.
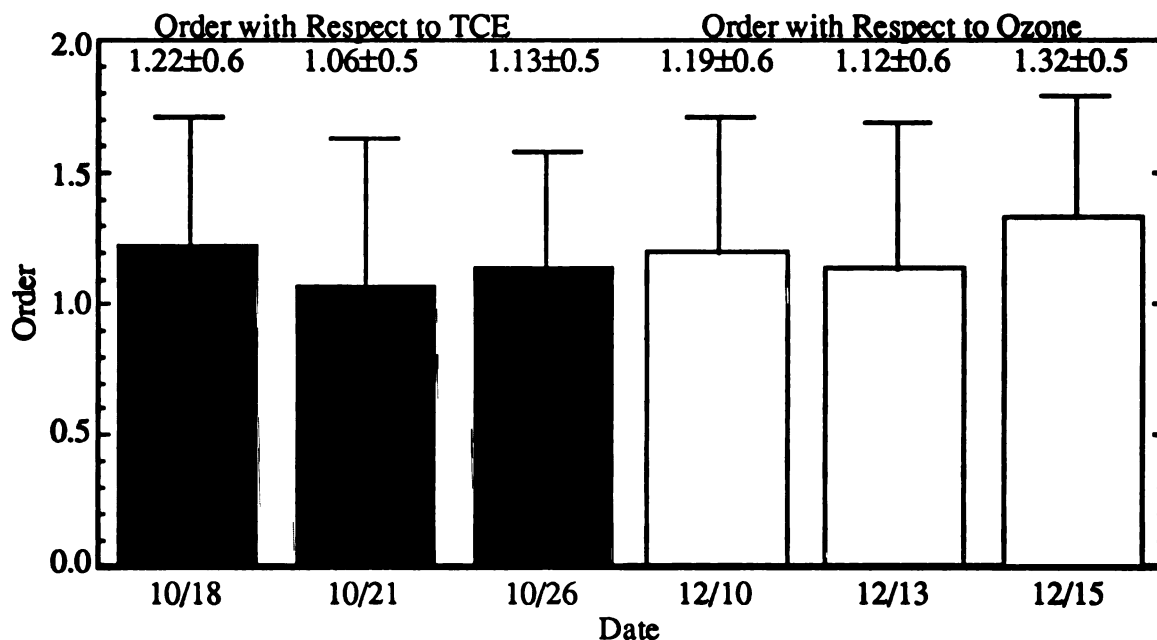
Figure 14. Summary of Order Results
Actual Value ± 95% Confidence Interval Shown
(Error Bars Show 95% Confidence Interval)

The results of the order determination indicated that the reaction is second order
overall, or first order with respect to each reactant. The calculated order agrees with the
order predicted by the Criegee mechanism. These results indicated that the Criegee
mechanism cannot be rejected as being a possible mechanistic pathway that describes the

overall reaction. Agreement of the calculated order with the predicted order is not sufficient experimental evidence to suggest that the reaction occurs only by the pathway described by the Criegee mechanism. For example, the reaction could have proceeded by another second order overall mechanistic pathway other than the Criegee mechanism and produced the same results. The practical mechanistic information revealed by the results of the order determination experiment were that the rate determining step of the mechanism has 1:1 (ozone to VOC) stoichiometry and this happens to be the same as the Criegee mechanism. The order results also confirmed that Equation 9 was the correct form of the reaction rate law expression to be used in the derivation of the kinetic modeling expressions. Equations 14 and 18 were supported by the experimental results.

DETERMINATION OF REACTION STOICHIOMETRY

Measuring the Ratio of Stoichiometry Coefficients. An original objective of this study was to determine the overall stoichiometry of the reaction between ozone and chlorinated olefinic compounds. The stoichiometry coefficient of each reactant cannot be measured directly, but the ratio of the stoichiometry coefficients ($\upsilon M/\upsilon O_3$) was experimentally measured by plotting the change in the aqueous ozone concentration during a time interval versus the change in the measured VOC concentration during the same time interval. Figure 15 shows a typical plot used to determine the stoichiometry of the overall reaction. A linear relationship was observed, with the slope of the line being the ratio of the stoichiometry coefficients. Pictured on the figure is the line showing the least-squares linear regression of the data, in addition to the 95% confidence interval of the line. The ratio of stoichiometry coefficients for the reaction between ozone and the other compounds was calculated.

$$y = -7.1052e-8 + 2.7105x \quad R^2 = 0.904$$
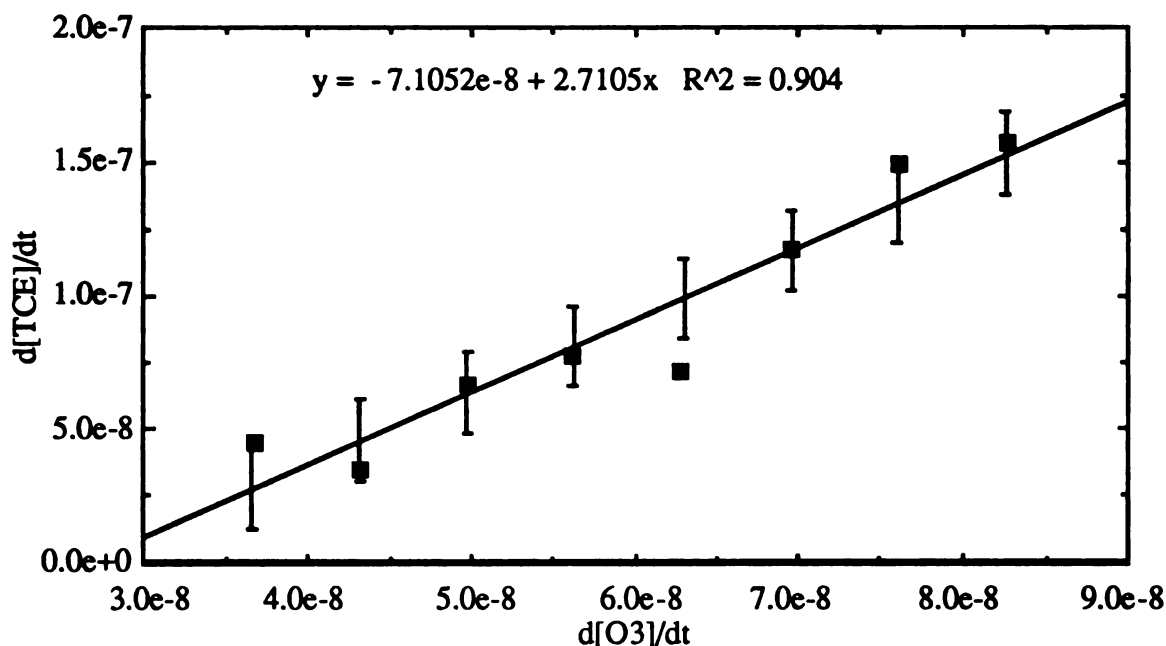
Figure 15. Typical Plot to Determine Ratio of Stoichiometry Coefficients. 11/15/94 (Error Bars Show 95% Confidence Interval for the Line)

The ratio of stoichiometry coefficients can be interpreted in one of two different ways. The ratio can be used to express the coefficients in terms of either one mole of VOC or one mole of ozone. For example, if the calculated ratio was 3, than the two interpretations are that one mole of VOC reacts with 0.33 moles of ozone OR 3 moles of VOC reacts with one mole of ozone. The latter is a more logical interpretation in terms of Criegee mechanism where it is postulated that the reaction stoichiometry is one mole of VOC reacts with one mole of ozone.

A summary of the experimentally determined ratio of the stoichiometry coefficients for the reaction between ozone and three chlorinated compounds can be seen in Table 5. The reaction was conducted using 2:1 (ozone:VOC) initial molar ratio of the reactant concentration. For each compound, two trials each consisting of two experimental runs was performed. The ratio observed for the compounds was significantly greater than what would be expected based on the Criegee mechanism. The results indicated that about three moles of TCE reacted per mole of ozone. This value is

significantly greater than observed for the chlorinated propenes. These results were reproducible and any variation of the calculated ratios between runs was within experimental error.

Table 5. Summary of Calculated Stoichiometry Ratios

| Date | Ratio of Stoichiometry Coefficients ($\upsilon M/\upsilon O_3$) | |
	Run I	Run II
	TCE	
11/11/94	3.1±0.2	2.9±0.2
11/15/94	2.7±0.2	2.4±0.2
	1,1,3-TCP	
02/14/95	1.9±0.3	1.3±0.2
02/20/95	1.9±1.9	2.0±1.0
	1,1-DCP	
03/08/95	1.4±0.2	1.5±0.1
03/13/95	1.2±0.1	1.1±0.2

Actual Value ± 95% Confidence Interval

CALCULATION OF THE REACTION RATE COEFFICIENT

The final objective of this study was to calculate the reaction rate coefficient for the reaction between ozone and chlorinated olefinic compounds using second order reaction conditions. The reaction rate coefficient was calculated using three different methods because the reaction was being monitored by measuring the concentration of both reactants. A nonlinear kinetic modeling expression (Equation 14) was used with the concentration data of one reactant to determine the reaction rate coefficient by finding the value of the coefficient which produced the best fit of the model to the concentration data. This model, called Model I, was used to model the concentration of each reactant independently. Model II was a linear model requiring concentration data from both reactants. A least-squared linear regression was used to determine the slope of the line and the reaction rate coefficient was calculated based on the slope of the line.

Fit of Concentration Data to Kinetic Models. Figure 16, 17, and 18 shows graphically a typical fit of the measured concentration data from one run to the two

kinetic modeling expressions. The control runs shown in Figure 16 and 17 were used to verify that any decrease in the concentration of the reactants was due to the reaction and not due to other sources of losses.
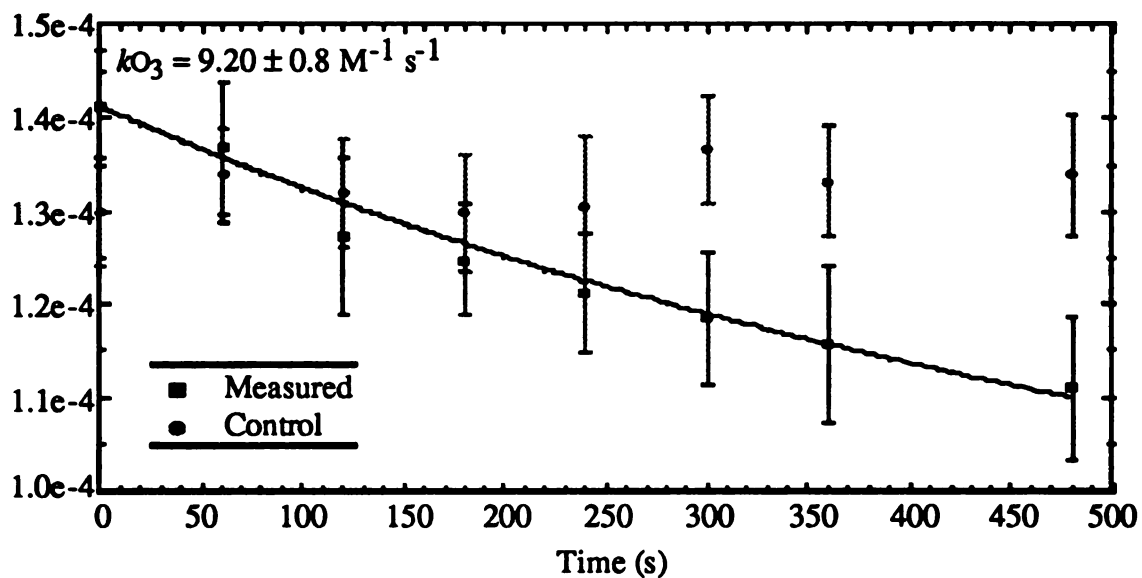
Figure 16. Typical Fit of Ozone Concentration Data to Model I
11/15/94. Run I
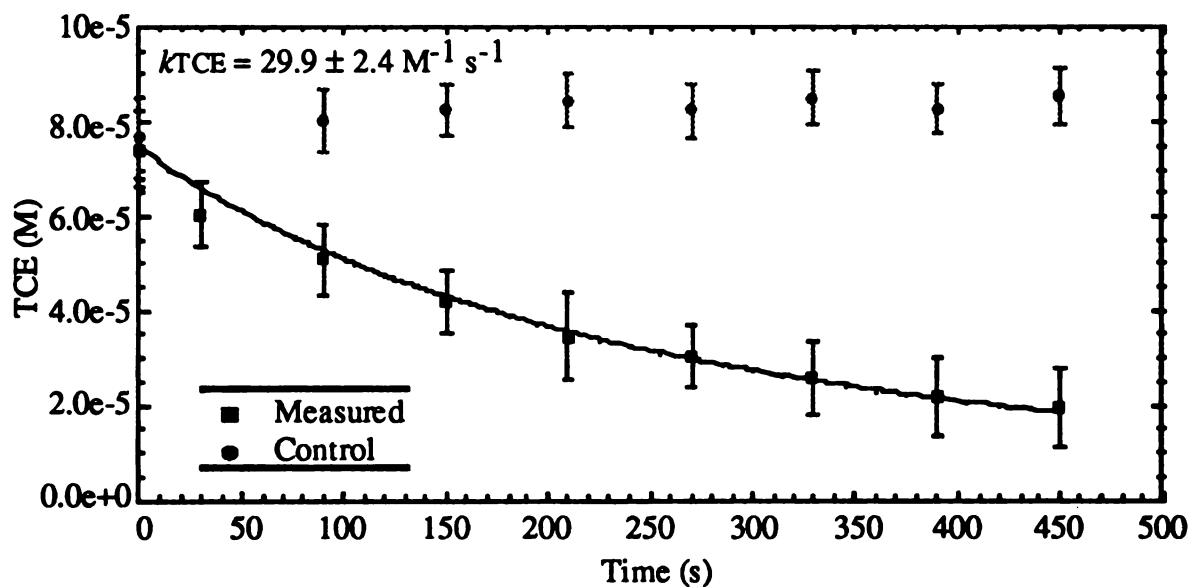
Figure 17. Typical Fit of TCE Concentration Data to Model I
11/15/94. Run I
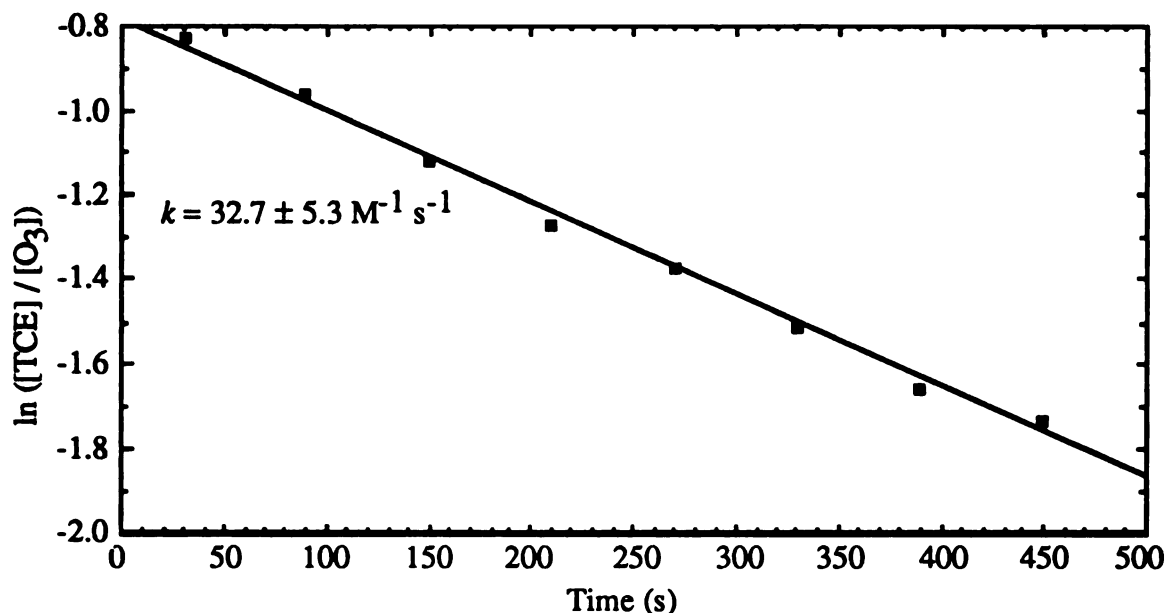
Figure 18. Typical Fit of Ozone and TCE Concentration Data to Model II
11/15/94. Run I

The control run ensured that no losses from volatilization was occurring. Figure 17

shows that the reaction was monitored for a sufficient period of time to be able to observe

a 77% decrease in the measured TCE concentration. Monitoring the reaction for a

significant extent of the reaction was important to ensure an accurate determination of the

reaction rate coefficient.

The best fit of the concentration data to the modeling expression can be observed

on Figures 16 and 17 as the solid black line. The measure used to describe the goodness

of fit to the non-linear expression was the coefficient of determination (CD). The value,

expressed as a percent, is the proportion of the variation that is explained by the model

(Devore, 1991). For example, the CD for model I using ozone data was 0.979, indicating

97.9% of the variation can be explained by the model. The black line on Figure 18 is the

line representing the linear least-squares regression analysis of the data. The measure

used to describe the goodness of fit to the linear model was the correlation coefficient

(r^2). An r^2 of 0.997 was calculated for the fit of the data to the modeling expression

shown on Figure 18.

The values for the second order reaction rate coefficient calculated using the two models are shown on the figures. The error term is the 95% confidence interval for the value. It was observed that the reaction rate coefficients calculated using the three models did not agree as expected. The value of the reaction rate coefficient calculated using model I using the VOC data and model II were about three times greater than the value calculated by model I using ozone data. The cause of this observation will be discussed later.

Effect of Stoichiometry on the Kinetic Model: Substitution in Rate Law Expression. It was observed during the analysis of the data that the value of the stoichiometry coefficient greatly affected the fit of the concentration data to the non-linear model but had no affect on the linear model. The stoichiometry coefficient term was incorporated into the non-linear model in two places. First, the stoichiometry coefficient of the reactant not being used to fit the model was introduced into the modeling expression through Equation 12. In this step of the derivation, a substitution was made into the second order rate law expression to insert the expression terms of the concentration of one reactant. Figure 19 shows the effect of including the measured TCE stoichiometry coefficient into Model I on the fit of the model. The modeling expression fit the data better when the stoichiometry coefficient for TCE was 1.0 compared to when the measured coefficient of 2.7 included in the model. Significant deviation of the model from the measured experimental data occurred towards the end of the run only when the measured stoichiometry coefficients were used in the model.
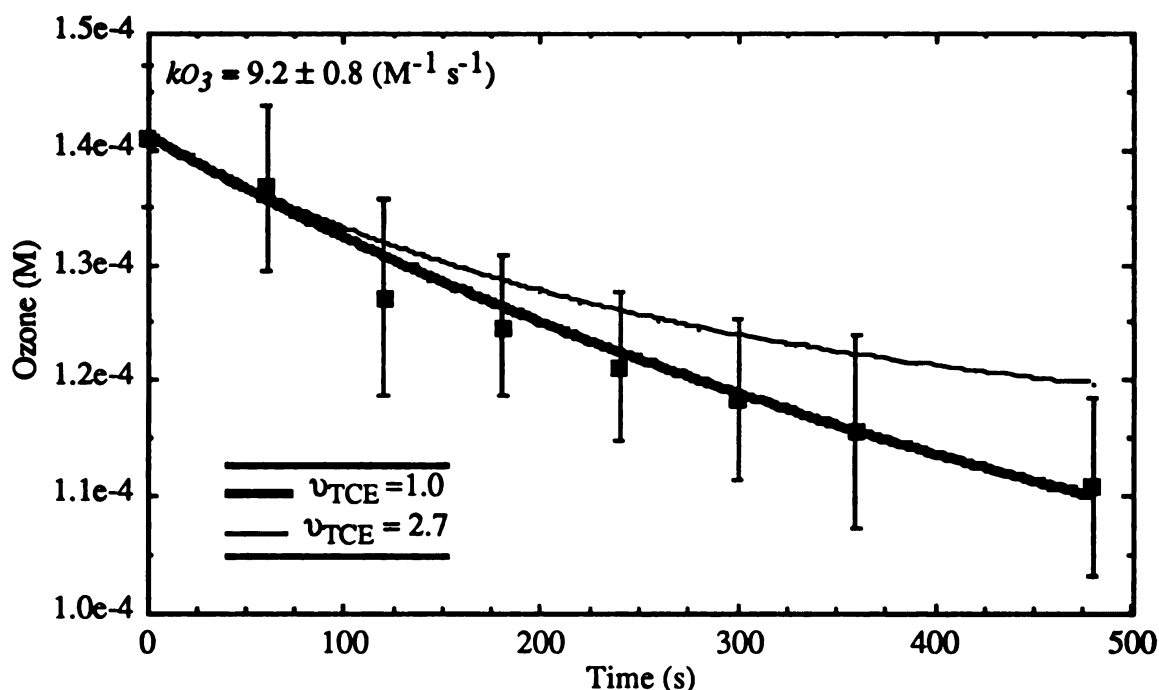
Figure 19. Typical Fit of Ozone Concentration Data to Model I
When Varying the Value of the Stoichiometry Coefficient in the Model
11/15/94. Run I

Effect of Stoichiometry on the Kinetic Model: Value of Reaction Rate

Coefficient. The stoichiometry coefficients were observed to affect the value of the

reaction rate coefficient that was determined using two kinetic models. The

stoichiometry coefficients were incorporated into the non-linear kinetic modeling

expression through an additional term. Equation 14 included the term ($kO_3/\upsilon O_3$), where

the reaction rate coefficient was divided by the stoichiometry coefficient of the reactant

being used to fit the modeling expression. This term was included in the modeling

expression (Equation 14) because the second order reaction rate law expression (Equation

6) defined the rate of the reaction in terms of one mole of reaction. The stoichiometry

coefficients were also incorporated into model II through Equation 19, where the reaction

rate coefficient was calculated from the slope of the line. The measured stoichiometry

coefficients were observed to affect the value of the reaction rate coefficients through

these two terms. Table 6 shows the observed effects on the calculated reaction rate

coefficients when the measured stoichiometry coefficients were used in the modeling

expressions in the terms previously discussed. The values of the coefficients for model I

(using VOC data) and model II were observed to agree to within experimental error of the

values obtained using model I (using ozone data) when the measured stoichiometry

coefficient was included in the model. A potential cause for this observation will be

discussed later.

Table 6. Effect of Stoichiometry Coefficient of the Value
of the Calculated Reaction Rate Coefficient

Date	Stoichiometry Coefficients	Second Order Reaction Rate Coefficient, k (M^{-1} s^{-1})		
		Model I (Ozone)	Model I (VOC)	Model II
11/11/94 Run I	$v_{O_3}=1$, $v_{TCE}=1$	9.64±1.7	27.0±2.1	31.7±5.9
	$v_{O_3}=1$, $v_{TCE}=3.1$	9.64±1.7	8.74±0.6	5.57±0.9
11/11/94 Run II	$v_{O_3}=1$, $v_{TCE}=1$	10.9±1.2	29.3±1.7	35.1±4.4
	$v_{O_3}=1$, $v_{TCE}=2.9$	10.9±1.2	10.2±0.5	7.07±0.7
11/15/94 Run I	$v_{O_3}=1$, $v_{TCE}=1$	9.20±0.8	29.8±2.4	32.7±5.3
	$v_{O_3}=1$, $v_{TCE}=2.7$	9.20±0.8	11.0±0.3	7.1±1.1
11/15/94 Run II	$v_{O_3}=1$, $v_{TCE}=1$	11.2±1.5	29.3±0.7	31.8±4.1
	$v_{O_3}=1$, $v_{TCE}=2.4$	11.2±1.5	12.3±0.6	8.7±1.1

Final Reaction Rate Coefficient Calculations. Based upon the previously

observed effects of the stoichiometry coefficients on the kinetic models, the reaction rate

coefficients have been corrected for stoichiometry. Table 7 shows the corrected second

order reaction rate coefficients obtained using the two kinetic models for three

chlorinated alkene compounds. The values reported in Table 7 have been corrected for

stoichiometry by not including stoichiometry in the fit of the non-linear model, but

including stoichiometry in the calculation of the reaction rate coefficient value.

Table 7. Overall Summary of Calculated Reaction Rate Coefficients[1]

Date	vVOC/vO$_3$	Second Order Reaction Rate Coefficient (M^{-1} s^{-1})		
		Ozone Data Model I	VOC Data Model I	O$_3$ and VOC Model II
		TCE		
11/11/94. Run I	3.1±0.2	9.5±1.5	8.7±0.7	5.6±1.0
11/11/94. Run II	2.9±0.2	11.1±1.6	10.4±0.4	7.1±0.9
11/15/94. Run I	2.7±0.2	9.2±0.8	11.0±0.9	7.1±1.1
11/15/94. Run II	2.4±0.2	11.2±1.2	12.3±0.7	8.7±1.1
		1,1,3-TCP		
02/14/95. Run I	1.9±0.3	70.8±17.4	58.6±16.0	49.2±10.0
02/14/95. Run II	1.3±0.2	53.2±6.8	106±25	58.0±13.0
02/20/95. Run I	1.9±0.2	53.5±8.1	88.4±18.0	47.9±37.0
02/20/95. Run II	2.0±1.0	59.0±10.0	97.5±30.0	48.1±42.0
		1,1-DCP		
03/08/95. Run I	1.4±0.2	3260±400	1757±521	1600±1300
03/08/95. Run II	1.5±0.2	1420±230	1980±1300	1790±1500
03/13/95. Run I	1.2±0.1	1330±850	2223±370	1677±1000
03/13/95. Run II	1.1±0.2	5380±2780	2589±390	1766±1240

(1) at 22.0±2.0°C

The trends that have been observed in previous research have also been observed in this study. The rate of the reaction, as reflected by the reaction rate coefficient, was observed to decrease as chlorine was added and an alkyl group was removed at the site of the double bond (comparing 1,1-DCP with TCE). The reaction rate coefficient was observed to decrease when chlorine was added to the molecule but not to the site of the double bond (comparing 1,1-DCP with 1,1,3-TCP). The effect of shifting the chlorine substitution away from the site of the double bond was observed to increase the rate of the reaction (comparing TCE to 1,1,3-TCP). These trends support the conclusion that chlorine acts as an electron-withdrawing substitute causing the electron density at the site of the double bond to decrease. Less electron density cause the initial attack of ozone at the site of the double bond to be slowed thus causing the observed rate of the reaction to decrease.

The experimentally determined reaction rate coefficients showed significantly greater accuracy to the literature values in this study than compared to the previous study on this series of compounds by Bandemehr (1992). In some cases, the rate constants

determined by Bandemehr (1992) deviated from literature values by as much as an order of magnitude. In comparison to this study, the calculated reaction rate coefficient values for TCE were just slightly less that the literature value of 17 M^{-1} s^{-1} reported by Hoigné and Bader (1983). The difference in the accuracy of the values between the two studies may have been the result of using a reaction vessel which prevented the loss of the reactants due to partitioning. The slight deviation between literature and calculated values in this study can be explained by understanding some important deficiencies of the experimental procedure used by Hoigné and Bader which may have contributed towards causing the reported values to be biased upwards. A second order reaction rate coefficient was calculated from the observed second half-life of the reaction using pseudo-first order reaction conditions. Under these reaction conditions, any volatilization of the VOCs (present in 10-fold molar ratio excess) may have caused the value of the reported rate coefficient to be greater that the actual value. Photolysis of ozone caused by the adsorption of high energy UV radiation due to the spectrophotometric method of monitoring the ozone concentration introduced an additional mechanism to cause the decrease in ozone concentration.

The only other reported literature values for the ozonation of these compounds is a value of 960 ± 100 M^{-1} s^{-1} for 1,1-DCP reported by Masten and Hoigné (1992). Depending on the trial and model, significant deviation from the reported literature values was observed. This deviation can be explained from an understanding of the sensitivity of the nonlinear model to the initial concentration of the reactants.

The results shown in Table 7 showed a greater precision of the calculated reaction rate coefficients between the trials for TCE and 1,1,3-TCP. The ability to reproduce experimental results is a general indication that the experimental procedures have been developed sufficiently to minimize both random and bias error. General agreement was also observed between the values of the models for TCE and to a lesser extent for 1,1,3-TCP. Theoretically, the reaction rate coefficient from the three determinations using the

two models should agree to within experimental error. The degree of agreement decreased as the rate of the reaction was observed to increase. TCE showed the best agreement between the models but 1,1-DCP showed the poorest agreement between the models. The problem with the agreement of the models was believed related to the importance of the initial concentration of the reactants for each model.

A sensitivity analysis was performed on Model I using the ozone concentration data from Run I on 03/08/95. Assuming an uncertainty of the measured absorbance of ± 0.001 and uncertainty of ± 100 M^{-1} cm^{-1} for the molar absorbance coefficient for ozone, the initial ozone concentration has an associated uncertainty of ± 0.006 μM or about 3.6%. This level of uncertainty was quite reasonable considering the accuracy and precision of spectrophotometric methods in general. Figure 20 shows the effect of this level of uncertainty of the initial concentration of ozone on the reaction rate coefficient determined using Model I. The calculated reaction rate coefficient was observed to vary by as much as 50% in either direction. The value of the reaction rate coefficient calculated using Model I with VOC concentration was also observed to vary by about 5% in either direction due to the uncertainty of the initial ozone concentration. The initial concentration of the reactant not being used to fit the model was incorporated into the model through Equation 13. A 5% level of uncertainty in the initial VOC concentration is rather insignificant compared to the uncertainty in the model due to the initial concentration of the reactant being modeled (ozone). A similar sensitivity analysis can be performed for Model I using VOC concentration data, but the level of uncertainty will be much greater because of the VOC analysis by GC has a level of uncertainty of about 10%. For this reason, the kinetic modeling expressions were observed to be very sensitive to the initial concentration of the reactants. This problem had a greater effect on the calculated reaction rate coefficients as the rate of the reaction was observed to increase. The sensitivity of the nonlinear model to the initial concentration was the cause

for the deviation observed between the models for 1,1-DCP and to a lesser extent for 1,1,3-TCP.
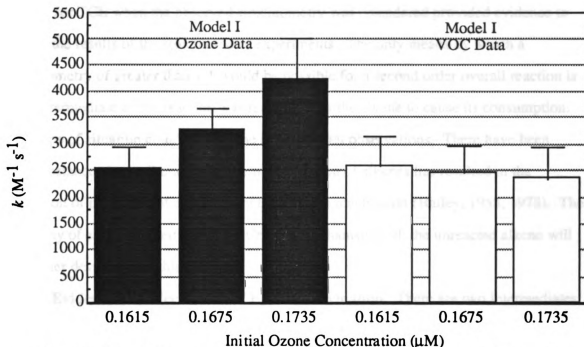
Figure 20. Sensitivity Analysis of Initial Ozone Concentration on the Calculated Reaction Rate Coefficient
03/08/95. Run I

EVIDENCE OF AN INDIRECT REACTION

Evidence of Other Reactions . The reaction order and stoichiometry results strongly suggest that another reaction after the rate determining step was occurring to cause the consumption of the VOC. The effects of the reaction stoichiometry on the kinetic modeling expressions provided further evidence to support this conclusion. The calculated order indicated that the rate determining step of the overall mechanism was occurring with a 1:1 (VOC:ozone) stoichiometry. The improved fit of the nonlinear model when the stoichiometry coefficient was set to one provided further evidence that the stoichiometry of the rate determining step was 1:1. The kinetic modeling expression was derived to describe the rate determining step of the overall mechanism. The presence

of an additional reaction causing the consumption of the VOC became evident when the overall reaction stoichiometry was calculated to be greater than 1:1 for the three compounds tested in this study. The agreement of the reaction rate coefficients from the models for TCE when the observed stoichiometry was considered provided evidence to further the results of the stoichiometry experiments. The only means by which a stoichiometry of greater than 1:1 would be possible for a second order overall reaction is if an intermediate of the reaction was reacting with the alkene to cause its consumption. This type of situation could explain the experimental observations. There have been many instances in the literature where the ozonation of alkenes has resulted in the formation of products not predicted by the Criegee mechanism (Bailey, 1958, 1978). The reactivity of each intermediate of the Criegee mechanism with the unreacted alkene will be further developed in this chapter.

Evidence and Mechanism of Epoxide Formation. There are two intermediates of the Criegee mechanism (primary ozonide and carbonyl oxide) along with ozone itself that have been suggested in the literature as being possibly responsible for the formation of non-Criegee mechanism products during the ozonation of alkenes. One of the most commonly observed products not predicted by the Criegee mechanism are epoxides (e.g., see Bailey, 1958, 1978). These compounds are formed from the transfer of one oxygen atom from the reactive species to the alkene at the site of the carbon-carbon double bond. The epoxide products are known in the literature as "partial cleavage" products because the alkene reacts with the oxygen atom to cause only the π−bond of the carbon-carbon double bond to be broken. Normally complete cleavage of the double bond (breakage of both the sigma and the pi bonds) is predicted by the Criegee mechanism. The cause of the epoxidization of alkenes became apparent by examining the structures of the parent alkene compounds when epoxide products were produced.

In almost all cases, "partial cleavage" products formation was reported for compounds with bulky substituent groups on one or both sides of the double bond. Table

8 shows the observed percent yield of epoxide products upon the ozonation of highly

hindered alkene compounds.

Table 8. Percent Yield of Epoxide Products upon
Ozonation of Hindered Alkene Compounds

Compound	% Yield of Epoxide Products
R₁=R₂=neopentyl	35
R₁=R₂=phenyl	15
R₁=R₂=t-butyl	15
R₁=t-butyl and R₂=isoproply	10

(from Bailey and Lane, 1967)

The results in Table 8 show that substitution at the β–position of the alkyl groups had a

much greater effect on the yield of epoxide products than substitution at the α–position.

The alkyl substituent groups to the double bond had the effect of increasing the electron

density at the site of the double bond making the bond more electron rich. To explain the

production of epoxides, Bailey and Lane (1967) proposed a mechanism involving the

formation of a π–complex between ozone and the double bond. The complex would

form prior to reacting further via a 1,3-dipolar cycloaddition mechanism to form the

primary ozonide or react by releasing molecular oxygen to form an epoxide species. The

degree of the bulk of the substituent groups dictated which pathway by which the reaction

would occur. Highly hindered alkenes would react via the epoxide formation pathway

while less hindered species would react via the Criegee mechanistic pathway. The two

competing reaction schemes can be seen in Figure 21. In addition to product

identification as a means of suggesting these pathways, there has been UV and IR

spectrophotometric identification of the π–complex between ozone and the π–electron

system of some double bond containing compounds (Bailey et al., 1974; Hull, Hisatsune,

and Heicklen, 1972).
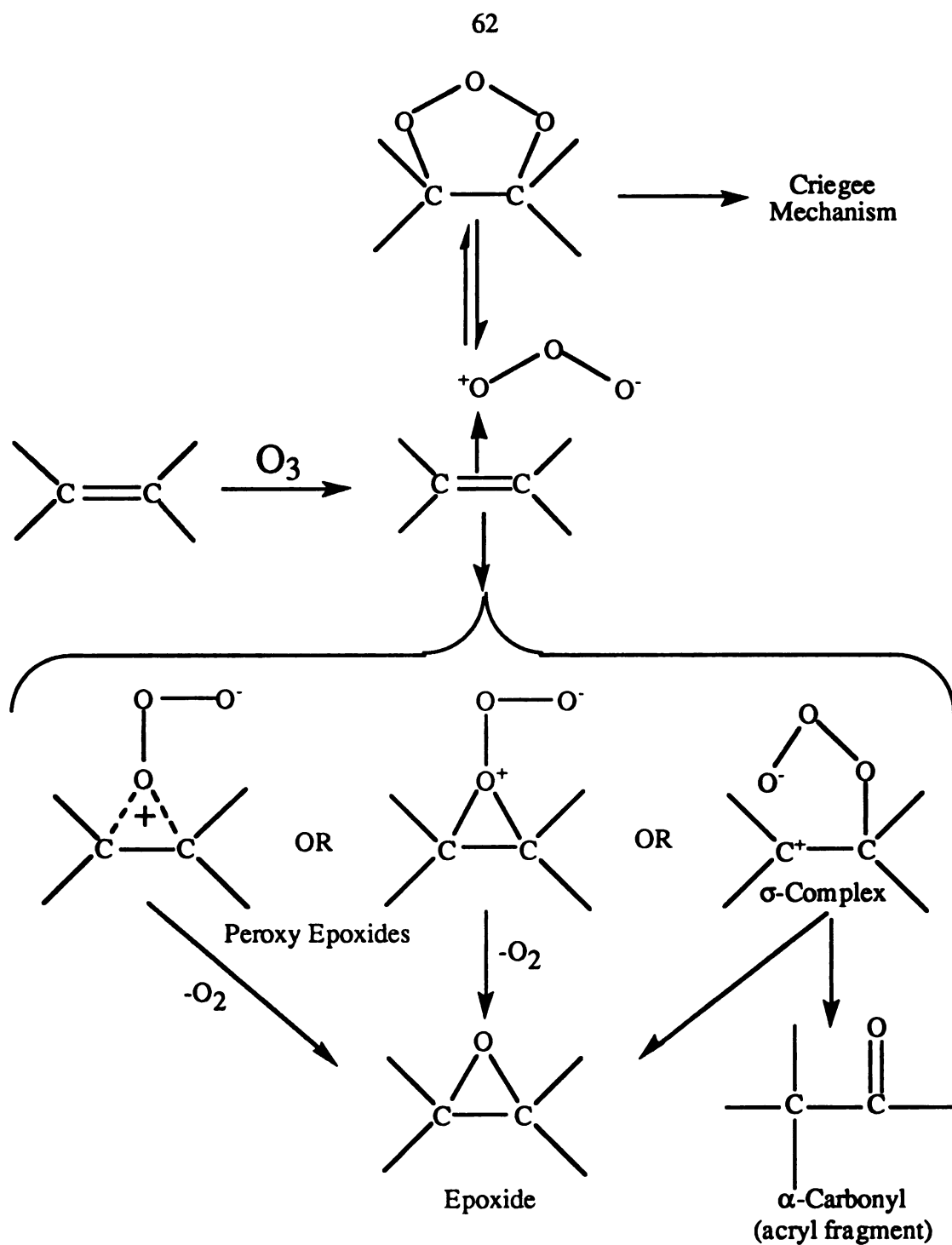
Figure 21. Mechanism of Complete and Partial Cleavage of Alkenes

The formation of a π–complex between ozone and alkenes with the subsequent loss of molecular oxygen is a logical explanation of the formation of epoxides upon the ozonation of highly hindered alkene compounds.

Epoxide formation through the reaction of the π-complex by the release of molecular oxygen is a reaction scheme that is inconsistent with the experimental results obtained in this study. As, the stoichiometry of the mechanism as shown remains 1:1, this is inconsistent with the measured stoichiometry being greater than 1:1 for the three compounds in this study. Secondly, chlorine is not as bulky as the alkyl and phenyl groups listed in Table 8. Steric hindrance due the size of the chlorine group would not be expected to be a factor to prevent the expected 1,3-dipolar cycloaddition mechanism as suggested by the Criegee mechanism. Finally, the π-complex formation has been observed when the substituent groups to the double bond have been electron-donating groups such as alkyl groups. The chlorine group has the exact opposite effect causing the electron density at the site of the double bond to decrease. For these reasons, the epoxide formation mechanism via a reaction between ozone and the alkene cannot be the postulated indirect reaction responsible for the experimental observations and results.

In addition to ozone, the primary ozonide may be considered as a potential epoxide forming agent towards alkenes. The primary ozonide species is the five member ringed structure produced upon the 1,3-dipolar cycloaddition of ozone to the double bond. Figure 22 shows a possible orientation by which the apex oxygen atom on the primary ozonide could interact with the π–electrons of the double bond to cause the formation of an epoxide at the site of the double bond. The transfer of an oxygen atom from the primary ozonide to the alkene through the formation of an epoxide could occur through a HOMO-HOMO interaction between the species (Boch and Wolber, 1984). However, theoretical calculations by Boch and Wolber (1984) indicate that the activation energy of this reaction (~35 kcal/mol) is much to great to be favored when compared to
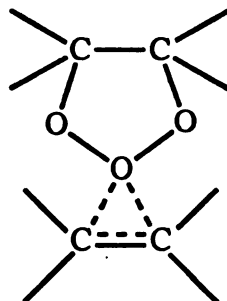
Figure 22. Attack of Primary Ozonide To Form an Epoxide with the Alkene
(from Cremer and Bock, 1986)

the cleavage of the primary ozonide to release an aldehyde and carbonyl oxide (see Figure 4). The Criegee mechanism is the energetically favored pathway by which the primary ozonide can be stabilized as compared to reacting with the alkene to form an epoxide. While the oxygen transfer type of reaction would be consistent with the experimentally observed stoichiometry, as such the very high activation energy would disfavor this reaction to form epoxide products. The reaction between the primary ozonide and the alkene is not expected to occur due to a high activation energy.

The final example of an intermediate of the Criegee mechanism that has been implicated for being responsible for epoxide formation is the carbonyl oxide zwitterion. According to the Creigee mechanism, the carbonyl oxide is formed as a product of the stabilization of the primary ozonide (see Figure 4). The ability of the carbonyl oxide to form epoxides with alkenes has been reported for carbonyl oxides generated from reactions other than ozonation. Kwart and Hoffman (1966) reported that hydroxyl-substituted carbonyl oxide species derived from peracids (RCO_3H) are capable of forming epoxides with alkenes. Carbonyl oxides produced via singlet oxygen oxidation of diazo compounds have been observed to form epoxides with alkenes (Hinrichs, Ramachandran, and Murry, 1979). The decomposition of an unusually stable 1,2,3-trioxylane (or primary ozonide) to a carbonyl oxide was used to demonstrate that the carbonyl oxide acted as the epoxidization agent towards alkenes rather than the primary ozonide (Pryor and Covindan, 1981). In their experiment, the addition of methanol was

used to scavenge the carbonyl oxide species to prevent epoxide formation. These reports in the literature provided empirical evidence that a reaction of a carbonyl oxide with an alkene was a possible source for the formation of epoxide products.

In addition to the reports of the formation of epoxides by a reaction of the carbonyl oxide species with alkenes, there have been two mechanisms proposed to explain these reactions. Figure 23 shows a mechanism by which the terminal oxygen atom on the carbonyl oxide can be oriented to interact with the double bond to form an epoxide (Cremer and Bock, 1986).
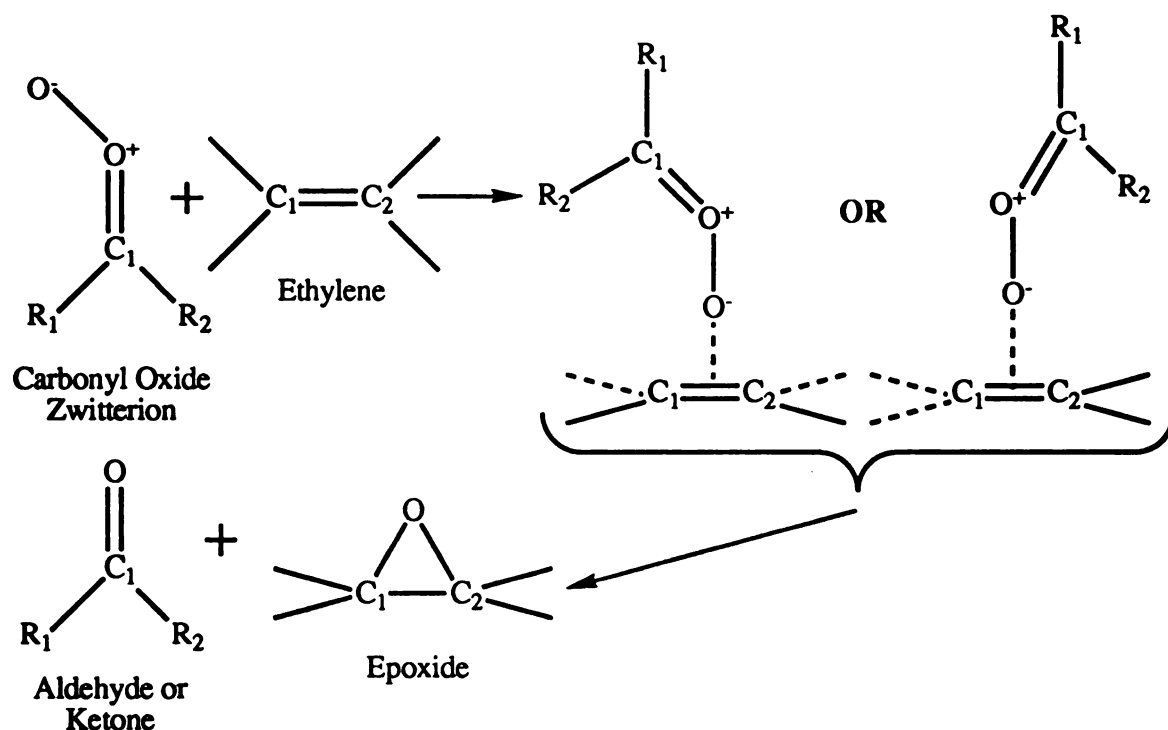
Figure 23. Epoxide Formation Mechanism for "Edge-Directed" Orientation

Such an attack would permit the interaction of the HOMO of the carbonyl oxide with the LUMO of the alkene to form the epoxide species. Cremer and Bock (1986) reported that theoretical calculations for this reaction showed an activation energy of 4.7 kcal/mol, which compares well to the low activation energy observed for the ozonation of chlorinated ethylenes.

Kwart and Hoffman (1966) presented an additional mechanism by with epoxides can be formed via an oxygen atom transfer to an alkene. This mechanism is shown in Figure 24.
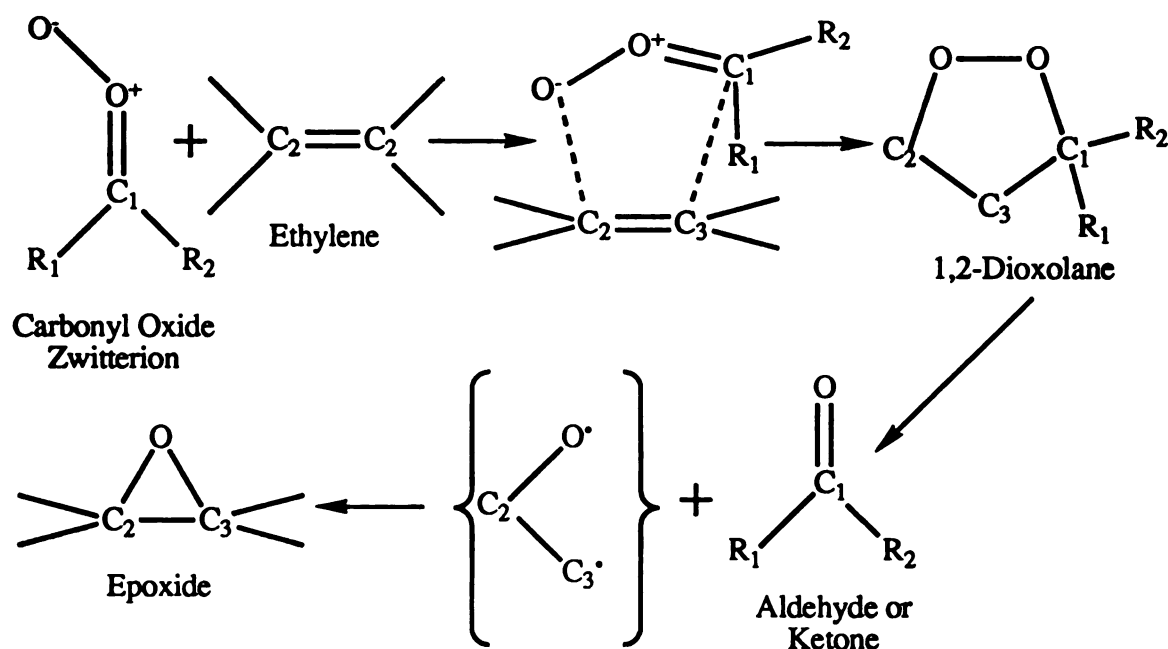
Figure 24. Epoxide Formation Mechanism Through 1,3-Dipolar Cycloaddition

In this case, the carbonyl oxide is acting similar to ozone and reacting with the alkene through a concerted 1,3-dipolar cycloaddition mechanism. The theoretical calculations showed that the activation energy of this reaction is 12.4 kcal/mol (Cremer and Bock, 1986). The calculated activation energy is about three times greater than the "edge-directed" attack shown in Figure 23, but is reasonably close to the observed activation energy for the series of chlorinated ethylenes. Further evidence supporting this type of attack of the alkene by the carbonyl oxide species was provided by the identification of the key intermediate of this mechanism, 1,2-dioxolane, by NMR identification of the molecule (Kwart, 1967). Thus, in the literature there has been two proposed mechanisms to describe the experimentally observed reaction between the carbonyl oxide and the alkene to produce an epoxide species.

Epoxide formation through the reaction of the carbonyl oxide with the alkene cannot be the indirect reaction suggested by the order and stoichiometry results. From an energy standpoint, the "edge-directed" mechanism would be the favored mechanism in comparison to the concerted 1,3-dipolar cycloaddition mechanism because of the lower calculated activation energy of this mechanism. The stoichiometry of this reaction would be greater than 1:1, which would be consistent with the experimental observations. However, the reaction cannot be the indirect reaction because the solvent (H_2O) used in this study is a participating solvent and the reaction between the water and the carbonyl oxide would be expected to predominate over a reaction with the alkene. Water is present in an aqueous solution in excess relative to the concentration of the alkene. A reaction with a participating solvent, methanol, was the method used by Pryor and Covindan (1981) to scavenge the carbonyl oxide species to prevent the epoxide formation reaction with the alkene. For these reasons, the reaction of the carbonyl oxide with the alkene cannot be the theoretical indirect reaction responsible for causing the experimental results.

Hydroxy Hydroperoxide as a Reactant in the Indirect Reaction. The only other intermediate of the Criegee mechanism that has not been previously discussed as a reactant being involved in the indirect reaction with the alkene is the hydroxy hydroperoxide species [XII]. This species is produced through the reaction of the carbonyl oxide zwitterion with the participating solvent ([XI] ---> [XII]; see Figure 4). The Criegee mechanism predicts that the hydroxy hydroperoxide species will be short lived and decompose to a simple carbonyl containing compound by releasing either water or hydrogen peroxide. However, recent work with this species would suggest that organic hydroperoxides as a class of compounds are more stable that previously thought to be true when the Criegee mechanism was developed. Hellpointner and Gäb (1989) and the more recent work by Kurth et al (1991) used HPLC with a fluoresence detector to measure various organic peroxides including hydroxy hydroperoxide species in cloud and

rainwater. A theory to explain the presence of these compounds in the environment was proposed by Hewitt, Kok, and Fall (1990) and Gäb *et al.* (1986). Organic hydroperoxides are believed produced by the reaction of gas phase ozone with biotic alkenes released by tree species. Tress such as the red spruce, Norway spruce, and firs are all known emitters of monoterpenes and other reactive alkenes. The organic hydroperoxides produced in the gas phase are readily water soluble in rainwater. This class of compounds, which are toxic to plants, has been associated with the observed death of large areas (*Waldsterben*) of forested lands in Europe and the Western United States (Hellpointner and Gäb, 1989). The reaction of hydroxy hydroperoxide species with the alkene may be the indirect reaction responsible for the observed experimental results.

Because of its stability in the environment, the identification of hydroxy hydroperoxide species in the environment would tend to indicate that the species is stable in the environment and does not decompose as readily as expected by the Criegee mechanism. For the hydroxy peroxide species to be involved in a indirect reaction which consumes the alkene, the species must also be stable in acidic solutions. Zhou and Lee (1992) determined the reaction between hydrogen peroxide (H_2O_2) and formaldehyde (H_2CO) to form hydroxymethyl hydroperoxide (HMP) as shown below:

$$H_2CO + H_2O_2 <\text{---}> HOCH_2O_2H \qquad (20)$$
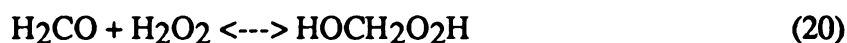
HMP is the simplest of the hydroxy hydorperixide species and would be the expected product of the ozonation of ethylene. The reaction shown in equation (20) is the reverse of the decomposition reaction included as part of the Criegee mechanism. The equilibrium constant (K) for the reaction as written at a temperature of 25°C is 150 M^{-1}, indicating that the equilibrium position for this reaction lies far to the right favoring the production of HMP from the reactants and disfavors its decomposition. Zhou and Lee (1992) demonstrated that the equilibrium constant was independent of pH between 4.0

and 8.4. The reaction is base-catalyzed so that the HMP species was observed to be very stabile only at a pH $\leq$ 5.5. This report in the literature would suggest that the hydroxy hydroperoxide species would not decompose as predicted by the Criegee mechanism and would a stable product of the ozonation reaction if the reaction was conducted at a pH of 2.0, as was done in the experiments described here.

The reactivity of the hydroxy hydroperoxide specie towards the unreacted alkene is determined by the exact chemical structure of the intermediate of the compounds used in this study. A mechanism for the reaction can be postulated subsequent to determining the exact structures of the reaction intermediates. Figure 4 showed the generalized representation of the Criegee mechanism, but the structures of the intermediate from the three specific compounds used in this study (TCE, 1,1,3-TCP, and 1,1-DCP) will be dictated by which carbon atom will be involved in the formation of the carbonyl oxide zwitterion. Figure 25 depicts a portion of the Criegee mechanism for the specific compounds used in this study. The carbonyl oxide will be formed from the carbon moiety not having the chlorine atoms as a subsistent group. The chlorine atom acts as an electron withdrawing group causing a shift of the electron density towards the C_1 carbon atom. This is shown in Figure 25 by the direction of the arrows for [IX]. The electrons necessary to satisfy the electron withdrawing effect of the chlorine must come from another part of the molecule, resulting in electrons being taken from the bond between the oxygen atom attached to C_1 and the apex oxygen atom. In this case the shift of the electron density is sufficiently strong as to cause the bond to be completely broken. The carbon atom containing the chlorine group will form the carbonyl compound while the other carbon atom will form the carbonyl oxide zwitterion species. This explanation is consistent with the experimental observations by Meister, Zwick, and Griesbaum (1983) who observed that the carbon atom containing the chlorine moiety was transformed into the carbonyl fragment while the other carbon atom was transformed into the zwitterion fragment upon the ozonation of vinyl chlorine in a participating solvent.
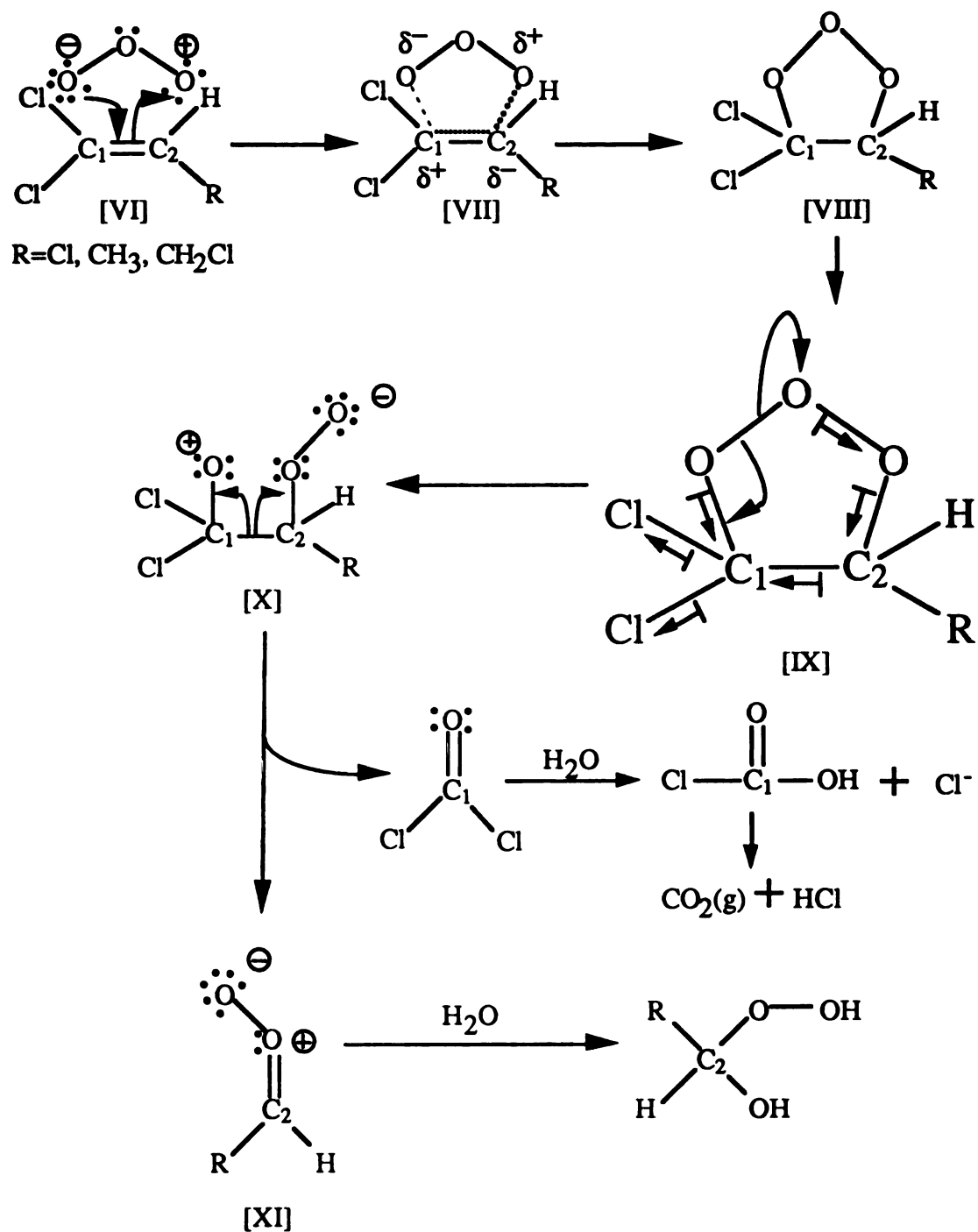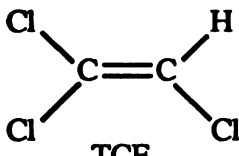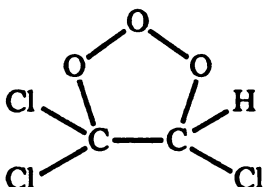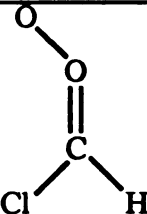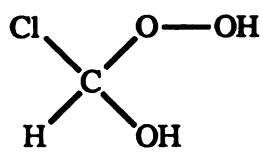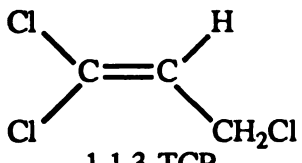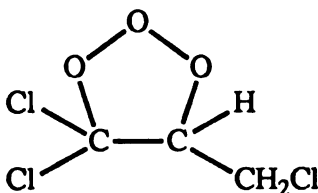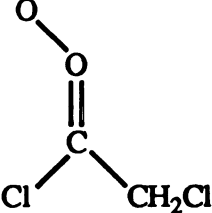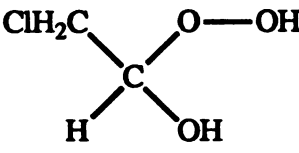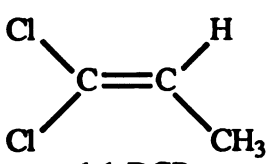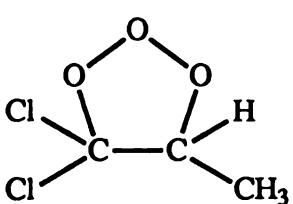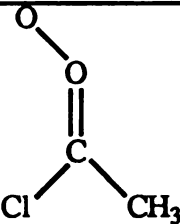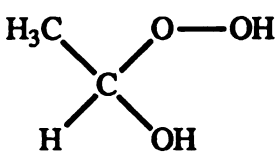
Figure 25. The Specific Criegee Mechanism Representation for TCE, 1,1,3-TCP, and 1,1-DCP.

For the three compounds used in this study, the carbon atom containing the two chlorine substituent groups will form the same carbonyl fragment (phosgene) while the other carbon atom will yield the zwitterion fragment.

The reactivity of the hydroxy hydroperoxide species with the alkene will be dictated by the structure of the species. Table 9 shows the expected chemical structures of the intermediate predicted by the Criegee mechanism upon the ozonation of the three compounds used during this study. The structure of the hydroxy hydroperoxide species will be different for each of the compounds because the substitution of C_2 is different for each compound.

Table 9. Expected Chemical Structure of the Criegee Intermediates

The hydroxy hydroperoxide species expected from the three compounds will all contain two hydroxy groups (-OH) each having a specific pK_a value to reflect the acidic character of this group. Organic alcohols generally are weakly acidic compounds which

is reflected by a very high pK$_a$ value. For example, methanol has a pK$_a$ value of 15.54

(McMurry, 1988) as compared to a pK$_a$ of 14.00 for water. Equation 21 can be used to

estimate the fraction of an acidic compound that will exists in the protonated or acid form

at a given pH value (Schwarzenbach, Gschwend, and Imboden, 1993).

$$\alpha_a = \frac{1}{1 + 10^{(pH - pK_a)}}$$ (21)

where α_a = fraction of the compound in the acidic form.

Methanol is such a weak acid that it will exist in the protonated form over the entire pH

range. For a significant (>10%) percentage of the compound to exists in the

nonprotonated from at a pH=2.0, the pK$_a$ of the compound must be greater than 3.0.

Electron withdrawing groups are known to have a great influence on the pK$_a$ value of a

compound. Chlorine acts to pull the electron density of the molecule away from the

hydroxyl group increasing the ability of the compound to release the proton and to

stabilize the ionized form of the molecule. The increased in the acidity of the compounds

will be reflected by a decreased pK$_a$ value. The proximity of the electron withdrawing

group to the double bond also effects the strength of the acidic functional group. The

closer the electron withdrawing group is to the double bond, the lower the pK$_a$ value of

the acidic functional group. From the structures of the hydroxy hydroperoxide species for

each compound shown in Table 9, the hydroxy hydroperoxide from TCE will have the

lowest pK$_a$ value followed by the peroxide from the 1,1,3-TCP and the weakest acid will

be the peroxide from the 1,1-DCP. The trend in the acidity of the hydroxy hydroperoxide

species was also reflected in the order of the observed ratio of the stoichiometry

coefficients of the three compounds used in this study. The parent compound (TCE) with

the most acidic hydroxy hydroperoxide species was observed to have the greatest ratio of

stoichiometry coefficients. Likewise, the parent compound (1-1-DCP) with the least

acidic hydroxy hydroperoxide species was observed to have a stoichiometry ratio closer

to 1:1. Form the correlation between acidity and observed stoichiometry, it would appear that the acidity of the hydroxy hydroperoxide species or more importantly, the extent of the species which exists in the nonprotonated form at a pH of 2.0, is related to the reactivity of the intermediate species with the alkene.

The nonprotonated or ionized form of the hydroxy hydroperoxide species for the three compounds may have acted as a nucleophile in the reaction with the alkene. A reaction between the alkene and the hydroxy hydroperoxide is consistent with the theory put forth to explain the experimental observations. The hydroxy hydroperoxide species is formed as an intermediate of the Criegee mechanism after the rate determining step. The nonprotonated from of the hydroxy hydroperoxide species could act as a nucleophile in the reaction with the unreacted alkene via an attack similar to the "edge-directed" orientation of the attack described by Cremer and Bock (1986) for the reaction of the carbonyl oxide with the alkene as shown in Figure 23. Figure 26 shows the orientation required for the two compounds to facilitate the interaction of the HOMO of the hydroxy hydroperoxide species with the LUMO of the alkene to form an epoxide as a product of the reaction. A low activation energy would be expected for this reaction mechanisms because a theoretical calculation for a similar mechanism between the carbonyl oxide and the alkene showed a low activation energy (Cremer and Bock, 1986). This reaction would cause the observed stoichiometry to be greater than 1:1 (VOC:ozone), and a reaction stoichiometry of 3:1 (VOC:ozone) from this scheme could also be possible if either species [XX] or [XXI] reacted further with the alkene. From an examination of the exact chemical structure of the hydroxy hydroperoxide species produced as an intermediate of the Creigee mechanisms, an indirect reaction between the hydroxy hydroperoxide species with the unreacted alkene after the rate determining step is consistent with the experimental observations and postulated explanation of this observation.
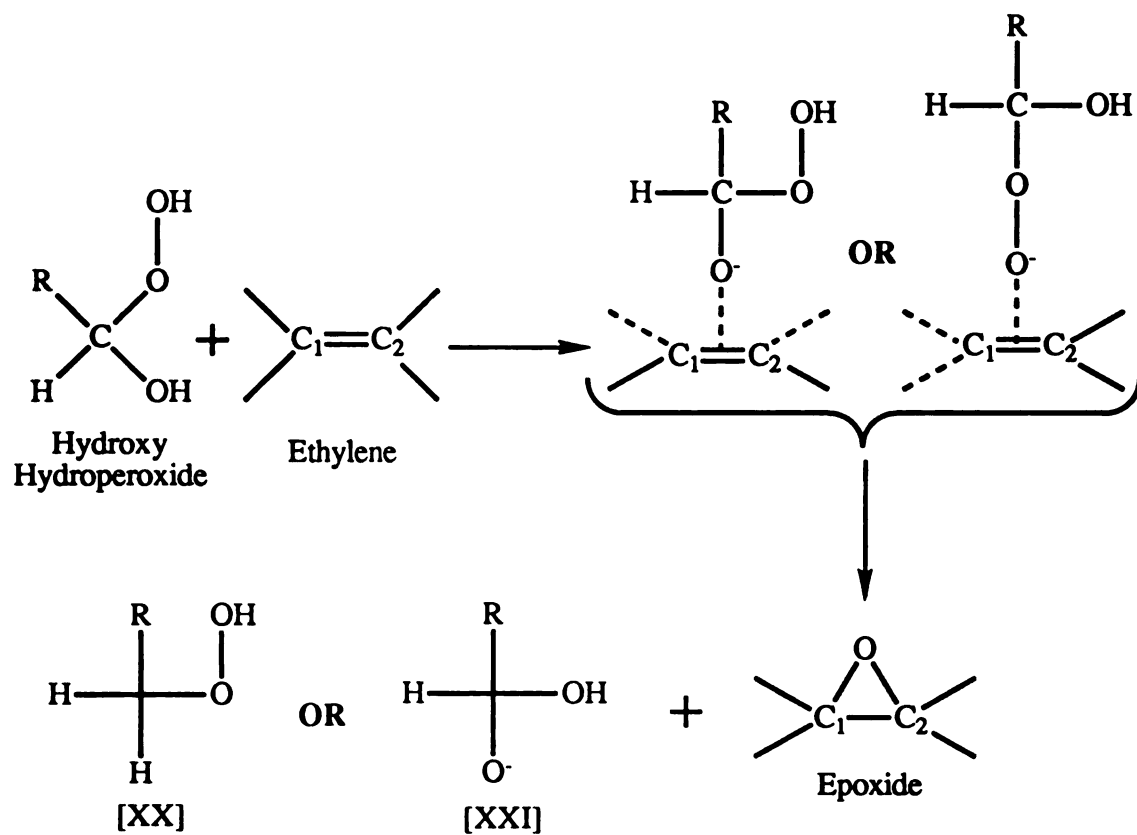
Figure 26. Epoxide Formation Mechanism for an "Edge-Directed" Attack
of the Hydroxy Hydroperoxide Species with the Alkene

CHAPTER 5

CONCLUSION

SUMMARY OF OBJECTIVES AND SIGNIFICANCE OF RESULTS

The first objective of this study was to develop an experimental apparatus and/or experimental procedure to obtain kinetic data for the reaction between two volatile reactants. Partitioning of ozone from the aqueous phase to the gas headspace above the solution was observed to be significant in a ten minute interval for three mixing schemes employing a 22 mL GC headspace vial as the reaction vessel. Even when the volume of the headspace was reduced to approximately 9% of the total volume of the vessel, a 30% decrease in the aqueous ozone concentration was observed after a ten minute interval. A reaction vessel with no headspace (a 50 mL airtight, glass syringe) and an experimental procedure for conducting kinetic experiments was developed to overcome the problems encountered with losing the reactants from the aqueous phase to the gas headspace above the solution.

The significance of this observation is that the determination of the kinetics for any reaction involving a volatile reactant must be questioned if any gas phase headspace above the solution was present. The loss of the reactants due to partitioning will occur and the extent of partitioning be determined before accepting kinetic data from the system. The observations from this study raise serious concern with any data obtained using the "solution ozone test" as proposed by Hoigné and Bader (1994). A modified bottle-top dispenser on a dark glass reagent bottle was proposed as the reaction vessel for a standard test to determine the ozone demand and the half-live of ozone in a natural water. A headspace above the solution develops as aliquots are removed from the bottle for analysis. This situation would result in the partitioning of ozone from the aqueous phase to the gas headspace above the solution, thus causing erroneous results.

75

Partitioning of the reactants must be a factor in the consideration of a reaction vessel when any gas phase headspace above the solution will be present.

The second objective of this study was to measure the order of the reaction with respect to each reactant. The Van't Hoff Plot analysis method was used to analyze concentration data for the reaction using pseudo-first order reaction conditions to determine the order of the reaction with respect to each reactant. The reaction was calculated to be second order overall, or first order with respect to each reactant. This observation confirmed that the correct form of the reaction rate law was being used to derive the nonlinear kinetic modeling expression. The other purpose of the order determination experiments was to provide experimental evidence to reject a proposed mechanism. In this case, the result of the experimental order determination agreed with the order predicted by the Criegee mechanism and as such the Criegee mechanism cannot be rejected as the mechanistic pathway by which the reaction occurred. At the same time, the results of the order determination alone did not provide sufficient experimental evidence to positively confirm that the reaction was occurring through the Criegee mechanism. From the results of the order determination, it was concluded that the rate determining step of the overall reaction occurred with a 1:1 (VOC:ozone) reaction stoichiometry.

The third objective of this study was to measure the overall reaction stoichiometry coefficients with respect to each reactant. Measuring the stoichiometry of the reaction was important to understand the overall reaction mechanism and to fit the concentration data to the kinetic modeling expression. The stoichiometric determination was performed by plotting the change in the VOC concentration over a time interval versus the change in the ozone concentration over the same time interval where the slope of the resulting linear relationship was the ratio of the stoichiometry coefficients (v_M/v_{O_3}). The most logical interpretation of the ratio in light of the Criegee reaction mechanism was to express it in terms of one mole of ozone. The stoichiometric coefficient for the three compounds used

in this study (TCE, 1,1,3-TCP, and 1,1-DCP) were found to be significantly greater than the expected 1:1 (VOC:ozone) stoichiometry as predicted by the Criegee mechanism. The most significant deviation from the expected value occurred with TCE where a 3:1 (VOC:ozone) reaction stoichiometry was observed for the reaction with ozone. The stoichiometry coefficient determination experiments were performed using second order reaction conditions where a 2:1 (ozone:VOC) initial molar ratio of the reactant concentrations were used.

The final objective of this study was to calculate the reaction rate coefficient (k) for the reaction between ozone and low molecular weight chlorinated alkenes. Second order reaction conditions were used in this study as compared to the pseudo-first order reaction conditions utilized in previous studies because those experimental conditions are not feasible for an engineered treatment system. A nonlinear model derived by Bandemenhr (1992) and corrected in this study was used in conjunction with concentration data from one reactant to determine the reaction rate coefficient which provided the best fit of the experimental data to the modeling expression. A linear model requiring concentration data from both reactants was used to calculate the reaction rate coefficient from the slope of the line determined by the linear model. For each set of concentration data, the reaction rate coefficient was determined using three models with the values from the three models expected to agree. It was observed that the inclusion of the measured stoichiometry coefficients into the kinetic nonlinear model negatively affected the fit of the model to the concentration data but positively affected the agreement of the calculated values from the three models.

For all four trials, the reaction rate coefficients calculated for TCE using the three models agreed to within experimental error. The values were slightly less than the literature values, but the experimental conditions used in the previous studies could have biased the reported values. The significance of the reaction rate coefficient values agreeing for the three models was that it demonstrated that a reaction rate coefficient

value could be obtained using second order reaction conditions using concentration data for only one reactant. This conclusion has a significant on the methodology for studying environmental systems where the concentration of a reactant cannot be measured or for other data limited situations. The observations that the reaction rate coefficient values three models did not agree for the other two compounds was attributed to the significant influence of the initial concentration of the reactants on the kinetic models for very fast reactions ($k > 25$ M^{-1} s^{-1}).

In general, the expected trends in the reaction rate coefficients for the three compounds were observed after the being corrected for the observed stoichiometry. The addition of chlorine at the site of the double bond caused the observed rate to decrease. Shifting the chlorine substitution away from the site of the double bond caused the rate of the reaction to increase. The observed trends for the three compounds in this study support the notion previously suggested by others that chlorine acts as an electron-withdrawing group decreasing the electron density of the molecule at the site of the double bond and slowing the rate of the reaction.

The difference in the measured stoichiometry of the rate determining step of the reaction as suggested by the order results as compared to the results from the determination of the overall stoichiometry of the reaction suggested that another reaction was occurring to cause the consumption of the unreacted alkene. The effect of the stoichiometry coefficients on the kinetic models further supported this conclusion. An indirect reaction between an intermediate of the Criegee mechanism was proposed as a hypothesis to explain the cause of the results produced in this study. The yield of products not predicted by the Criegee mechanism have been observed for the ozonation of alkenes. Epoxides are the predominant non-Criegee mechanism products. The reaction of ozone, the primary ozonide, and the carbonyl oxide zwitterion with the alkene have been implied as being responsible for the production of epoxide products, but these reactions are inconsistent with the experimental observations or were not an energetically

favorable reaction during the ozonation of alkenes in aqueous phase. The only intermediate of the Criegee mechanism that fits the criteria to explain the experimental observations was the hydroxy hydroperoxide species. The identification of this species in atmospheric samples has been reported in the literature (Hewitt, Kok, and Fall, 1990; Gäb *et al.*, 1986), which suggests that the species may be more stable the previously thought. The hydroxy hydroperoxide species contains two weakly acidic hydroxyl functional groups. Chlorine, acting as a electron-withdrawing group, is known to shift the electron density in acidic compounds so as to make the compound more acidic, resulting in the ionization of the hydroxyl groups by the release of a proton. Because of the structures of the chlorinated alkenes used in this study, the resulting hydroxy hydroperoxide species produced by the ozonation of TCE would be most acidic while the species produced by the ozonation of 1,1-DCP would be least acidic. The nonprotonated or ionized form of the hydroxy hydroperoxide species could have acted as a nucleophilie in an indirect reaction with the unreacted alkene via an "edge-directed" orientation to form an epoxide species. In certain circumstances, the product of the reaction will contain another nonprotonated hydroxyl group available for further reaction. The trend in the acidity of the hydroxy hydroperoxide species for the three compounds used in this study correlated to the order of the parent compounds with regards to the results of the stoichiometry results. A measured stoichiometry of 3:1 (VOC:ozone) measured for TCE would be consistent with a reaction between the alkene and the products of the previous reaction. A reaction mechanism of this type would be consistent with the experimental observations of this study.

There is great environmental engineering significance of an indirect reaction occurring during the ozonation of alkenes in water. Because the observed reaction stoichiometry was greater than the 1:1 (VOC:ozone) reaction stoichiometry predicted by the Criegee mechanisms, a smaller dose of ozone on a molar basis would be required to degrade the aqueous VOCs than previously thought. The major disadvantage seen with

ozone treatment systems, in general, are the capital costs associated with supplying the ozone. Any design parameter (reaction stoichiometry) which reduced the ozone capacity requirements of an ozone treatment system will greatly benefit the economics of the project. However, further experimental testing will be required to demonstrate that a stoichiometry of greater than 1:1 occurs at other pH values and at different initial molar ratio concentration conditions.

The other significance of this observation involves the yield of products upon the ozonation of chlorinated alkenes. The toxicity of the by-products of ozone treatment of drinking water has been offered as a concern of this technology. This study would imply that the organic peroxides (including hydroxy hydroperoxide species) may be more stable than previously thought and the human toxicity of this class of compounds must be further investigated.

FUTURE WORK

Any future research on this topic should be directed towards confirming the indirect reaction hypothesis and then towards confirming the exact mechanism of the indirect reaction. First, the reaction stoichiometry should be determined for the reaction at different pH conditions while taking steps to minimize hydroxyl radical formation and radical reactions at the higher pH conditions. Zhou and Lee (1992) determined that the hydroxy hydroperoxide species would not be a stable product above a pH of 5.5. The indirect reaction hypothesis would be supported if the stoichiometry of the reaction became 1:1 (VOC:ozone) at pH values greater than 5.5 where a radical scavenger compound, like *tert*-butyl alcohol, has been added to minimize the formation of hydroxyl radicals.

Secondly, future research should be directed towards confirming the proposed mechanisms to explain the experimental observations. Following along the studies referenced in this study, analytical methods should be developed to detect the proposed

products of the direct and indirect reaction. An HPLC method has been reported to measure organic peroxides in atmospheric samples (Hellpointer and Gäb, 1989; Kurth *et al.*, 1991). The methods of Zhou and Lee (1992) could be used to synthesize hydroxy hydroperoxide compounds by the reaction of hydrogen peroxide with formaldehyde or chlorinated aldehydes under basic conditions. The acidity of the compounds could be measured and compared to the theoretical analysis of the acid dissociation constants of the compounds discussed in this study. The reactivity of the synthesized hydroxy hydroperoxide compounds with the corresponding chlorinated alkenes could be determined using the 50 mL airtight, glass syringe as the reaction vessel. Aliquots of the reaction solution could be withdrawn and analyzed to identify the products of the reaction. Taken as a whole, these two research directions should be able to confirm the hypothesis proposed in this study regarding the presence of an indirect reaction between the alkene and the hydroxy hydroperoxide species produced as an intermediate predicted by the Criegee mechanism for the ozonation of alkenes in water.

APPENDICES

APPENDIX A

CHEMICAL PROPERTIES

Table A-1. Chemical Properties of Low Molecular Weight Chlorinated Alkenes

Name	Molecular Weight (g/mol)	Boiling Point (°C)	Vapor Pressure (mm Hg)[1]	Water Solubility (mg/L)	Henry's Law Constant (C_a/C_w)[1]
1,1-dichloroethylene	96.95	32	591		
cis 1,2-dichloroethylene	96.95	60	200	800	1.305
trans 1,2-dichloroethylene	96.95	48	200	600	1.739
trichloroethylene	131.5	86.7	74	1200	0.423
1,1,2,2-tetrachlorethylene	165.8	121.4	19	150	0.727
cis 1,3-dichloropropene	110.97	104	43	2700	0.095
trans 1,3-dichloropropene	110.97	112	53	2800	0.072
2,3-dichloropropene	110.97	94	34	2150	0.147

(Taken from Schwarzenbach, Gschwend, and Imboden, 1993. Verschueren, K. 1983)
(1) at 25°C

Table A-2. Chemical Properties of Ozone

Name	Molecular Weight (g/mol)	Boiling Point (°C)	Vapor Pressure (mm Hg)	Water Solubility (mg/L)[1]	Henry's Law Constant (C_a/C_w)[2]
ozone	48.0			58.1	3.1245

(Taken from Roth and Sullivan, 1981)
(1) at pH=2.0 and T=20°C. (2) at pH=2.0 and T=25°C

APPENDIX B

VOC ANALYSIS BY HEADSPACE GAS CHROMATOGRAPHY

GC Program and Conditions for Headspace Autosampler

Flame Ionization Detector (FID)

Detector Temperature:	250°C
Hydrogen Flow Rate:	30 mL/min(est.)
Air Flow Rate:	200 mL/min(est.)
Make-up Gas Rate:	15 mL/min(est.)
Injector Temperature:	200°C
Equilibrium Time	1.0 min

Gas Chromatograph Conditions

Oven

Temperature:	39°C
Total Time:	10.0 min
Carrier Gas	Helium
Flow Rate:	4.0 mL/min

Headspace Autosampler Conditions

Sample Temperature	90°C
Needle Temperature	95°C
Transfer Tube Temperature	95°C
Auxiliary Pressure	21 psi

Headspace Autosampler Program

Cycle Time	12.0 min
Thermostat Time	40.0 min
Pressurization Time	2.0 min
Injection Time	0.2 min
Withdraw Time	0.2 min

The following is a typical GC chromatograph for TCE produced using these conditions.
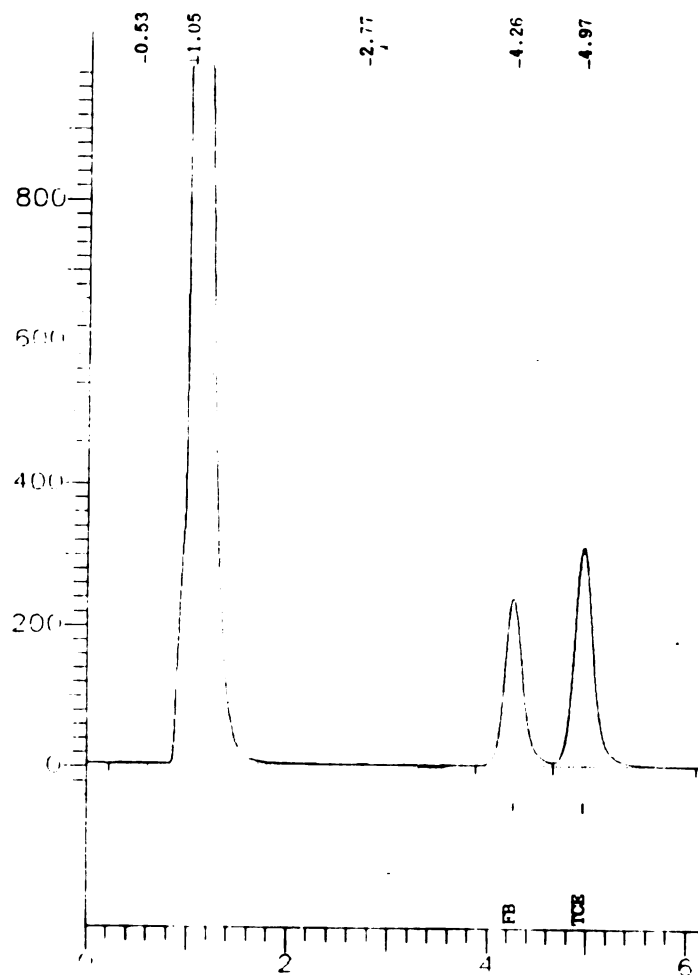
Figure B-1. Typical Chromatograph for TCE.
20 μg TCE Standard with 7.0 μg Flurobenzene as Internal Standard
10/26/94. VOC Order Determination. VOC Sample #12.

APPENDIX C

RAW DATA

DETERMINATION OF OZONE LOSSES WITH DIFFERENT MIXING SCHEMES

07/01/94. Determination of ozone losses with mixing. 10 mL of ozonated 0.05 M phosphate buffer solution at pH 2.0 in 20 mL GC headspace vial. Mixing was provided by Rotomix Type 50800 Shaker Table set at 200 rpm. Temp. = 22°C

Table C-07/01/94-Experimental Run 1 and 2

RUN 1	Ozone Concentration			RUN 2	Ozone Concentration		
Time	Initial	Final		Time	Initial	Final	
(s)	(mg/L)	(mg/L)	95% CI	(s)	(mg/L)	(mg/L)	95% CI
0	1.232	1.265	0.10	0	1.348	1.346	0.10
30	1.220	1.089	0.10	30	1.348	1.320	0.10
60	1.231	0.913	0.10	60	1.342	1.047	0.10
90	1.215	0.834	0.10	90	1.346	1.080	0.10
120	1.234	1.124	0.10	120	1.350	1.005	0.10
150	1.251	1.031	0.10	150	1.381	0.802	0.10
180	1.253	0.969	0.10	180	1.382		
210	1.290	0.737	0.11	210	1.370	1.093	0.10
240	1.284	0.591	0.12	240	1.321	0.748	0.11
270	1.301	0.924	0.10	270	1.296	0.570	0.12
300		0.579	0.12	300	1.310	0.860	0.10
360	1.279	0.798	0.11	360	1.320	0.902	0.10
420	1.275	0.866	0.10	420	1.345	0.773	0.11
480	1.255	0.419	0.13	480	1.342	0.635	0.11
540	1.277	0.804	0.10	540	1.328	0.732	0.11
600	1.286	0.782	0.11	600	1.331	0.738	0.11
CSTD	(mg/L)	95% CI	%	CSTD	(mg/L)	95% CI	%
1.305	1.282	0.10	98.24	1.357	1.362	0.10	100.4
				1.308	1.299	0.10	99.31

Observed Ozone Self-Decomposition Rate = $1.17e^{-4}$ s^{-1}

07/06/94. Determination of ozone losses with mixing. 10 mL of ozonated 0.05 M phosphate buffer solution at pH 2.0 in 20 mL GC headspace vial. Mixing was provided by Rotomix Type 50800 Shaker Table set at 200 rpm. Temp. = 22°C

Table C-07/06/94-Experimental Run 1

Time (s)	Ozone Concentration		
	Initial (mg/L)	Final	
		(mg/L)	95% CI
0	1.212	1.200	0.06
15	1.214	1.164	0.06
30	1.222	1.131	0.06
45	1.248	1.086	0.06
60	1.278	1.084	0.06
75	1.294	1.055	0.06
90	1.321	1.194	0.06
105	1.325	0.884	0.06
120	1.338	1.001	0.06
150	1.350	1.070	0.06
180	1.347	0.633	0.06
210	1.349	0.736	0.06
240	1.349	0.457	0.06
270	1.360	0.636	0.06
300	1.367	0.523	0.06
360	1.394	0.667	0.06
420	1.388	0.460	0.06
480	1.381	0.784	0.06
560	1.391	0.845	0.06
600	1.403	0.852	0.06
CSTD	(mg/L)	95% CI	%
1.380	1.341	0.06	97.17
1.374	1.327	0.06	96.58

Ozone Decomposition Rate=$9.38e^{-5}$ s^{-1}

07/10/94. Determination of ozone losses with mixing. 10 mL of ozonated 0.05 M phosphate buffer solution at pH 2.0 in 20 mL GC headspace vial. Mixing was provided by mirco-stirbar. Temp. = 22°C

Table C-07/10/94-Experimental Run 1

Time	Initial	Final	
(s)	(mg/L)	(mg/L)	95% CI
0	1.126	1.130	0.03
10	1.115	0.972	0.03
20	1.126	0.984	0.03
30	1.118	0.935	0.03
40	1.123	0.983	0.03
50	1.115	0.932	0.03
60	1.115	0.966	0.03
70	1.115	0.916	0.03
80	1.111	0.912	0.03
90	1.111	0.919	0.03
120	1.201	0.976	0.03
150	1.190	0.995	0.03
180	1.197	0.918	0.03
210	1.198	0.934	0.03
240	1.189	0.791	0.03
270	1.202	0.760	0.03
300	1.206	0.654	0.03
330	1.199	0.684	0.03
360	1.218	0.750	0.03
390	1.205	0.843	0.03
420	1.200	0.665	0.03

CSTD	(mg/L)	95% CI	%
1.123	1.145	0.03	101.9

Ozone Self-Decomposition Rate = $8.83e^{-5}$ s^{-1}

07/12/94. Determination of ozone losses with mixing. 10 mL of ozonated 0.05 M
phosphate buffer solution at pH 2.0 in 20 mL GC headspace vial. Mixing was
provided by mirco-stirbar. Temp. = 22°C

Table C-07/12/94-Experimental Run 1

| | | Ozone Concentration | |
| Time | Initial | Final | |
(s)	(mg/L)	(mg/L)	95% CI
0	1.216	1.196	0.03
15	1.221	1.055	0.03
30	1.210	1.007	0.03
45	1.199	0.963	0.03
60	1.170	0.927	0.03
75	1.113	0.884	0.03
90	1.096	0.834	0.03
105	1.107	0.856	0.03
120	1.080	0.838	0.03
135	1.082	0.823	0.03
150	1.045	0.742	0.03
165	1.115	0.713	0.03
180	1.110	0.761	0.03
195	1.197	0.785	0.03
210	1.157	0.828	0.03
225	1.144	0.795	0.03
240	1.149	0.757	0.03
255	1.163	0.813	0.03
270	1.140	0.640	0.03
285	1.147	0.773	0.03
300	1.133	0.639	0.03
330	1.128	0.475	0.03
360	1.201	0.722	0.03
390	1.255	0.563	0.03
450	1.228	0.392	0.03
480	1.226	0.475	0.03
510	1.138	0.476	0.03
540	1.101	0.390	0.03
570	1.051	0.446	0.03
600	1.039	0.863	0.03

CSTD	(mg/L)	95% CI	%
1.144	0.947	0.03	83.78

Ozone Self-Decomposition Rate = $1.15e^{-4}$
s^{-1}

07/14/94. Determination of ozone losses with mixing. 20 mL of ozonated 0.05 M phosphate buffer solution at pH 2.0 in 20 mL GC headspace vial. Mixing was provided by mirco-stirbar. Temp. = 22°C

Table C-07/14/94-Experimental Run 1

Time (s)	Ozone Concentration		
	Initial (mg/L)	Final	
		(mg/L)	95% CI
0	1.138	1.091	0.07
15	1.136	1.004	0.07
30	1.115	0.981	0.07
45	1.102	0.965	0.07
60	1.093	0.936	0.07
75	1.111	0.932	0.07
90	1.128	0.941	0.07
105	1.116	0.963	0.07
120	1.125	0.955	0.07
135	1.127	0.914	0.07
150	1.122	0.959	0.07
165	1.128	0.951	0.07
180	1.113	0.897	0.07
195	1.129	0.912	0.07
210	1.139	0.896	0.07
225	1.141	0.897	0.07
240	1.168	0.937	0.07
255	1.118	0.868	0.07
270	1.154	0.896	0.07
285	1.157	0.876	0.07
300	1.164	0.850	0.07
330	1.098	0.830	0.07
360	1.101	0.790	0.07
390	1.102	0.812	0.07
420	1.123	0806	0.07
450	1.154	0.815	0.07
480	1.182	0.851	0.07
510	1.201	0.799	0.07
540	1.192	0.799	0.07

CSTD	(mg/L)	95% CI	%
1.085	1.069	0.07	98.53
1.094	1.066	0.07	97.44

Ozone Self-Decomposition Rate = $6.55e^{-5}$ s^{-1}

08/21/94. Determination of ozone losses with mixing. 20 mL of ozonated 0.05 M phosphate buffer solution at pH 2.0 in 20 mL GC headspace vial. Mixing was provided by mirco-stirbar. Temp. = 22°C

Table C-08/21/94-Experimental Run 1

Time	Initial	Final	
(s)	(mg/L)	(mg/L)	95% CI
0	1.148	1.108	0.14
15	1.154	1.093	0.14
30	1.152	1.040	0.14
45	1.135	1.074	0.14
60	1.148	1.075	0.14
75	1.144	1.043	0.14
90	1.160	1.049	0.14
105	1.151	1.027	0.14
120	1.161	1.029	0.14
135	1.185	1.046	0.14
150	1.197	1.066	0.14
165	1.188	1.042	0.14
180	1.189	1.013	0.14
195	1.209	0.985	0.14
210	1.221	1.028	0.14
225	1.205	1.031	0.14
240	1.194	1.009	0.14
255	1.198	0.995	0.14
270	1.198	0.979	0.14
285	1.200	0.965	0.14
300	1.197	0.963	0.14

CSTD	(mg/L)	95% CI	%
1.197	1.177	0.14	98.33
1.203	1.174	0.14	97.59

Ozone Self-Decomposition Rate = $9.18e^{-5}$ s^{-1}

08/29/94 and 09/16/94. Determination of ozone or TCE losses with mixing. 50 mL Hamlton (Reno, NV) Glass Syringe as the reaction vessel. Mixing was provided by mirco-stirbar. Temp. = 22°C

Table C-08/29/94-and 09/16/94 Experimental Run

Time	Ozone Concentration				Time	TCE Concentration			
(s)	(mg/L)	95% CI	μM	95% CI	(s)	(mg/L)	95% CI	μM	95% CI
0	4.540	0.63	94.58	13.1	0	11.59	0.31	88.14	2.4
30	4.625	0.60	96.35	12.5	30	11.47	0.33	87.22	2.5
60	5.039	0.52	105.0	10.8	60	11.66	0.33	88.67	2.5
90	4.687	0.46	97.65	9.6	90	11.64	0.32	88.52	2.4
120	5.158	0.54	107.4	11.2	120	11.32	0.32	86.08	2.4
150	5.059	0.55	105.4	11.4	150	11.66	0.32	88.67	2.4
180	5.043	0.57	105.1	11.9	180	11.44	0.31	87.00	2.4
210	4.953	0.53	103.2	11.0	210	11.20	0.32	85.17	2.4
240	5.074	0.52	105.7	10.8	240	11.85	0.32	90.11	2.4
270	5.044	0.50	105.1	10.4	270	11.59	0.33	88.14	2.5
300	4.820	0.58	100.4	12.1	300	12.12	0.33	92.17	2.5
360	4.775	0.52	99.48	10.8	360	11.65	0.32	88.59	2.4
420	4.806	0.47	100.1	9.8	420	11.75	0.33	89.35	2.5
480	4.607	0.46	95.98	9.6	480	11.33	0.32	86.16	2.4
560	4.568	0.53	95.17	11.0	560	11.78	0.33	89.58	2.5
					600	11.55	0.32	87.83	2.4
CSTD	(mg/L)	95% CI	%		CSTD	(μg)	%		
4.794	4.759	0.47	99.27		8.0	7.903	98.79		
					14	14.03	100.2		

Observed Ozone Self-Decomposition Rate = $7.34e^{-5}$ s^{-1}

TCE ORDER DETERMINATION

10/18/94. Ozonation of TCE. TCE Order Determination. Ozone in Excess.
0.05 M Phosphate Buffer Solution at pH 2.0. Temp = 22.0°C

Table C-10/18/94-Experimental Run 1

Time	Ozone Concentration				Time	TCE Concentration			
(s)	(mg/L)	95% CI	μM	95% CI	(s)	(mg/L)	95% CI	μM	95% CI
0	17.76	0.56	370.0	11.6	0	4.558	0.34	34.66	2.6
					10	4.075	0.33	30.99	2.5
					20	3.827	0.34	29.10	2.6
					30	3.305	0.33	25.13	2.5
					40	2.924	0.33	22.24	2.5
					50	2.713	0.35	20.63	2.7
					60	2.480	0.37	18.86	2.8
					70	2.225	0.52	16.92	4.0
CSTD	(mg/L)	95% CI	%		CSTD	(μg)	%		
	No Check Standards Prepared				6.0	5.900	98.33		
					16.0	12.55	78.44		

Table C-10/18/94-Experimental Run 2

Time	Ozone Concentration				Time	TCE Concentration			
(s)	(mg/L)	95% CI	μM	95% CI	(s)	(mg/L)	95% CI	μM	95% CI
0	17.85	0.56	372.0	11.6	0	4.487	0.34	34.17	2.6
					10	3.728	0.42	28.35	3.2
					20	3.149	0.41	23.95	3.1
					30	2.924	0.36	22.24	2.7
					40	2.546	0.39	19.36	3.0
					50	2.391	0.42	18.18	3.2
					60	2.208	0.40	16.79	3.0
					70	2.004	0.40	15.24	3.0
					80	1.945	0.77	14.79	5.9
CSTD	(mg/L)	95% CI	%		CSTD	(μg)	%		
	No Check Standards Prepared				6.0	5.959	99.32		
					16.0	15.54	97.12		

10/18/94. Ozonation of TCE. TCE Order Determination. Ozone in Excess.
0.05 M Phosphate Buffer Solution at pH 2.0. Temp = 22.0°C

Table C-10/18/94-Experimental Run 3

Time		Ozone Concentration			Time		TCE Concentration		
(s)	(mg/L)	95% CI	µM	95% CI	(s)	(mg/L)	95% CI	µM	95% CI
0	16.73	0.52	348.4	10.9	0	2.740	0.42	20.84	3.2
					10	2.328	0.39	17.70	3.0
					20	2.133	0.37	16.22	2.8
					30	2.000	0.45	15.21	3.4
					40	1.736	0.33	13.20	2.5
					50	1.569	0.36	11.93	2.7
					60	1.135	0.27	8.631	2.0
					70	1.282	0.41	9.749	3.1
CSTD	(mg/L)	95% CI	%		CSTD	(µg)	%		
	No Check Standards Prepared				No Additional Check Standards Prepared				

10/18/94. Summary of Data to Prepare and the Results of theVan't Hoff Plots

Table C-10/18/94-Van't Hoff Plot Data and Results

Run	[TCE] at t=0s (µM)	X-Axis ln [TCE]$_O$	(d[TCE]/dt) at t=0s 10^{-2} (M s^{-1})	Y-Axis ln (d[TCE]/dt)$_O$
1	34.66	-10.2697	4.7016	-3.0573
2	34.17	-10.2856	6.0152	-2.8109
3	20.84	-10.7788	2.8729	-3.5498
		Slope	1.2162±1.9741	
		Intercept	9.5634±20.6241	
		R^2	0.8753	
	Order with Respect to Ozone	1.22±1.97		

10/21/94. Ozonation of TCE. TCE Order Determination. Ozone in Excess.
0.05 M Phosphate Buffer Solution at pH 2.0. Temp = 22.0°C

Table C-10/21/94-Experimental Run 1

Time	Ozone Concentration				Time	TCE Concentration			
(s)	(mg/L)	95% CI	μM	95% CI	(s)	(mg/L)	95% CI	μM	95% CI
0	16.46	0.51	342.8	10.6	0	2.567	0.34	19.52	2.6
					10	2.278	0.38	17.32	2.9
					20	1.931	0.37	14.68	2.8
					30	1.785	0.37	13.57	2.8
					40	1.712	0.37	13.02	2.8
					50	1.555	0.53	11.83	4.0
					60	1.271	0.45	9.665	3.4
					70	1.247	0.36	9.483	2.7
					80	1.079	0.32	8.205	2.4
CSTD	(mg/L)	95% CI	%		CSTD	(μg)	%		
	No Check Standards Prepared				6.0	4.760	79.33		
					16.0	15.08	97.25		

Table C-10/21/94-Experimental Run 2

Time	Ozone Concentration				Time	TCE Concentration			
(s)	(mg/L)	95% CI	μM	95% CI	(s)	(mg/L)	95% CI	μM	95% CI
0	16.12	0.50	335.9	10.5	0	2.874	0.35	21.86	2.7
					10	2.347	0.43	17.85	3.3
					20	1.731	0.30	13.16	2.3
					30	1.999	0.34	15.20	2.6
					40	1.789	.037	13.60	2.8
					50	1.508	0.36	11.47	2.7
					60	1.314	0.39	9.992	3.0
					70	1.224	0.43	9.308	3.3
					80	1.154	0.55	8.776	4.2
CSTD	(mg/L)	95% CI	%		CSTD	(μg)	%		
	No Check Standards Prepared				6.0	5.696	94.93		
					16.0	16.51	103.2		

10/21/94. Ozonation of TCE. TCE Order Determination. Ozone in Excess.
0.05 M Phosphate Buffer Solution at pH 2.0. Temp = 22.0°C

Table C-10/21/94-Experimental Run 3

Time	Ozone Concentration				Time	TCE Concentration			
(s)	(mg/L)	95% CI	µM	95% CI	(s)	(mg/L)	95% CI	µM	95% CI
0	18.33	0.57	381.8	11.9	0	4.383	0.32	33.33	2.4
					10	3.583	0.27	27.25	2.0
					20	3.429	0.28	26.08	2.1
					30	3.135	0.31	23.84	2.3
					40	2.539	0.29	19.31	2.2
					50	2.456	0.28	18.68	2.1
					60	2.048	0.30	15.57	2.3
					70	1.866	0.78	14.19	5.9
CSTD	(mg/L)	95% CI	%		CSTD	(µg)		%	
					6.0	5.509		91.82	
					16.0	14.59		91.19	

10/21/94. Summary of Data to Prepare and the Results of the Van't Hoff Plots

Table C-10/21/94-Van't Hoff Plot Data and Results

Run	[TCE] at t=0s (µM)	X-Axis ln [TCE]$_O$	(d[TCE]/dt) at t=0s 10^{-2} (M s^{-1})	Y-Axis ln (d[TCE]/dt)$_O$
1	19.52	-10.8440	2.6453	-3.6324
2	21.86	-10.7310	3.3203	-3.4051
3	33.33	-10.3090	4.8280	-3.0307

Slope	1.0595±0.8370
Intercept	7.9047±8.8973
R^2	0.9674
Order with Respect to Ozone	1.06±0.84

10/26/94. Ozonation of TCE. TCE Order Determination. Ozone in Excess.
0.05 M Phosphate Buffer Solution at pH 2.0. Temp = 22.0°C

Table C-10/26/94-Experimental Run 1

Time	Ozone Concentration				Time	TCE Concentration			
(s)	(mg/L)	95% CI	μM	95% CI	(s)	(mg/L)	95% CI	μM	95% CI
0	19.20	0.60	400.0	12.5	0	3.954	0.44	30.07	3.3
					10	3.320	0.32	25.25	2.4
					20	3.057	0.29	23.25	2.2
					30	2.704	0.29	20.56	2.2
					40	2.310	0.28	17.57	2.1
					50	2.134	0.28	16.23	2.1
					60	1.909	0.29	14.52	2.2
					70	1.675	0.26	12.74	2.0
					80	1.544	0.29	11.74	2.2
CSTD	(mg/L)	95% CI	%		CSTD	(μg)	%		
	No Check Standards Prepared				6.0	4.748	79.13		
					16.0	13.30	83.12		

Table C-10/26/94-Experimental Run 2

Time	Ozone Concentration				Time	TCE Concentration			
(s)	(mg/L)	95% CI	μM	95% CI	(s)	(mg/L)	95% CI	μM	95% CI
0	18.81	0.59	391.8	12.3	0	4.162	0.34	31.65	2.6
					10	3.566	0.37	27.12	2.8
					20	3.245	0.35	24.68	2.7
					30	2.726	0.34	20.73	2.6
					40	2.454	0.29	18.66	2.2
					50	2.116	0.39	16.09	3.0
					60	1.991	0.33	15.14	2.5
					70	1.780	0.33	13.54	2.5
					80	1.705	0.24	12.97	1.8
					90	1.531	0.33	11.64	2.5
CSTD	(mg/L)	95% CI	%		CSTD	(μg)	%		
	No Check Standards Prepared				6.0	5.013	83.55		
					16.0	13.73	85.81		

10/26/94. Ozonation of TCE. TCE Order Determination. Ozone in Excess.
0.05 M Phosphate Buffer Solution at pH 2.0. Temp = 22.0°C

Table C-10/26/94-Experimental Run 3

Time	Ozone Concentration			Time	TCE Concentration		
(s)	(mg/L)	95% CI	μM	95% CI	(s)	(mg/L)	95% CI	μM	95% CI

Time (s)	(mg/L)	95% CI	μM	95% CI	Time (s)	(mg/L)	95% CI	μM	95% CI
0	18.74	0.59	390.3	12.3	0	2.428	0.34	18.46	2.6
					10	1.881	0.37	14.30	2.8
					20	1.730	0.39	13.16	3.0
					30	1.605	0.31	12.20	2.4
					40	1.474	0.36	11.21	2.7
					50	1.234	0.37	9.384	2.8
					60	1.166	0.38	8.867	2.9
					70	0.979	0.38	7.445	2.9
					80	0.905	0.33	6.882	2.5
					90	0.891	0.32	6.776	2.4
CSTD	(mg/L)	95% CI	%		CSTD	(μg)	%		
No Check Standards Prepared					6.0	5.342	89.03		
					16.0	13.44	84.00		

10/26/94. Summary of Data to Prepare and the Results of the Van't Hoff Plots

Table C-10/26/94-Van't Hoff Plot Data and Results

Run	[TCE] at t=0s (μM)	X-Axis ln [TCE]$_O$	(d[TCE]/dt) at t=0s 10^{-2} (M s^{-1})	Y-Axis ln (d[TCE]/dt)$_O$
1	30.37	-10.4120	4.7001	-3.0576
2	31.62	-10.3608	5.2929	-2.9388
3	18.46	-10.8997	2.8126	-3.5711

Slope	1.1249±0.4438
Intercept	8.6874±4.6867
R^2	0.9917
Order with Respect to Ozone	1.12±0.44

OZONE ORDER DETERMINATION

12/10/94. Ozonation of TCE. Ozone Order Determination. TCE in Excess.
0.05 M Phosphate Buffer Solution at pH 2.0. Temp = 22.0°C

Table C-12/10/94-Experimental Run 1

Time	Ozone Concentration				Time	TCE Concentration			
(s)	(mg/L)	95% CI	μM	95% CI	(s)	(mg/L)	95% CI	μM	95% CI
0	2.857	0.17	59.52	3.5	0	125	13	951	99
20	2.347	0.16	48.90	3.3	200	114	12	867	91
40	2.280	0.16	47.50	3.3					
60	1.690	0.13	35.21	2.7					
80	1.860	0.16	38.75	3.3					
100	1.688	0.16	35.17	3.3					
120	1.547	0.15	32.23	3.1					
140	1.503	0.16	31.31	3.3					
160	1.491	0.16	31.06	3.3					
180	1.591	0.17	33.15	3.5					
200	1.397	0.16	29.10	3.3					
CSTD	(mg/L)	95% CI	%		CSTD	(μg)	%		
2.605	2.198	0.15	84.38		15	17.44	116.3		
3.285	3.245	0.17	98.78		30	34.20	114.0		

Table C-12/10/94-Experimental Run 2

Time	Ozone Concentration				Time	TCE Concentration			
(s)	(mg/L)	95% CI	μM	95% CI	(s)	(mg/L)	95% CI	μM	95% CI
0	2.926	0.09	60.96	1.9	0	125	13	951	99
20	2.261	0.16	47.10	3.3	200	109	12	829	91
40	2.068	0.16	43.08	2.3					
60	2.315	0.20	48.23	4.2					
80	1.780	0.16	37.08	3.3					
100	1.775	0.17	36.98	3.5					
120	1.684	0.16	35.08	3.3					
140	1.713	0.17	35.69	3.5					
160	1.528	0.16	31.83	3.3					
180	1.665	0.18	34.69	3.7					
200	1.581	0.17	32.94	3.5					
CSTD	(mg/L)	95% CI	%		CSTD	(μg)	%		
1.790	1.964	0.16	109.7		15	15.83	105.5		
3.096	3.186	0.16	102.9		30	34.09	113.6		

12/10/94. Ozonation of TCE. Ozone Order Determination. TCE in Excess.
0.05 M Phosphate Buffer Solution at pH 2.0. Temp = 22.0°C

Table C-12/10/94-Experimental Run 3

Time	Ozone Concentration				Time	TCE Concentration			
(s)	(mg/L)	95% CI	μM	95% CI	(s)	(mg/L)	95% CI	μM	95% CI
0	2.348	0.15	48.92	3.1	0	125	13	951	99
20	1.970	0.15	41.04	3.1	200	112	12	852	91
40	1.968	0.16	41.00	3.3					
60	1.941	0.18	40.44	3.7					
80	1.508	0.15	31.42	3.1					
100	1.596	0.16	33.25	3.3					
120	1.412	0.15	29.42	3.1					
140	1.543	0.17	32.16	3.5					
160	1.406	0.17	29.29	3.5					
180	1.431	0.17	29.81	3.5					
200	1.445	0.19	30.10	3.9					
CSTD	(mg/L)	95% CI	%		CSTD	(μg)	%		
1.695	1.849	0.13	109.1		30	35.08	116.9		
2.376	2.671	0.15	112.4						

Table C-12/10/94-Experimental Run 4

Time	Ozone Concentration				Time	TCE Concentration			
(s)	(mg/L)	95% CI	μM	95% CI	(s)	(mg/L)	95% CI	μM	95% CI
0	2.216	0.16	46.17	3.3	0	125	13	951	99
20	1.983	0.17	41.31	3.5	200	107	12	814	91
40	1.889	0.18	39.35	3.7					
60	1.473	0.15	30.69	3.1					
80	1.611	0.17	33.56	3.5					
100	1.563	0.18	32.56	3.7					
120	1.467	0.17	30.56	3.5					
140	1.422	0.17	29.62	3.5					
160	1.442	0.18	30.04	3.7					
180	1.227	0.16	25.56	3.3					
200	1.354	0.18	28.21	3.7					
CSTD	(mg/L)	95% CI	%		CSTD	(μg)	%		
1.293	1.646	0.16	127.3		No Additional Check Standards Prepared				
1.996	2.354	0.17	117.9						

12/13/94. Ozonation of TCE. Ozone Order Determination. TCE in Excess.
0.05 M Phosphate Buffer Solution at pH 2.0. Temp = 22.0°C

Table C-12/13/94-Experimental Run 1

Time	Ozone Concentration			Time	TCE Concentration			
(s)	(mg/L)	95% CI	μM	95% CI	(s)	(mg/L)	95% CI	μM	95% CI
0	2.936	0.054	61.17	1.1	0	112	10	852	76
20	2.700	0.055	56.25	1.1	200	101	10	768	76
40	2.313	0.054	48.19	1.1					
60	2.076	0.054	43.25	1.1					
80	2.113	0.056	44.02	1.2					
100	1.855	0.060	38.65	1.2					
120	1.704	0.057	35.50	1.2					
140	1.640	0.058	34.17	1.2					
160	1.669	0.061	34.77	1.3					
180	1.493	0.054	31.10	1.1					
200	1.456	0.055	30.33	1.1					

CSTD	(mg/L)	95% CI	%		CSTD	(μg)	%		
1.552	1.553	0.060	100.1		15	15.02	100.1		
3.166	3.220	0.056	101.7		30	31.20	104.0		

Table C-12/13/94-Experimental Run 2

Time	Ozone Concentration			Time	TCE Concentration			
(s)	(mg/L)	95% CI	μM	95% CI	(s)	(mg/L)	95% CI	μM	95% CI
0	2.909	0.053	60.60	1.1	0	112	10	852	76
20	2.408	0.051	50.17	1.1	200	97	9	738	68
40	2.294	0.055	47.79	1.1					
60	2.006	0.053	41.79	1.1					
80	1.943	0.054	40.48	1.1					
100	1.600	0.050	33.33	1.0					
120	1.623	0.055	33.81	1.1					
140	1.508	0.057	31.42	1.2					
160	1.657	0.059	34.82	1.2					
180	1.352	0.054	28.17	1.1					
200	1.562	0.064	32.54	1.3					

CSTD	(mg/L)	95% CI	%		CSTD	(μg)	%		
1.288	1.278	0.058	99.22		15	14.31	95.4		
3.007	3.058	0.056	101.7		30	29.02	96.7		

12/13/94. Ozonation of TCE. Ozone Order Determination. TCE in Excess.
0.05 M Phosphate Buffer Solution at pH 2.0. Temp = 22.0°C

Table C-12/13/94-Experimental Run 3

Time	Ozone Concentration			Time	TCE Concentration			
(s)	(mg/L)	95% CI	μM	95% CI	(s)	(mg/L)	95% CI	μM	95% CI
0	2.109	0.042	43.94	0.9	0	112	10	852	76
20	2.094	0.056	43.62	1.2	200	99	9	753	68
40	1.955	0.059	40.73	1.2					
60	1.723	0.056	35.90	1.2					
80	1.582	0.056	32.96	1.2					
100	1.696	0.065	35.33	1.3					
120	1.370	0.054	28.54	1.1					
140	1.439	0.060	29.98	1.2					
160	1.304	0.054	27.17	1.1					
180	1.202	0.057	25.04	1.2					
200	1.309	0.063	27.27	1.3					
CSTD	(mg/L)	95% CI	%		CSTD	(μg)	%		
1.348	1.321	0.07	98.00		15	15.41	102.7		
2.287	2.369	0.06	103.6		30	31.50	105.0		

Table C-12/13/94-Experimental Run 4

Time	Ozone Concentration			Time	TCE Concentration			
(s)	(mg/L)	95% CI	μM	95% CI	(s)	(mg/L)	95% CI	μM	95% CI
0	2.282	0.065	47.54	1.3	0	112	10	852	76
20	2.046	0.056	42.62	1.2	200	96	9	730	68
40	1.820	0.054	37.92	1.1					
60	1.653	0.057	34.44	1.2					
80	1.554	0.059	32.38	1.2					
100	1.452	0.059	30.25	1.2					
120	1.351	0.064	28.15	1.3					
140	1.306	0.063	27.21	1.3					
160	1.302	0.061	27.13	1.3					
180	1.229	0.063	25.60	1.3					
200	1.302	0.069	27.12	1.4					
CSTD	(mg/L)	95% CI	%		CSTD	(μg)	%		
1.26	1.236	0.06	98.09		No Additional Check Standards Prepared				
2.232	2.263	0.06	101.4						

12/15/94. Ozonation of TCE. Ozone Order Determination. TCE in Excess.
0.05 M Phosphate Buffer Solution at pH 2.0. Temp = 22.0°C

Table C-12/15/94-Experimental Run 1

Time	Ozone Concentration				Time	TCE Concentration			
(s)	(mg/L)	95% CI	μM	95% CI	(s)	(mg/L)	95% CI	μM	95% CI
0	2.596	0.15	54.08	3.1	0	106	14	806	106
20	2.128	0.17	44.33	3.5	200	92	14	700	106
40	1.940	0.18	40.42	3.7					
60	1.646	0.17	34.29	4.0					
80	1.541	0.19	32.10	3.3					
100	1.284	0.16	26.75	3.3					
120	1.150	0.16	23.96	3.5					
140	1.129	0.17	23.52	3.7					
160	1.129	0.18	23.52	3.7					
180	1.100	0.18	22.92	3.7					
200	1.599	0.28	33.31	5.8					
CSTD	(mg/L)	95% CI	%		CSTD	(μg)	%		
1.301	1.343	0.16	103.2		15	14.81	98.73		
3.078	3.123	0.18	101.5		30	29.20	97.33		

Table C-12/15/94-Experimental Run 2

Time	Ozone Concentration				Time	TCE Concentration			
(s)	(mg/L)	95% CI	μM	95% CI	(s)	(mg/L)	95% CI	μM	95% CI
0	2.532	0.14	52.75	2.9	0	106	14	806	106
20	2.328	0.19	48.50	4.0	200	89	14	677	106
40	1.880	0.16	39.17	3.3					
60	1.897	0.21	39.52	4.4					
80	1.518	0.18	31.62	3.7					
100	1.196	0.16	24.92	3.3					
120	1.209	0.17	25.19	3.5					
140	1.232	0.19	25.67	4.0					
160	1.172	0.19	24.42	4.0					
180	0.936	0.17	19.50	3.5					
200	0.950	0.17	19.75	3.5					
CSTD	(mg/L)	95% CI	%		CSTD	(μg)	%		
1.138	1.212	0.18	106.5		15	15.19	101.3		
2.928	2.992	0.17	102.2		30	28.47	94.9		

12/15/94. Ozonation of TCE. Ozone Order Determination. TCE in Excess.
0.05 M Phosphate Buffer Solution at pH 2.0. Temp = 22.0°C

Table C-12/15/94-Experimental Run 3

Time	Ozone Concentration			Time	TCE Concentration			
(s)	(mg/L)	95% CI	μM	95% CI	(s)	(mg/L)	95% CI	μM	95% CI
0	1.810	0.16	37.71	3.3	0	106	14	806	106
20	1.508	0.16	31.42	3.3	200	92	14	700	106
40	1.469	0.20	30.60	4.2					
60	1.340	0.20	27.92	4.2					
80	1.055	0.17	21.98	3.5					
100	0.967	0.16	20.15	3.3					
120	0.959	0.18	19.98	3.7					
140	0.999	0.19	20.81	4.0					
160	0.867	0.18	18.06	3.7					
180	0.967	0.21	20.15	4.4					
200	0.798	0.18	16.62	3.7					
CSTD	(mg/L)	95% CI	%		CSTD	(μg)	%		
1.173	1.324	0.16	112.9		15	14.59	97.3		
1.778	2.007	0.16	112.9		30	29.34	97.8		

Table C-12/15/94-Experimental Run 4

Time	Ozone Concentration			Time	TCE Concentration			
(s)	(mg/L)	95% CI	μM	95% CI	(s)	(mg/L)	95% CI	μM	95% CI
0	1.884	0.15	39.25	3.1	0	106	14	806	106
20	1.572	0.16	32.75	3.3	200	91	14	692	106
40	1.397	0.16	29.10	3.3					
60	1.348	0.19	28.08	4.0					
80	1.098	0.17	22.87	3.5					
100	1.048	0.17	21.83	3.5					
120	1.086	0.19	22.62	4.0					
140	0.831	0.16	17.31	3.3					
160	0.923	0.18	19.23	3.7					
180	0.884	0.18	18.42	3.7					
200	0.696	0.16	14.50	3.3					
CSTD	(mg/L)	95% CI	%		CSTD	(μg)	%		
1.173	1.328	0.19	113.2		No Additional Check Standards Prepared				
1.794	2.005	0.15	111.8						

Summary of Data to Prepare and the Results of the Van't Hoff Plots

Table C-12/10/94-Van't Hoff Plot Data and Results

Run	[O3] at t=0s (μM)	X-Axis ln [O3]o	(d[O3]/dt) at t=0s 10⁻² (M s⁻¹)	Y-Axis ln (d[O3]/dt)o
1	59.52	-9.7292	1.4807	-4.2127
2	60.96	-9.7053	1.5810	-4.1471
3	46.17	-9.9831	1.1173	-4.4943

Slope	1.1919 ± 0.52
Intercept	7.4029 ± 5.09
R^2	0.9898
Order with Respect to Ozone	1.19 ± 0.52

Table C-12/10/94-Van't Hoff Plot Data and Results

Run	[O3] at t=0s (μM)	X-Axis ln [O3]o	(d[O3]/dt) at t=0s 10⁻² (M s⁻¹)	Y-Axis ln (d[O3]/dt)o
1	61.17	-9.7019	1.4878	-4.2079
2	60.60	-9.7111	1.5818	-4.1466
3	43.94		0.7880	-4.8434
4	47.54	-9.9539	-1.1598	-4.4569

Slope	1.1225 ± 1.0782
Intercept	$6.7173 \pm$
R^2	0.9525
Order with Respect to Ozone	1.12 ± 1.1

Table C-12/10/94-Van't Hoff Plot Data and Results

Run	[O3] at t=0s (μM)	X-Axis ln [O3]o	(d[O3]/dt) at t=0s 10⁻² (M s⁻¹)	Y-Axis ln (d[O3]/dt)o
1	54.08	-9.8250	-1.8054	-4.0144
2	52.75	-9.8499	-1.4635	-4.2243
3	37.71	-10.1856	-1.0476	-4.5587
4	39.25	-10.1456	-1.0710	-4.5366

Slope	1.3199 ± 0.8668
Intercept	8.8678 ± 8.6704
R^2	0.9214
Order with Respect to Ozone	1.32 ± 0.87

OZONATION OF TCE USING SECOND ORDER CONDITIONS

11/11/94. Ozonation of TCE using Second Order Kinetic Reaction Conditions.
0.05 M Phosphate Buffer Solution at pH 2.0. Temp = 22.0°C

Table C-11/11/94-Control Run

Time	Ozone Concentration			Time	TCE Concentration		
(min)	(mg/L)	95% CI	μM	95% CI	(min)	(mg/L)	95% CI	μM	95% CI

Time (min)	(mg/L)	95% CI	μM	95% CI	Time (min)	(mg/L)	95% CI	μM	95% CI
0	6.227	0.17	129.7	3.5	0.0	11.35	1.10	86.31	8.4
1	6.365	0.19	132.6	4.0	0.5	11.63	0.89	88.44	6.8
2	6.522	0.25	135.9	5.2	1.5	11.89	0.90	90.42	6.8
3	6.312	0.23	131.5	4.8	2.5	11.53	0.99	87.68	7.5
4	6.311	0.21	131.5	4.4	3.5	11.68	0.97	88.82	7.3
5	6.365	0.26	132.6	5.4	4.5	11.42	1.07	86.84	8.1
6	6.416	0.27	133.7	5.6	5.5	11.55	1.04	87.83	7.9
7	6.528	0.22	136.0	4.6	6.5	11.50	0.97	87.45	7.4

CSTD	(mg/L)	95% CI	%		CSTD	(μg)	%		
3.752	3.982	0.22	106.1		15	13.39	89.3		
5.812	6.086	0.22	104.7		30	29.83	99.4		

Table C-11/11/94-Experimental Run I

Time (min)	(mg/L)	95% CI	μM	95% CI	Time (s)	(mg/L)	95% CI	μM	95% CI
0	6.430	0.23	133.9	4.8	0.0	9.65	1.3	73.37	9.9
1	6.098	0.26	127.0	5.4	0.5	8.50	1.1	64.66	8.4
2	5.818	0.24	121.2	5.0	1.5	6.78	1.4	51.58	10.6
3	5.901	0.25	122.9	5.2	2.5	5.82	1.6	44.24	12.2
4	5.686	0.32	118.5	6.6	3.5	5.06	1.3	38.50	9.9
5	5.247	0.23	109.3	4.8	4.5	4.39	1.1	33.35	8.4
6	5.323	0.25	110.9	5.2	5.5	4.16	1.2	31.62	9.1
7	5.066	0.30	105.5	6.2	6.5	3.27	1.0	24.87	7.6
					7.5	2.76	1.5	21.02	11.4

CSTD	(mg/L)	95% CI	%		CSTD	(μg)	%		
3.549	3.734	0.22	105.2		15	15.24	101.6		
5.519	5.955	0.21	107.9		30	29.58	98.6		

Table C-11/11/94-Experimental Run 2

Time (min)	(mg/L)	95% CI	μM	95% CI	Time (s)	(mg/L)	95% CI	μM	95% CI
0	6.909	0.23	143.9	4.8	0.0	9.932	0.9	75.53	6.8
1	6.651	0.27	138.6	5.6	0.5	8.629	0.9	65.62	6.8
2	6.287	0.24	131.0	5.0	1.5	6.960	0.9	52.93	6.8
3	6.168	0.24	128.5	5.0	2.5	5.498	1.4	41.81	10.6
4	5.838	0.24	121.6	5.0	3.5	4.779	0.8	36.34	6.1
5	5.737	0.25	119.5	5.2	4.5	3.932	1.0	29.90	7.6
6	5.361	0.22	111.7	4.6	5.5	3.370	1.0	25.63	7.6
					6.5	2.808	1.4	21.35	10.6

CSTD	(mg/L)	95% CI	%		CSTD	(μg)	%		
3.741	3.900	0.21	104.3		15	13.96	93.1		
6.426	6.647	0.22	103.4		30	29.45	98.2		

11/15/94. Ozonation of TCE using Second Order Kinetic Reaction Conditions.
0.05 M Phosphate Buffer Solution at pH 2.0. Temp = 22.0°C

Table C-11/15/94-Control Run

Time	Ozone Concentration			Time	TCE Concentration			
(min)	(mg/L)	95% CI	μM	95% CI	(min)	(mg/L)	95% CI	μM	95% CI
0	6.066	0.28	126.4	5.8	0.0	10.07	1.13	76.58	8.6
1	6.420	0.24	133.7	5.0	0.5	11.04	0.99	83.95	7.5
2	6.331	0.28	131.9	5.8	1.5	10.53	0.88	80.95	6.7
3	6.236	0.30	129.9	6.2	2.5	10.84	0.73	82.43	5.5
4	6.248	0.38	130.2	7.9	3.5	11.10	0.74	84.41	5.5
5	6.555	0.28	136.5	5.8	4.5	10.83	0.74	82.36	5.5
6	6.392	0.28	133.2	5.8	5.5	11.17	0.73	84.94	5.5
7	6.424	0.31	133.8	6.5	6.5	10.85	0.68	82.51	5.1
CSTD	(mg/L)	95% CI	%		CSTD	(μg)	%		
4.381	4.423	0.26	101.0		15	14.57	97.13		
6.104	6.075	0.24	99.5		30	29.71	99.03		

Table C-11/15/94-Experimental Run I

Time	Ozone Concentration			Time	TCE Concentration			
(min)	(mg/L)	95% CI	μM	95% CI	(s)	(mg/L)	95% CI	μM	95% CI
0	6.773	0.30	141.1	6.2	0.0	9.758	1.06	74.21	8.1
1	6.562	0.34	136.7	7.1	0.5	7.930	0.93	60.30	7.1
2	6.112	0.40	127.3	8.3	1.5	6.694	0.99	50.96	7.5
3	5.991	0.29	124.8	6.0	2.5	5.520	0.86	41.98	6.5
4	5.820	0.31	124.2	6.4	3.5	4.584	1.22	34.86	9.3
5	5.681	0.33	118.3	6.9	4.5	4.019	0.84	30.56	6.4
6	5.550	0.40	116.2	8.3	5.5	3.394	1.06	25.81	8.1
7	5.706	0.39	118.9	8.1	6.5	2.863	1.09	21.77	8.3
8	5.324	0.37	110.9	7.7	7.5	2.583	1.10	19.64	8.4
CSTD	(mg/L)	95% CI	%		CSTD	(μg)	%		
3.693	3.550	0.25	96.1		15	15.55	103.7		
6.129	6.744	0.27	110.0		30	31.05	103.5		

Table C-11/15/94-Experimental Run 2

Time	Ozone Concentration			Time	TCE Concentration			
(min)	(mg/L)	95% CI	μM	95% CI	(s)	(mg/L)	95% CI	μM	95% CI
0	7.372	0.28	153.6	5.8	0.0	9.601	1.04	73.01	7.9
1	7.091	0.34	147.7	7.1	0.5	8.012	1.03	60.93	7.9
2	6.568	0.27	136.8	5.6	1.5	6.388	0.77	48.58	5.8
3	6.345	0.35	132.2	7.3	2.5	5.314	0.80	40.41	6.1
4	6.291	0.37	131.1	7.7	3.5	4.358	0.99	33.14	7.5
5	6.175	0.38	128.6	7.9	4.5	3.576	0.81	27.19	6.1
6	5.976	0.37	124.5	7.7	5.5	3.004	0.76	22.84	5.8
7	5.706	0.33	118.9	6.9	6.5	2.559	0.82	19.46	6.2
8	5.598	0.53	116.6	11.0	7.5	2.199	1.10	16.72	8.4
CSTD	(mg/L)	95% CI	%		CSTD	(μg)	%		
3.770	3.725	0.24	98.8		15	14.02	93.5		
6.916	7.340	0.26	106.1		30	31.64	105.5		

01/12/95. Ozonation of TCE using Second Order Kinetic Reaction Conditions.
0.05 M Phosphate Buffer Solution at pH 2.0. Temp = 22.0°C. Initial Molar
ratio of the reactants was 2:1 (VOC:ozone).

Table C-01/12/95-Control Run

Time	Ozone Concentration				Time	TCE Concentration			
(min)	(mg/L)	95% CI	μM	95% CI	(min)	(mg/L)	95% CI	μM	95% CI
0	2.926	0.10	60.96	2.1					
1	2.955	0.11	61.56	2.3					
2	2.952	0.08	61.50	1.7					
3	2.935	0.09	61.15	1.9		Control Sample Not Analyzed			
4	2.908	0.12	60.58	2.5		Data Not Available			
5	2.805	0.11	58.44	2.3					
6	2.923	0.09	60.89	1.9					
7	2.856	0.10	59.50	2.1					
CSTD	(mg/L)	95% CI	%		CSTD	(μg)	%		
1.717	1.809	0.08	105.4		15	15.99	106.6		
3.009	3.038	0.10	109.0		30	33.25	110.8		

Table C-01/12/95-Experimental Run I

Time	Ozone Concentration				Time	TCE Concentration			
(min)	(mg/L)	95% CI	μM	95% CI	(s)	(mg/L)	95% CI	μM	95% CI
0	3.082	0.11	64.20	2.3	0.0	22.96	0.94	174.6	7.1
1	2.650	0.09	55.20	1.9	0.5	21.30	0.96	162.0	7.3
2	2.326	0.09	48.45	1.9	1.5	19.70	0.89	149.8	6.8
3	2.053	0.10	42.78	2.1	2.5	18.47	0.96	140.4	7.3
4	1.902	0.13	39.63	2.7	3.5	16.94	1.04	128.8	7.9
5	1.531	0.09	31.89	1.9	4.5	16.36	0.84	124.4	6.4
6	1.445	0.11	30.10	2.3	5.5	15.42	0.98	117.2	7.4
					6.5	14.89	0.89	113.3	6.8
CSTD	(mg/L)	95% CI	%		CSTD	(μg)	%		
1.681	1.726	0.08	102.7		15	15.61	104.1		
3.012	3.027	0.08	100.5		30	32.71	109.0		

Table C-01/12/95-Experimental Run 2

Time	Ozone Concentration				Time	TCE Concentration			
(min)	(mg/L)	95% CI	μM	95% CI	(s)	(mg/L)	95% CI	μM	95% CI
0	3.139	0.09	65.39	1.9	0.0	23.45	1.00	178.3	7.6
1	2.800	0.10	58.32	2.1	0.5	21.79	0.91	165.7	6.9
2	2.249	0.09	46.85	1.9	1.5	19.77	0.83	150.3	6.3
3	1.965	0.09	40.94	1.9	2.5	18.20	0.80	138.4	6.1
4	1.771	0.10	36.89	2.1	3.5	17.32	0.89	131.7	6.8
5	1.470	0.09	30.63	1.9	4.5	16.35	1.00	124.3	7.6
6	1.330	0.11	27.71	2.3	5.5	15.79	0.80	120.1	6.1
7	1.319	0.25	27.48	5.7	6.5	15.24	0.76	115.9	5.8
CSTD	(mg/L)	95% CI	%		CSTD	(μg)	%		
1.380	1.311	0.10	95.0		15	16.34	108.9		
3.331	3.280	0.08	98.5		30	33.47	111.6		

OZONATION OF 1,1,3-TCP

02/14/95. Ozonation of 1,1,3-TCP using Second Order Kinetic Reaction Conditions. 0.05 M Phosphate Buffer Solution at pH 2.0. Temp = 22.0°C

Table C-02/14/95-Control Run

Time	Ozone Concentration			Time	1,1,3-TCP Concentration			
(min)	(mg/L)	95% CI	μM	95% CI	(min)	(mg/L)	95% CI	μM	95% CI
0	5.90	0.14	12.3	3.0	0	10.9	1.3	75.0	8.9
1	5.91	0.14	12.3	3.0	1	11.4	1.2	78.4	8.2
2	6.01	0.14	12.5	3.0	2	11.7	1.3	80.5	8.9
3	5.96	0.13	12.4	2.7	3	11.6	1.1	79.8	7.6
4	5.87	0.13	12.2	2.7	4	10.9	1.1	75.0	7.6
5	5.87	0.15	12.2	2.7	5	10.4	1.0	71.5	6.9
7	5.73	0.13	11.9	2.7	7	11.3	1.2	77.7	8.2
10	5.75	0.13	12.0	2.7	10	10.8	1.0	74.3	7.6

CSTD	(mg/L)	95% CI	%		CSTD	(μg)	95% CI	%	
2.85	2.81	0.14	98.6		10	9.53		95.3	
5.87	5.78	0.13	98.5		20	19.25		96.3	

Table C-02/14/95-Experimental Run I

Time	Ozone Concentration			Time	1,1,3-TCP Concentration			
(s)	(mg/L)	95% CI	μM	95% CI	(s)	(mg/L)	95% CI	μM	95% CI
0	5.875	0.15	122	3.1	0	11.2	1.1	77.0	7.6
10	5.203	0.13	108	2.7	5	9.40	1.2	64.7	8.3
40	4.641	0.15	96.7	3.1	25	7.39	1.0	50.8	6.9
70	4.181	0.15	87.1	3.1	55	5.63	1.0	38.7	6.9
100	4.003	0.13	83.4	2.7	85	4.52	1.0	31.1	6.9
130	3.805	0.12	79.3	2.5	115	3.92	0.9	26.9	6.2
160	3.643	0.12	75.9	2.5	145	3.43	1.0	23.6	6.9
190	3.531	0.13	73.6	2.7	175	3.17	1.4	21.8	9.6

CSTD	(mg/L)	95% CI	%		CSTD	(μg)	95% CI	%	
3.540	3.508	0.13	99.1		10	9.36		93.6	
6.232	6.102	0.14	97.9		20	17.8		89.0	

Table C-02/14/95-Experimental Run 2

Time	Ozone Concentration			Time	1,1,3-TCP Concentration			
(s)	(mg/L)	95% CI	μM	95% CI	(s)	(mg/L)	95% CI	μM	95% CI
0	5.103	0.15	106	3.1	0	11.2	1.1	77.0	7.6
10	4.874	0.16	101	3.3	5	9.28	1.2	63.8	8.3
40	4.286	0.12	89.3	2.5	25	7.23	1.1	49.7	7.6
70	3.957	0.12	82.4	2.5	55	5.83	1.0	40.1	6.9
100	3.629	0.12	75.6	2.5	85	4.75	1.0	32.7	6.9
130	3.459	0.11	72.1	2.3	115	3.89	1.0	26.7	6.9
160	3.392	0.14	70.7	2.9	145	3.94	1.2	27.1	8.3
					175	2.90	0.9	19.9	6.2

CSTD	(mg/L)	95% CI	%		CSTD	(μg)	95% CI	%	
3.001	3.03	0.13	101.0		10	9.95		99.5	
5.103	5.04	0.12	98.8		20	18.7		93.5	

02/20/95. Ozonation of 1,1,3-TCP using Second Order Kinetic Reaction Conditions.
0.05 M Phosphate Buffer Solution at pH 2.0. Temp = 22.0°C

Table C-02/20/95-Control Run

Time (min)	Ozone Concentration				Time (min)	1,1-TCP Concentration			
	(mg/L)	95% CI	µM	95% CI		(mg/L)	95% CI	µM	95% CI
0	6.22	0.38	129.6	7.9	0	11.93	1.20	82.0	8.3
1	6.13	0.43	127.7	9.9	1	10.76	0.95	74.0	6.5
2	6.32	0.37	131.7	7.7	2	11.02	1.06	75.8	7.3
3	6.38	0.37	132.9	7.7	3	10.71	0.93	73.6	6.4
4	6.26	0.38	130.4	7.9	4	11.69	1.03	80.4	7.1
5	6.29	0.41	131.0	8.5	5	11.45	1.09	78.7	7.5
7	6.24	0.39	130.0	8.1	7	10.45	0.79	71.9	5.4
10	6.16	0.40	128.3	8.3	10	11.23	0.97	77.2	6.7

CSTD	(mg/L)	95% CI	%		CSTD	(µg)	%		
3.10	3.01	0.38	97.1		10.0	8.69	86.9		
6.45	6.23	0.36	96.6		20.0	19.52	97.6		

Table C-02/20/95-Experimental Run I

Time (s)	Ozone Concentration				Time (s)	1,1-DCP Concentration			
	(mg/L)	95% CI	µM	95% CI		(mg/L)	95% CI	µM	95% CI
0	5.81	0.37	121	7.7	0	11.04	1.03	75.9	7.1
10	5.57	0.37	116	7.7	5	9.28	0.93	63.8	6.4
40	4.81	0.38	100	7.9	25	6.36	0.88	43.7	6.1
70	4.50	0.44	93.8	9.2	55	4.61	0.75	31.7	5.2
100	4.33	0.42	90.3	8.7	85	3.32	0.69	22.9	4.7
130	4.04	0.43	84.1	9.0	115	2.82	0.71	19.4	4.9
160	3.87	0.53	80.7	11.0	145	1.96	0.76	13.5	5.2
					175	1.78	0.80	12.2	5.5

CSTD	(mg/L)	95% CI	%		CSTD	(µg)	%		
2.715	2.71	0.39	99.8		10	9.48	94.8		
5.805	5.79	0.40	99.7		20	19.36	96.8		

Table C-02/20/95-Experimental Run 2

Time (s)	Ozone Concentration				Time (s)	1,1-DCP Concentration			
	(mg/L)	95% CI	µM	95% CI		(mg/L)	95% CI	µM	95% CI
0	5.81	0.38	121	7.9	0	11.04	1.03	75.9	7.1
10	5.64	0.37	118	7.7	5	8.70	0.94	59.8	6.5
40	4.75	0.41	98.9	8.5	25	6.00	1.00	41.3	6.9
70	4.47	0.36	93.2	7.5	55	3.82	0.77	26.3	5.3
100	4.19	0.37	87.3	7.7	85	3.22	0.81	22.2	5.6
130	4.00	0.37	83.3	7.7	115	2.41	0.77	16.6	5.3
160	3.95	0.37	82.3	7.7	145	1.89	0.72	13.0	5.0
					175	1.40	0.69	9.61	4.7

CSTD	(mg/L)	95% CI	%		CSTD	(µg)	%		
2.745	2.67	0.36	97.3		10	9.04	90.4		
5.287	5.34	0.37	101.0		20	19.37	96.8		

OZONATION OF 1,1-DCP

03/08/95. Ozonation of 1,1-DCP using Second Order Kinetic Reaction Conditions.
0.05 M Phosphate Buffer Solution at pH 2.0. Temp = 22.0°C

Table C-03/08/95-Control Run

Time	Ozone Concentration				Time	1,1-DCP Concentration			
(min)	(mg/L)	95% CI	µM	95% CI	(min)	(mg/L)	95% CI	µM	95% CI
0	0.778	0.08	16.2	1.7	0	0.920	0.09	8.29	0.81
1	0.795	0.07	16.6	1.5	1	0.933	0.08	8.41	0.72
2	0.827	0.06	17.2	1.2	2	0.931	0.08	8.39	0.72
3	0.804	0.08	16.7	1.7	3	0.979	0.07	8.82	0.63
4	0.837	0.07	17.4	1.5	4	0.958	0.08	8.63	0.72
5	0.803	0.08	16.7	1.2	5	0.975	0.07	8.79	0.63
7	0.782	0.08	16.3	1.2	7	0.950	0.08	8.56	0.72
10	0.764	0.08	15.9	1.2					
CSTD	(mg/L)	95% CI	%		CSTD	(µg)	%		
0.585	0.576	0.08	98.5		1.0	1.07	100.7		
0.819	0.811	0.08	99.0		2.0	2.30	115.0		

Table C-03/08/95-Experimental Run I

Time	Ozone Concentration				Time	1,1-DCP Concentration			
(s)	(mg/L)	95% CI	µM	95% CI	(s)	(mg/L)	95% CI	µM	95% CI
0	0.804	0.08	16.7	1.7	0	0.949	0.08	8.55	0.72
10	0.636	0.08	13.3	1.7	5	0.691	0.06	6.23	0.54
30	0.512	0.07	10.7	1.5	20	0.429	0.07	3.87	0.63
50	0.461	0.09	9.60	1.9	40	0.290	0.06	2.61	0.54
70	0.472	0.08	9.82	1.7	60	0.196	0.06	1.77	0.54
90	0.422	0.09	8.79	1.9	80	0.135	0.07	1.22	0.63
110	0.397	0.08	8.27	1.7	100	0.104	0.06	0.94	0.54
CSTD	(mg/L)	95% CI	%		CSTD	(µg)	%		
0.46	0.384	0.08	83.5		1.0	1.050	105.0		
0.75	0.726	0.08	96.8		2.0	2.067	103.3		

Table C-03/08/95-Experimental Run 2

Time	Ozone Concentration				Time	1,1-DCP Concentration			
(s)	(mg/L)	95% CI	µM	95% CI	(s)	(mg/L)	95% CI	µM	95% CI
0	0.776	0.09	16.2	1.9	0	0.949	0.08	8.55	0.72
10	0.679	0.09	14.1	1.9	5	0.604	0.13	5.44	1.17
40	0.554	0.08	11.5	1.7	25	0.361	0.07	3.25	0.63
70	0.496	0.07	10.3	1.5	55	0.201	0.07	1.81	0.63
100	0.447	0.09	9.31	1.9	85	0.117	0.07	1.05	0.63
130	0.471	0.09	9.80	1.9	115	0.091	0.10	0.820	0.90
160	0.467	0.08	9.73	1.7	145	0.061	0.08	0.055	0.72
					175	0.064	0.10	0.058	0.90
CSTD	(mg/L)	95% CI	%		CSTD	(µg)	%		
0.586	0.560	0.08	95.6		1.0	1.102	110.2		
0.858	0.837	0.08	97.5		2.0	2.207	110.3		

110

03/13/95. Ozonation of 1,1-DCP using Second Order Kinetic Reaction Conditions.
0.05 M Phosphate Buffer Solution at pH 2.0. Temp = 22.0°C

Table C-03/13/95-Control Run

Time (min)	Ozone Concentration				Time (min)	1,1-DCP Concentration			
	(mg/L)	95% CI	µM	95% CI		(mg/L)	95% CI	µM	95% CI
0	0.880	0.10	18.3	2.1	0	0.784	0.06	7.06	0.54
1	0.882	0.11	18.4	2.3	1	0.726	0.09	6.54	0.81
2	0.863	0.11	8.0	2.3	2	0.734	0.09	6.61	0.81
3	0.902	0.12	18.8	2.5	3	0.744	0.08	6.70	0.72
4	0.884	0.10	18.4	2.1	4	0.743	0.07	6.70	0.63
5	0.864	0.10	18.0	2.1	5	0.757	0.07	6.82	0.63
7	0.838	0.09	17.5	1.9	7	0.723	0.07	6.52	0.72
10	0.786	0.11	16.4	2.3	10	0.732	0.07	6.60	0.63

CSTD	(mg/L)	95% CI	%		CSTD	(µg)	%		
0.50	0.535	0.10	107		1.0	0.969	96.9		
0.90	0.944	0.10	104		2.0	1.907	95.4		

Table C-03/13/95-Experimental Run I

Time (s)	Ozone Concentration				Time (s)	1,1-DCP Concentration			
	(mg/L)	95% CI	µM	95% CI		(mg/L)	95% CI	µM	95% CI
0	0.874	0.10	18.2	2.1	0	0.748	0.08	6.74	0.72
10	0.760	0.11	15.8	2.3	5	0.606	0.10	5.46	0.90
30	0.621	0.10	12.9	2.1	20	0.284	0.08	2.56	0.72
50	0.647	0.10	12.5	2.1	40	0.161	0.09	1.45	0.81
70	0.650	0.08	13.5	1.7	60	0.094	0.10	0.85	0.72
90	0.611	0.11	12.7	2.3	80	0.063	0.08	0.56	0.72
110	0.597	0.10	12.4	2.1	100	0.049	0.10		0.90
130	0.584	0.11	12.2	2.1	120	0.034	0.08		0.72

CSTD	(mg/L)	95% CI	%		CSTD	(µg)	%		
0.52	0.599	0.09	115.2		1.0	0.909	90.9		
0.76	0.820	0.11	107.9		2.0	1.930	96.5		

Table C-03/13/95-Experimental Run 2

Time (s)	Ozone Concentration				Time (s)	1,1-DCP Concentration			
	(mg/L)	95% CI	µM	95% CI		(mg/L)	95% CI	µM	95% CI
0	0.840	0.10	17.5	2.1	0	0.748	0.06	6.74	0.54
10	0.676	0.09	14.1	1.9	5	0.550	0.06	4.96	0.54
30	0.553	0.10	11.5	2.1	20	0.296	0.06	2.67	0.54
50	0.512	0.11	10.7	2.3	40	0.170	0.06	1.53	0.54
70	0.467	0.11	9.74	2.3	60	0.075	0.08	0.68	0.72
90	0.437	0.13	9.10	2.7	80	0.062	0.08	0.56	0.72
110	0.462	0.11	9.61	2.3	100	0.039	0.07	0.35	0.63
					120	0.026	0.05	0.23	0.45

CSTD	(mg/L)	95% CI	%		CSTD	(µg)	%		
0.54	0.472	0.11	87.4		1.0	0.994	99.4		
0.82	0.743	0.10	90.6		2.0	2.34	117.0		

APPENDIX D

HENRY'S LAW CONSTANT FOR OZONE

The Determination of the Henry's Law constant for ozone is a more diffucult experimental procedure than for VOCs because the compound must be introduced into solution as a gas. Additional processes such as mass transfer, self-decomposition, and oxidation of solvent inpurities are very important process to consider when determining the Henry's Law constant for ozone. Roth and Sullivan (1981) developed an emperical equation for the Henry's Law constant of ozone over a pH range of 0.65 to 10.2 and a temperature range of 3.5 to 60°C. The study by Roth and Sullivan is common referenced in the ozone literature because they took into account all the relivant processes in their determination. The following is the emperical equation:

$$K_H = 3.842 \times 10^7 ([OH^-]^{0.035})(exp(-2428/T)) \tag{D-1}$$

where K_H = Henry's Law Constant (atm/mole fraction)
[OH-] = Hydroxide Ion Concentration (mol/L)
T = Temperature (K)

The following is a table of values of the Henry's Law constant in dimensionless units that was adapted from values calculated from the empirical equation developed by Roth and Sullivan (1981).

Table D-1. Table of Dimensionless Henry's Law Constants (C_g/C_w)

pH	Temperature (°C)
	10	15	20	25	30	35	40
1.00	1.9656	2.2431	2.5482	2.8825	3.2475	3.6445	4.0751
1.50	2.0464	2.3353	2.6530	3.0011	3.3810	3.7944	4.2426
2.00	3.1306	2.4313	2.7621	3.1245	3.5200	3.9504	4.4171
2.50	2.2182	2.5313	2.8756	3.2529	3.6648	4.1128	4.5987
3.00	2.3094	2.6354	2.9939	3.3867	3.8155	4.2819	4.7878
3.50	2.4043	2.7437	3.1170	3.5259	3.9723	4.4580	4.9846
4.00	2.5032	2.8565	3.2452	3.6709	4.1357	4.6413	5.1896
4.50	2.6061	2.9740	3.3786	3.8219	4.3057	4.8321	5.4030
5.00	2.7133	3.0963	3.5175	3.9790	4.4828	5.0308	5.6251
5.50	2.8248	3.2236	3.6621	4.1426	4.6671	5.2377	5.8564
6.00	2.9410	3.3561	3.8127	4.3130	4.8590	5.4531	6.0973
6.50	3.0619	3.4941	3.9695	4.4903	5.0588	5.6773	6.3480
7.00	3.1878	3.6378	4.1327	4.6749	5.2668	5.9107	6.6090

APPENDIX E

TOTAL MASS TRANSFER VELOCITY CALCULATION

Determination of Chemical Properties

Table E-1. Compound Properties

Compound	FW	K_H
TCE	131.4	0.423
Ozone	48.0	3.124[1]

(1) at pH=2.0 and T=25°C

Using the following equations: (Schwarzenbach, Gschwend, and Imboden, 1993)

Molecular Diffusion Coefficient in Air: $D_a = \dfrac{1.55}{m^{0.65}}$ (cm^2 s^{-1}) at 25°C.   (E-1)

where m = formula weight (g/mol)

Molecular Diffusion Coefficinet in Water: $D_w = \dfrac{2.7 \times 10^{-4}}{m^{0.71}}$ (cm^2 s^{-1}) at 25°C.   (E-2)

Table E-2. Compound Properties

Compound	Molecular Diffusion Coefficient	
	D_a (cm^2 s^{-1})	D_w (cm^2 s^{-1})
TCE	0.065[1]	1.04e^{-5}[2]
Ozone	0.125[1]	1.74e^{-5}[3]

(1) Given by Equation E-1. (2) Given by Schwarzenbach, Gschwend, and Imboden, 1993. (3) Given by Masschelein, 1982; Bablon *et al.*, 1991.

Determination of Total Mass Transfer Velocity

General equation for v_{tot} was given by Schwarzenbach, Gschwend, and Imboden, 1993.

$$v_{tot} = \left(\frac{1}{\left({z_w}/{D_w} \right) + \left({z_w}/{D_a K_H} \right)} \right)$$ (E-3)

The estimated thickness of each stagnant layer as given by Schwarzenbach, Gschwend, and Imboden, 1993.

Water. $z_w = 0.001$ cm
Air. $z_a = 0.5$ cm

For Ozone

$$v_{tot} = \left(\frac{1}{\left(\frac{0.001}{1.74e^{-5}} \right) + \left(\frac{0.5}{0.125 * 3.124} \right)} \right)$$

$v_{tot} = 0.0170$ cm s^{-1}

For TCE

$$v_{tot} = \left(\frac{1}{\left(\frac{0.001}{1.04e^{-5}} \right) + \left(\frac{0.5}{0.065 * 0.423} \right)} \right)$$

$v_{tot} = 0.0087$ cm s^{-1}

LIST OF REFERENCES

LIST OF REFERENCES

Anderson, R. (1987) *Pratical Statistics for Analytical Chemists*. Van Nostrand Reinhold, New York, 89-121.

Atkins, D. (1990) *Physical Chemistry*, 4th Ed. W.H. Freeman, New York, 778-870.

Bach, R. and Wolber, C. (1984) Mechanism of Oxygen Transfer from Oxaziridine to Ethylene: The Consequence of HOMO-HOMO Interaction on Frontier Orbital Narrowing. *J. Am. Chem. Soc.*, **106**, 1410-1415.

Bader, H. and Hoigné, J. (1981) Determination of Ozone in Water By the Indigo-Method. *Wat. Res.*, **15**, 449-456.

Bader, H. and Hoigné, J. (1981) Determination of Ozone in Water By the Indigo-Method: A Submitter Standard Method. *Ozone Sci. Eng.*, **4**, 169-176.

Bailey, P. (1958) The Reactions of Ozone with Organic Compounds. *Chem. Rev.*, **58(2)**, 925-995.

Bailey, P. (1972) Organic Groupings Reactive Towards Ozone: Mechanisms in Aqueous Media in *Ozone in Water and Wastewater Treatment* (Edited by Evans, F.). Ann Arbor Science, Ann Arbor, MI., 29-59.

Bailey, P. (1978) *Ozonation in Organic Chemistry: Vol. 1, Olefinic Compounds,*. Academic Press, New York.

Bailey, P. *et al.* (1974) Studies Concerning Complexes of Ozone with Carbon π-Systems. *J. Am. Chem. Soc.*, **96(19)**, 6136-6139.

Bailey, P. and Lane, A. (1967) Competition Between Complete and Partial Cleavage During Ozonation of Olefins. *J. Am. Chem. Soc.*, **89(17)**, 4473-4479.

Bailey, P., Thompson, J., and Shoulders, B. (1966) Structure of the Initial Ozone-Olefin Adduct. *J. Am. Chem. Soc.*, **88(17)**, 4098-4099.

Bandemehr, A. (1992) *The Reactions of Ozone with VOCs in the Presence of Naturally Occuring Organic Matter*. MS Project Report, Michigan State University, Department of Civil and Environmental Engineering, East Lansing, MI.

Brink, D., Langlais, B., and Reckhow, D. (1991) Introduction. in *Ozone in Water Treatment: Application and Engineering* (Edited by Langlais, B., Reckhow, D., and Brink, D.). Lewis Publishers, Chelsea, MI. 1-11.

Carles, J., and Fliszár, S. (1972) Quantative Investagation of the Ozonolysis Reaction. XVI. Substituent Effects in the Ozonation Rates of Ethylenes. *Adv. Chem. Ser.*, **112**, 35-49.

Carlins, J. and Clark, R. (1982) Ozone Generation by Corona Discharge in *Handbook of Ozone Technology and Applications, Vol. 1* (Edited by Rice, R. and Netzer, A.). Ann Arbor Science, Ann Arbor, MI. 41-76.

The Conservation Foundation (1987) *Groundwater Protection. Groundwater: Saving the Unseen Resource. The final Report of the National Groundwater Policy Forum* (Austin, TX., 1985). The Conservation Foundation, Washington, DC., 76-85.

(1990) *CRC Handbook of Chemistry and Physics*, 70th Ed. (Edited by Weast, R.). CRC Press, Boca Raton, FL. D151-D158.

Cremer, D. (1981a) Theoretical Determination of Molecular Structure and Conformation. 7. Stereoselectivity of the Ozonolysis Reaction. *J. Am. Chem. Soc.*, **103(13)**, 3619-3626.

Cremer, D. (1981b) Theoretical Determination of Molecular Structure Conformation. 8. Energetics of the Ozonolysis Reaction. Primary Ozonide vs. Carbonyl Oxide Control of Stereochemistry. *J. Am. Chem. Soc.*, **103(13)**, 3627-3623.

Cremer, D. and Bock, C. (1986) Theoretical Determination of Molecular Structure and Conformation. 18. On the Formation of Epoxides during the Ozonation of Alkenes. *J. Am. Chem. Soc.*, **108(12)**, 3375-3379.

Davis, M. and Cornwell, D. (1991) *Introduction to Environmental Engineering*. McGraw Hill, New York. 431-433.

Dewar, M., Hwang, J., and Kuhn, D. (1991) An AM1 Study of the Reactions of Ozone with Ethylene and 2-Butene. *J. Am. Chem. Soc.*, **113(3)**, 735-742.

Durham, L. and Greenwood, F. (1968a) Ozonolysis. X. The Molozonide as an Intermediate in the Ozonolysis of Cis and Trans Alkenes. *J. Org. Chem.*, 33(4), 1629-1632.

Durham, L., and Greenwood, F. (1968b) The Cis-Molozonide. *Chem Comm.*, 24-5.

Devore, J. (1991) *Probability and Statistics for Engineering and the Sciences*, 3rd Ed. Brooks/Cole Publishing, Pacific Grove, CA.

Fliszár, S., and Carles, J. (1969a) A Quantiative Investigation of the Ozonolysis Reaction. VII. Ozonolysis of Phenylethylenes in the Presence of Oxygen -18-Labeled Benzaldehyde. *J. Am. Chem. Soc.*, 91(10), 2637-2643.

Fliszár, S., and Carles, J. (1969b) Quantiative Investigation of the Ozonolysis Reaction. IX. On the Mechanism of Ozonide Formation. *Can. J. Chem.*, 74(21), 3921-3929.

Fliszár, S., Carles, J., and Renard, J. (1968) On the Ozonolysis of cis and trans Stilbene in the Presence of Benzaldehyde-^{18}O, *J. Am. Chem. Soc.*, 90, 1364-1365.

Gäb, S. *et al.* (1985) Hydorxymethyl hydrogenperoxide and bis(hydroxymethyl) peroxide from Gas-phase Ozonolysis of Naturally Occurring Alkenes, *Nature*, 316, 535-536.

Grasso, D. and Weber, W. (1989) Mathematical Interpretation of Aqueous-Phase Ozone Decomposition Rates. *J Env.iron. Eng.*, 115(3), 541-559.

Greenwood, F. (1964) Studies in Ozonolysis. IV. Steric Effects in Determining the Existence of the Molozonide. *J. Org. Chem.*, 29, 1321-1324.

Greenwood, F. (1965) Ozonolysis. V. Reaction of the Ozonide with Isopropyl Grignard Reagent. *J. Org. Chem.*, 30, 1276-1277.

Greenwood, F., and Cohen, S. (1963) The Molozonide as an Intermediate in the Alkene-Ozone Reaction. *J. Org. Chem.*, 28, 1159-1160.

Griesbaum, K. and Brüggemann, J. (1972) The interaction of Ozone with Double Bonds Containing Vinyl Bromide Moieties. *Adv. Chem. Ser.*, 112, 50-65.

Hadler, M. (1982) Economic Poisons in *Enclopedia of Chemical Technology*, 3rd Ed., Vol. 18. (Edited by Othmer, D. and Raymond, K.) John Wiley, New York, 304-307.

(1986) *Handbook of Public Water Systems* (Editer by Williams, R. and Culp, G.). Van Nostrand Reichold, New York, 516-521.

Harding, L. and Goddard, W. (1978) Mechanisms of Gas-Phase and Liquid-Phase Ozonolysis. *J. Am. Chem. Soc.*, **100(23)**, 7180-7188.

Hellpointner, E. and Gäb, S. (1989) Detection of Methyl, Hydroxymethyl, and Hydorxyethyl Hydroperoxides in Air and Precipitation, *Nature*, **337**, 631-634.

Hewitt, C., Kok, G., and Fall, R. (1990) Hydroperoxides in Plants Exposed to Ozone Mediated Air Pollution Damage to Alkene Emitters, *Nature*, **344**, 56-58.

Hickmar, J. (1993) Tetrachlorethylene in *Enclopedia of Chemical Technology*, 4th Ed., Vol. 6. (Edited by Othmer, D. and Raymond, K.) John Wiley, New York, 50-59.

Hill, C. (1977) *An Introduction to Chemical Engineering*. John Wiley and Sons, New York, 29.

Hinrichs, T., Ramachandran, V., and Murry, R. (1979) Epoxidation of Olefins with Carbonyl Oxides. *J. Am. Chem. Soc.*, **101(5)**, 1282-1284.

Hoigné, J. (1982) Mechanimsm, Rates, and Selectivities of Oxidation of Organic Compounds Initiated by Ozonation of Water in *Handbook of Ozone Technology and Applications, Vol. 1* (Edited by Rice, R. and Netzer, A.). Ann Arbor Science, Ann Arbor, MI. 341-379.

Hoigné, J. (1995) Personal Communication. Federal Institute of Water Resources and Water Pollution Control (EAWAG), Swiss Federal Institute of Technology, Dübendorf, Switzerland.

Hoigné, J. and Bader, H. (1976) The Role of Hydroxyl Radical Reactions in Ozonation Processes in Aqueous Solutions. *Wat. Res.*, **10**, 377-386.

Hoigné, J. and Bader, H. (1983) Rate Constants of Reactions of Ozone with Organic and Inorganic Compounds in Water: I. Non-Dissociating Organic Compounds. *Wat. Res.*, **17**, 173-183.

Hughes, R. (1956) Structure of Ozone from the Microwave Spectrum between 9000 and 45000 Mc. *J. Chem. Phys.*, **24(1)**, 131-138.

Huisgen, R. (1963) Kinetics and Mechanism of 1,3-Dipolor Cycloadditions. *Angew. Chem., Int. Ed. Engl.*, **2(11)**, 633-645.

Hull, L., Hisatsune, I. and Heicklen, J. (1972) Low-temperature Infrared Studies of Simple Alkene-Ozone Reactions. *J. Am. Chem. Soc.*, **94(14)**, 4856-4865.

James M. Montgomery, Consulting Engineers (1985) *Water Treatment Principles and Design*, John Wiley, New York.

Kurth, H. *et al.* (1991) A High-Performance Liquid Chromatography System with an Immobilized Enzyme Reactor for Detertion of Hydrophilic Organic Peroxide, *Anal. Chem.*, **63**, 2586-2589.

Kwart, H. and Hoffman, D. (1966) Observations Regarding the Mechanism of Olefin Epoxidation with Peracids. *J. Org. Chem.*, **31**, 419-425.

Masten, S. (1986) *Mechanisms and Kinetics of Ozone and Hydroxyl Radical Reactions*. PhD Thesis, Harvard University, Division of Applied Sciences, Cambridge, MA.

Masten, S. and Hoigné, J. (1992) Comparison of Ozone and Hydroxyl Radical-Induced Oxidation of Chlorinated Hydrocarbons in Water. *Ozone Sci. Eng.*, **14**, 197-214.

McMurry, J. (1988) *Organic Chemistry*, 2nd Ed. Brooks/Cole Publishing, Pacific Grove, CA., 1077-1106.

Meister, M., Zwick, G., and Griesbaum, K. (1983) Ozonolysis of Vinyl Chloride in Methanol: A Convenient Entry to Methoxvmethylhydroperoxide and its Chemistry. *Can. J. Chem.*, **61**, 2385-2388.

Mertens, J. (1993) Dichloroethylene in *Enclopedia of Chemical Technology*, 4th Ed., Vol. 6. (Edited by Othmer, D. and Raymond, K.) John Wiley, New York, 36-40.

Mertens, J. (1993) Trichloroethylene in *Enclopedia of Chemical Technology*, 4th Ed., Vol. 6. (Edited by Othmer, D. and Raymond, K.) John Wiley, New York, 40-50.

Nakagawa, T., Andrews, L., and Keefer, R. (1960) The Kinetics of Ozonization of Polyalkylbenzenes. *J. Am. Chem. Soc.*, **82**, 269-276.

Pryor, W., Giamalva, D., and Church, D. (1983) Kinetics of Ozonation. 1. Electron-Deficient Alkenes. *J. Am. Chem. Soc.*, **105(23)**, 6858-6861.

Pryor, W., Govindan, C. (1981) Oxygen-Atom-Transfer Reactions from a Carbonyl Oxide (Porduced from 1 1,2,3-Trioxlane) to Electron-Deficinet Unsaturated Compounds. *J. Am. Chem. Soc.*, **103**, 7681-7683.

Ratkowski, D. (1983) *Nonlinear Regression Modeling*. Mackay Press, New York, 30-32.

Reed, D. (1993) Chlorocarbons and Chlorohydrocarbons in *Enclopedia of Chemical Technology*, 4th Ed., Vol. 5. (Edited by Othmer, D. and Raymond, K.) John Wiley, New York, 1017-1021.

Reich, D. and Cormany, C. (1982) Dry Cleaning and Laundering in *Enclopedia of Chemical Technology*, 3rd Ed., Vol. 8. (Edited by Othmer, D. and Raymond, K.) John Wiley, New York, 58-61.

Roth, J. and Sullivan, D. (1981) Solubility of Ozone in Water. *Ind. Eng. Chem. Fundam.*, **20**, 137-140.

Schwarzenbach, R., Gschwend, P., and Imboden, D. (1993) *Environmental Organic Chemistry*. John Wiley, New York.

Sehested, K. *et al.* (1991) The Primary Reaction in the Decomposition of Ozone in Acidic Aqueous Solutions. *Environ. Sci. Technol.*, **25**, 1589-1596.

Staehelin, J. and Hoigné, J. (1982) Decomposition of Ozone in Water: Rate of Initiation by Hydroxide Ions and Hydrogen Peroxide. *Environ. Sci. Technol.*, **16**, 676-681.

Staehelin, J. and Hoigné, J. (1985) Decomposition of Ozone in Water in the Presents of Organic Solutes Acting as Promoters and Inhibitors of Radical Chain Reactions. *Environ. Sci. Technol.*, **19**, 1206-1213.

Steinfeld, J., Francisco, J., and Hase, W. (1989) *Chemical Kinetics and Dynamics*. Prentice Hall, Englewood Cliffs, NJ., 1-40.

Trambarulo, R. *et al.* (1953) The Molecular Structure, Dipole Moment, and g Factor of Ozone from Its Microwave Spectrum. *J. Chem. Phys.*, **21(5)**, 851-855.

Verschueren, K. (1983) Handbook of Environmental Data on Organic Compounds, 2nd Ed. Van Nostrand Reinhold, New York.

Wadt, W. and Goddard, W. (1975) The Electronic Structure of the Criegee Intermediate: Ramifications for the Mechanism of Ozonolysis. *J. Am. Chem. Soc.*, **97(11)**, 3004-3021.

Weber, W., and Posselt, H. (1972) Chemical Oxidation in *Physicochemical Processes for Water Quality Control* (Edited by W. Weber). Wiley-Interscience, New York. 380-387.

Williamson, D. and Cvetanovic, R. (1968) Rates of Reaction of Ozone with Chlorinated and Conjugated Olefins. *J. Am. Chem. Soc.*, **90(10)**, 4248-4252.

Zhou, X. and Lee, Y. (1992) Aqueous Solubility and Reaction Kinetics of Hydroxymethyl Hydroperoxide, *J. Phys. Chem.*, **96**, 265-272.